Holocene and recent paleoclimate investigations using carbon and nitrogen isotopes from bulk sediment of two subarctic lakes, central Northwest Territories

by

Fritz Griffith

A thesis submitted to the Faculty of Graduate and Postdoctoral Studies in partial fulfillment of the requirements for the degree of

Master of Science

in

Earth Sciences

University of Ottawa
Ottawa, Ontario

Abstract

The Tibbitt-to-Contwoyto Winter Ice Road (TCWR) is the sole overland route servicing diamond mines north of Yellowknife, Northwest Territories (NWT), Canada. The road is 568 km long, 85% of which extends over frozen lakes. As such, its operational season is highly dependent upon the length of the winter season. This was exemplified in 2006, when an El Niño event caused an unusually short ice road season and resulted in a costly reduction of shipments to the mines. For future use and development of the TCWR, a comprehensive understanding of past regional climate variability is required.

This study is an integral component of a larger-scale study designed to develop a comprehensive database of high-resolution paleoclimate data for the NWT, using a variety of proxies. As part of the larger study, freeze cores were taken from numerous lakes along the TCWR and sliced at 1-mm intervals using a custom-designed sledge microtome. Bulk ^{13}C and ^{15}N isotope analysis was completed at preliminary 1-cm intervals through the cores of two lakes on opposite sides of the tree line. Results from this analysis show clear trends with distinct transitions in both cores, whose closely-matched timing suggests regional-scale climate events. These results indicate that the Early Holocene was warm and dry, with a sudden shift to wetter conditions around 7200-6900 cal yr BP. Another shift to cooler conditions occurred at 4000 cal yr BP, and a final transition to even cooler temperatures occurred around 755-715 cal yr BP, coinciding with the Little Ice Age.

Additionally, a modern lake survey was completed using surface sediments of numerous lakes throughout the Arctic and Subarctic. This survey verifies the strong influence of boreal forest vs. tundra conditions in affecting various environmental properties within lakes, including carbon and nitrogen isotopes.

Lastly, time-series analysis was completed on two sections of Danny's Lake core at high resolution (up to 2 mm), in order to determine short-term climate cycles. These results highlight specific climate frequencies which may be related to the Pacific Decadal Oscillation. These results offer insight to short-term climate phenomena in the Northwest Territories which will allow future climate modellers to make more accurate predictions of future climate and its impact on the ice road.

Acknowledgements

I would like to express my gratitude towards my supervisor, Ian Clark, for his excellent guidance and support throughout this experience. Ian's geochemistry expertise has been an invaluable source of knowledge, and his laid-back, friendly, and enthusiastic demeanor has fostered an enjoyable and creative learning environment which has challenged and improved my understanding of the research topic. I am grateful to have had the opportunity to work with such a reputable scientist (even if that work involves being a ballet stagehand!). It has been a truly enjoyable experience.

Thanks to Tim Patterson for organizing the Patterson Research Group and the Ice Road Project in the Northwest Territories, and allowing me the opportunity to participate in such a fascinating project. Tim's vision and leadership in coordinating the many components of the project has been instrumental in progressing my research and the project as a whole.

I'd also like to thank everyone else at the Patterson Research Group for their wonderful support. All of our group discussions and meetings proved to be invaluable to helping dissect much of the details of our interpretations. Thanks to Andrew for providing important mentorship in key aspects of the project, and for allowing me to use his grain size data. And Carley for her radiocarbon data and great times in the field, and April for her support, and Becky for helping in

various ways as well. It was great fun working with and hanging out with everyone at the PRG and I will miss all our good times.

Thanks to Jen Galloway and Kyle Sulphur for fieldwork assistance and pollen data as well as help with interpretations of this data. To Paul Trainor for his Horseshoe Lake pollen data, and Paul Gammon for his amazing insight into lake water geochemistry. To Hendrik Falck for his field work assistance and other support through the Northwest Territories Geoscience Office. And certainly to Graham Swindles for his important work with time-series analysis of the high-resolution data. His work is key to much of my interesting results.

A big thanks to Paul, Wendy and Patricia at the G.G. Hatch Isotope Lab for their friendly and important support. I learned a great deal about isotopes and was provided much-needed assistance in processing my samples.

I would also like to thank my parents, who have always supported me in all my endeavors, even if they really have no idea what I'm actually working on.

Finally, I would like to thank all my fellow grad students and friends here in Ottawa. I have greatly enjoyed my time here and it was all because I have been surrounded by wonderful friends. It would not have been the same without you.

Table of Contents

Table of Figures

Table of Tables

1. Introduction

Climate change is a crucial area of scientific research due to the major implications for ecosystems, agriculture, industry and well-being. For this reason, there has been a large array of paleoclimate studies through a great diversity of locations around the world. However, climate changes in northern latitudes are generally far more pronounced than anywhere else on the planet (Hassol, 2004). Additionally, this region hosts three ecoclimatic regions (Strong et al., 1989), transitioning sharply from an arctic to a boreal climate near the tree line. For these reasons, climate variations in the north can be of quite a large magnitude compared to other locations. This large climate sensitivity may also have environmental consequences and economic repercussions for northern residents in particular, underscoring the importance of paleoclimate research in the region.

One concern in the Northwest Territories is the future of the Tibbitt to Contwoyto Winter Ice Road (TCWR). The TCWR allows for supplies such as fuel, food, and machinery to be delivered to the Snap Lake, Diavik, Ekati, and Jericho diamond mines, as well as the Gahcho Kue Diamond Mine Project and the Lupin gold mine. As these mines are located in remote locations, an all-season route is not feasible and delivering supplies by air is extremely costly. Therefore, the TCWR provides the only economical method of supplying these mines. However, because the majority (85%) of the TCWR traverses frozen lakes, late freezing or early thawing of these lakes can drastically shorten the transportation season, imparting significant economic consequences on mining operations. This climate vulnerability was demonstrated in 2006, when a warm and stormy winter season associated with an El Niño Southern Oscillation (ENSO) event resulted in a significant and costly reduction of shipments to the mines. Such unusually warm temperatures may become even more prevalent, as climate predictions suggest a warming trend

in northern latitudes of 1-2ºC over the next few decades (IPCC AR4 WGI, 2007). The TCWR therefore faces a very uncertain future, despite the fact that its use is likely to increase in the coming years due to the potential addition of the Gahcho Kue diamond mine. Because the mining industry in this region is important to the economic health of the Northwest Territories and Nunavut, it is prudent for planners and policy makers to address these concerns. Strategic decisions must be made regarding the future of the road, such as the possible need to create an all-season road, or delivering supplies by sea or even by dirigible (Prentice and Thomson, 2004). Such important decisions can only be made reliably with a strong understanding of the future viability of the TCWR, and this will require the most accurate near-term climate predictions possible. These predictions can only be provided through a detailed and comprehensive understanding of recent past climate variability in the Northwest Territories and Nunavut.

Previous research has been valuable in gaining a broad understanding of regional long-term climate change in northern Canada. However, the number of studies conducted in the region in which the TCWR operates (central Northwest Territories) has been limited. Additionally, no research in the region has provided a climate record with a resolution high enough to identify medium- to short-term climate phenomena, such as sub-decadal ENSO cycles, or the decadal-scale Pacific Decadal Oscillation [PDO]) which have been shown to be present in the region (Bonsal et al., 2001; Labrecque et al., 2009; Pisaric et al., 2009).

1.1. Project Description

To address this research gap, an NSERC strategic grant-funded project, termed the "Paleoclimatological Assessment of the Central Northwest Territories: Implications for the Long-Term Viability of the Tibbitt to Contwoyto Winter Ice Road" Project (PANWT) was created in order to develop a high-resolution paleoclimate reconstruction for this region of the

NWT (Galloway et al., 2010; Macumber et al., 2011). The PANWT covers an area of the central Northwest Territories from near the border with Alberta (60.46° N) to Nunavut (65.38° N; fig. 1). This large latitudinal gradient extends through four ecoclimatic regions (Strong et al., 1989). Currently, 115 lakes have been sampled for water and lake sediment, both along and below the TCWR. In addition, lake sediment core samples have been taken from 12 of these lakes. Numerous researchers are currently conducting paleoclimate investigations with these cores at extremely high resolution using many different proxies, such as diatoms, thecamoebians, chironomids, and pollen. The PANWT is an ongoing project and the number of lakes and samples collected will only continue to expand. This data will be used to determine climate trends and cycles which have affected the region over its recent history, and will form the baseline for climate variability used in future climate models.

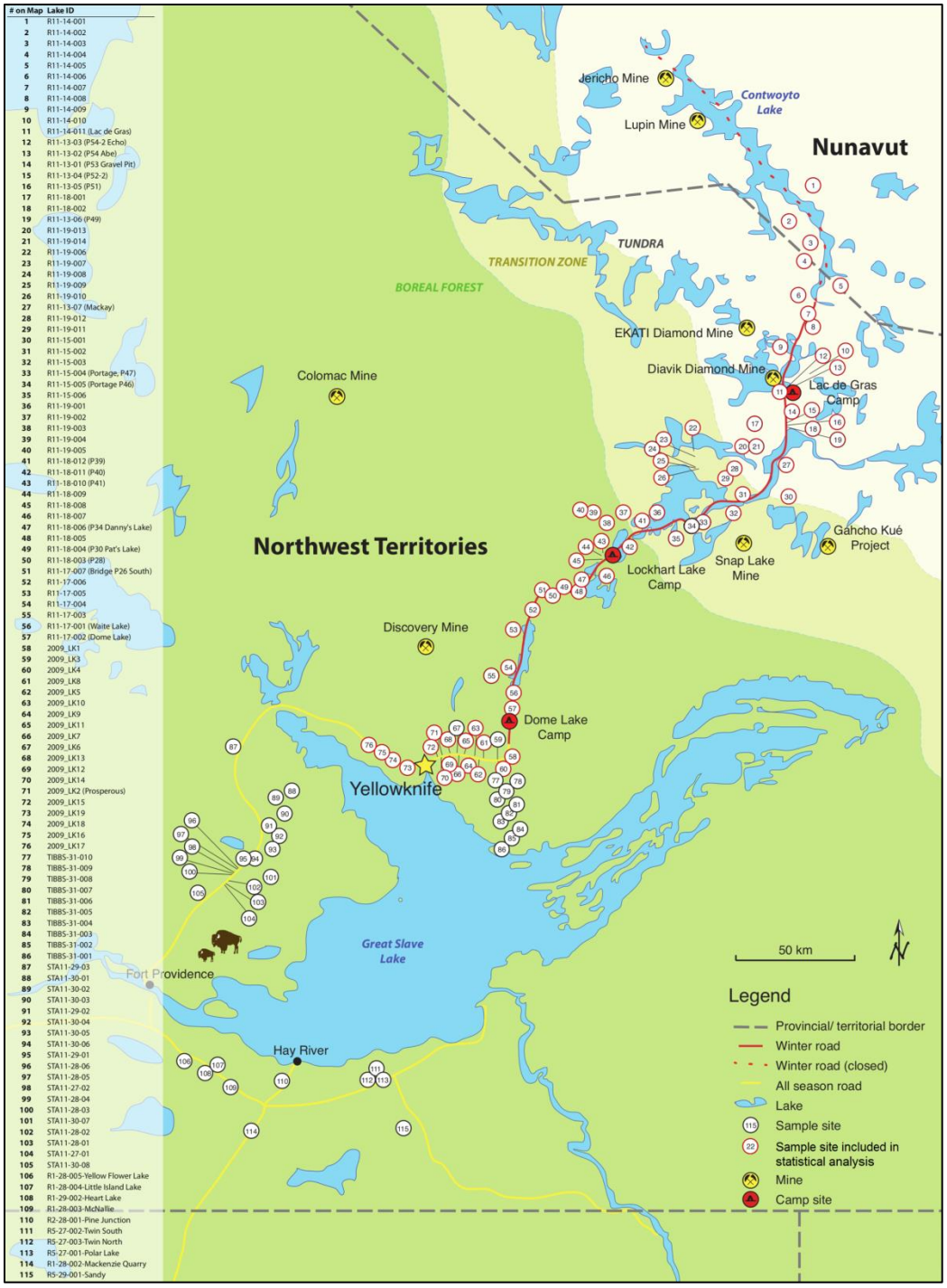

Figure 1. The study area, covering much of the Northwest Territories and a small part of Nunavut. Sample names and locations are shown, in which some or all of water, sediment, glew core and freeze core samples were taken. *Map modified from Carley Crann.*

1.2. Objectives

First, a modern lake survey will be completed in order to gain insight into important environmental changes across a varying climate over geographic space, as a tool for helping to interpret how down-core isotopic changes could relate to real-world environmental changes over time.

Second, a low-resolution (1 cm) carbon and nitrogen bulk sediment isotopic analysis of cores from two lakes will provide data which, in conjunction with grain size and pollen proxies, will be used to reconstruct the Holocene paleoclimate history for these regions. Carbon and nitrogen isotopes are useful because they can identify alterations in the relative amounts of input from various sources such as catchment soils and the atmosphere, as well as within-lake processes such as photosynthesis and respiration. Due to the complex nature of lake systems, multiple processes may alter isotopic values in the same way; however, when used in combination with other proxies, and with an adequate understanding of the physical environment, specific processes can often be determined using isotopes. Comparison of paleoclimate results for these two lakes allows for an indication of pervasive regional-scale environmental changes vs. local fluctuations throughout the Holocene.

Third, sections of Danny's Lake will be observed in higher detail (up to 2.5 mm) in order to discern short-term climate cycles and trends. These results will be compared with other regional high-resolution climate records in order to attribute a driving mechanism to climate variations in the region. Such analysis will be useful for climate models of the region which may allow for a greater ability to predict near-term future climate trends.

2. Background

2.1. Climate History

The Precambian Shield region of the Northwest Territories and Nunavut contains sedimentary deposits from as far back as the end of the most recent (Wisconsinan) glaciation, which retreated from most of the area within these territories approximately 10,000 yr BP (Dyke and Prest, 1987). These sediments have been slowly accumulating since that time in lakes and bogs with relatively little disturbance. As such, many of these deposits have been found to contain a continuous Holocene record of climatic and environmental variability.

2.1.1. Regional

2.1.1.1. Central Northwest Territories

The central Northwest Territories region encompasses Great Slave Lake and the area surrounding it, in particular the area north of Great Slave Lake where the forest-tundra boundary occurs. Previous research in this area is of particular importance to understanding expected local paleoclimate history for the current study, as the study is located within this region.

The earliest paleoclimate study in central Northwest Territories is by Sorenson (1977), who used paleopodzols for evidence of past northerly tree line extensions, and fossil frost-wedge polygons as evidence of southerly tree line extensions, at sites around Great Slave Lake. The study does not constrain any ages for the area, but gives a minimum past tree line fluctuation of 100 km north and 30 km south of its current location.

Further research was not completed until Moser and MacDonald (1990), who conducted a paleolimnological study of pollen in cores from two lakes (Queens Lake and McMaster Lake), just north of the tree line above Great Slave Lake. Their results suggest a northward tree line movement at 5000 yr BP and a southward tree line movement at 3500 yr BP. The Queens Lake

core was later analysed in greater detail for pollen, diatoms, organic content using Loss-On-Ignition (LOI), geochemistry, and ^{13}C and ^{18}O isotopes (MacDonald et al., 1993). While there is much fluctuation in the data, there is a clear trend across all proxies from 5000 – 4000 yr BP. Specifically, pollen indicates a northerly tree line shift, ^{18}O suggests an increase in precipitation, and diatoms, organic content, geochemistry and $\delta^{13}C$ all point to an increase in productivity. The same study also analysed pollen and organic content in cores from three other nearby lakes (McMaster Lake, Toronto Lake and Waterloo Lake) in conjunction with Queens Lake, and provided similar results, with the inclusion of an apparent secondary tree line advance and retreat at Toronto Lake around 2500 yr BP.

Wolfe et al. (1996) analysed the Toronto Lake core for ^{13}C isotopes in cellulose and bulk carbon, as well as ^{18}O isotopes in cellulose. The use of isotopes in cellulose minimizes the effects of contamination from catchment material, allowing for a purely lake-derived signal (Wolfe et al., 1996). Results of analysis of $\delta^{13}C$ from bulk carbon and cellulose proved to be extremely similar, suggesting very low catchment contamination. Depletion spikes in ^{18}O correlated fairly well with enrichment spikes in organic content (LOI) and pollen (*Picea mariana*), and were interpreted as a change to open-basin hydrological conditions during a warmer, high-productivity climate. The period from 5000-2500 yr BP contained the greatest number of depletion spikes, with the strongest spikes occurring at 5000, 4500, and 2400 yr BP. In contrast, $\delta^{13}C$ values did not correlate well with productivity increases, which the authors suggested may be due to 'flushing' of the lake during open-basin hydrological conditions, enhancing catchment-derived input of ^{13}C-depleted CO_2 into the dissolved inorganic carbon (DIC) pool of the lake.

Pienitz et al. (1999) analysed diatoms in the Queens Lake and Toronto Lake cores as an indicator of paleoclimate. A diatom-based transfer function was used which had been previously created

using 22 calibration lakes between Yellowknife and Contwoyto Lake (Pienitz and Smol, 1993). The transfer function linked diatom populations with dissolved organic carbon (DOC) levels in lakes. In Queens and Toronto Lakes, profound shifts in diatom populations and associated changes in DOC occurred from 5000-3000 yr BP, suggesting a warm, humid climate with increased productivity and a change from tundra to a forested environment during this time.

Pollen and organic content (LOI) analysis of a core from a new nearby site (UCLA Lake) was completed by Huang et al. (2004). Biostratigraphic zones were determined on the basis of changes in pollen assemblage, and, based on these zones, tree line was determined to have advanced at 6300 cal yr BP and retreated again at 3000 cal yr BP. The timing of tree line advancement for this site is noticeably earlier than similar nearby sites, which the authors hypothesize may be due to differences in local soil conditions.

Additional diatom analysis was completed on a core from Slipper Lake, in a slightly more northerly location (Ruhland and Smol, 2005). Biostratigraphic zones were computationally determined through cluster analysis of the diatom assemblage. Minor species changes attributed to colder conditions occurs at around 3000-4000 cal yr BP. However, the main focus of this study was on the most recent period of time, for which there is a large increase in planktonic diatom taxa over the past 200 years. This change is more dramatic than any other seen throughout the core, and is attributed to longer ice-free periods due to increasing temperature.

MacDonald et al. (2009) analyzed a core from Lake S41, located near Toronto Lake, focusing on the most recent 2000 years at a resolution of 0.5 cm (30-50 years per interval). Proxies analysed include biogenic silica (BSi) and organic content as indicators of productivity, and chironomids as a direct indicator of temperature. Results were compared with a northern hemisphere annual temperature reconstruction based off of tree rings, ice cores, and lake and ocean sediments

(Moberg et al., 2005). BSi and organic content were found to correlate well with each other and the temperature reconstruction, showing higher productivity during the medieval warm period, a reduction during the Little Ice Age, and a strong increase again over the last 300 years. Chironomids, however, did not show any apparent correlations with the other proxies or the temperature reconstruction.

The most recent study in the region was by Paul et al. (2010), who completed a diatom analysis of a core from Lake TK-2, located less than 100 km NE of Toronto Lake. Biostratigraphic zones were computationally determined through cluster analysis, similar to Ruhland and Smol (2005). Species abundances near the bottom of the core indicate that temperatures from 9000-8850 cal yr BP may have been surprisingly high, in contrast to records from similar studies in the region. From 8850-7000 cal yr BP, species abundances reflect more typically colder temperatures, with a possible warm episode around 8200 cal yr BP which may correlate with Greenland ice core records (Alley et al., 1997). From 7000 cal yr BP onward, much warmer temperatures are inferred, without much variance until recent times. A dramatic species abundance shift over the last 200 years indicates greatly warming temperatures in recent times.

Overall, previous studies in the central Northwest Territories region are in general agreement with a northward tree line shift at around 5000 yr BP, followed by a retreat at around 3000 yr BP. Differences in this timing can be noted in MacDonald et al. (1993), who found the retreat to occur at 4000 yr BP (uncalibrated), and Huang et al. (2004), who determined the advancement to occur at 6300 cal yr BP. Additionally, MacDonald et al. (1993) and Wolfe et al. (1996) found evidence of a secondary tree line advance and retreat at around 2500 yr BP (uncalibrated) in the Toronto Lake core. Lastly, it should be noted that Paul et al. (2010) did not see the excursion at all, except for a warming at around 7000 cal yr BP. This is likely because the location of the

studied lake is geographically too far northeast to have been greatly affected by a northward migration of the Arctic air front (Paul et al., 2010). Much of the discrepancies between these studies may be due to earlier research using uncalibrated dates.

Extracting useful paleoclimate information in terms of more recent, small-scale variability is difficult, due to the low sampling resolution of these studies. Some of the higher-resolution studies, such as Ruhland and Smol (2005), MacDonald et al. (2009) and Paul et al. (2010) provide hints of a possible Medieval Warm Period and Little Ice Age, although a higher sampling resolution is required to provide greater certainty. However, numerous studies did show clear evidence of a dramatic increase in productivity/temperature from around 150 cal yr BP to present (Ruhland and Smol, 2005; MacDonald et al., 2009; Paul et al., 2010).

2.1.1.2. Pacific Decadal Oscillation

While high-resolution paleoclimate information is scarce, there is evidence that short-term climate patterns in this region are largely controlled by the Pacific Decadal Oscillation (PDO), as shown from instrumental climate records (Bonsal et al., 2001), tree-ring studies (Pisaric et al., 2009), and satellite photo lake surface reconstructions (Labrecque et al., 2009).

The PDO is a decadal-scale oscillation in climate centered in the North Pacific, affecting climate throughout much of North America and Asia. It is defined by Park et al. (2012) as the first empirical orthogonal function mode of the North Pacific sea surface temperature anomalies. The state of the PDO is measured by the PDO Index, which is a measure of the average North Pacific sea surface temperature (SST; Hare, 1995; Zhang, 1996; Mantua et al., 1997). When the SST is anomalously high (low), the PDO is in a "positive" ("negative") phase.

2.1.1.2.1. Causes

The mechanics behind the PDO appear to be fairly complex and likely involve many different contributing factors. A clear contributing factor is the tropical ENSO cycle, which has been linked to the PDO through correlations in the instrumental climate record (Trenberth and Hurrell, 1994; Bonsal et al., 2001), as well as with climate modelling (Luksch et al., 1990; Lau and Nath, 1990; Alexander, 1992; Alexander et al., 2002). This connection is hypothesized to be due to the "atmospheric bridge", in which decadal-scale variations in North Pacific SST and sea level pressure (SLP) are caused by atmospheric alterations originating from the tropical ENSO (Alexander et al., 2002). During El Nino events, the anomalously warm tropical SST causes an increased heat flux to the atmosphere, generating Rossby Waves which circle the northern hemisphere as they oscillate from tropics to pole. These waves have a far-reaching effect on many atmospheric phenomena, including an intensification and southeasterly movement of the Aleutian Low (AL), which is a low-pressure system centered over the central North Pacific. The result is a strong, cold northwesterly wind in the central North Pacific, causing a reduced SST due to strengthened evaporative cooling, heat flux and Eckman transport advection; and an enhanced warm southwesterly wind near the Pacific North American coast, causing an increased SST through heat flux and Eckman transport advection (Park et al., 2012).

The western North Pacific, however, is more indirectly affected by these processes. Coupled General Circulation Models (CGCMs) indicate that SST in this region is greatly affected by decadal-scale variability of the Kuroshio Extension (KE; Pierce et al., 2001; Schneider et al., 2002; Wu et al., 2003; Kwon and Deser, 2007). Movement and intensification of the AL causes a strengthening and westerly movement of these Rossby waves through Eckman transport, which allows strengthened winds to reach and affect the Kuroshio Extension (Miller and Schneider,

2000; Miller et al., 2004; Taguchi et al., 2007). The KE is influenced by these winds due to its dynamic instability. In addition, these variations in Rossby waves result in an oscillation of the North Pacific Gyre from east to west, which also impacts the KE (Ceballos et al., 2009). The result is an alteration of current path and vertical mixing depth, causing a large SST variance which affects the entire western North Pacific. This SST response is generally consistent with, although lagged by a few years from, the SST variations observed in the eastern North Pacific (Miller et al., 2004).

2.1.1.2.2. Effects

The effects of the PDO can be clearly seen in the instrumental climate record (Trenberth and Hurrell, 1994; Mantua et al., 1997; Bonsal et al., 2001; Mantua and Hare, 2002). A positive PDO index, with anomalously high North Pacific SST, results in unusually wet conditions along the Gulf of Alaska and southwestern U.S. and Mexico, while unusually dry conditions predominate in interior Alaska and southern Canada from the Rockies to the Great Lakes. A positive index also results in unusually warm temperatures appearing most prominently in northwestern Canada and along the Pacific coast of the U.S., with further warming throughout western Canada; anomalous cooling occurs in southeastern U.S. and Mexico. During a negative PDO phase, these precipitation and temperature anomalies are reversed.

Tree ring records along coastal Alaska (Wiles et al., 1998; D'Arrigo et al., 2001) and California (Haston and Michaelson, 1994; Biondi et al., 2001; MacDonald and Case, 2005) also suggest a prominent role of the PDO in precipitation variations in these areas. Tree ring records within the continental interior of western Canada also display evidence of a PDO effect (MacDonald and Case, 2005).

2.1.1.2.3. Cyclicity

Numerous studies have used instrumental records, climate proxies and climate models to investigate the cyclicity of the PDO. The most obvious evidence of climate cyclicity is a stepwise shift in climate seen from instrumental data as well as salmon catches in North America in 1925, 1946-47, and 1976-77, indicating a 20-30 year oscillation (Mantua et al., 1997). A 20-year oscillation has also been reproduced by Latif and Barnett (1994; 1996), who used climate records on a coupled ocean-atmosphere climate model to reconstruct climate back to 1860. 19-23 year cycles have been seen in numerous tree ring records from Alaska down to California going back as far as 1600 AD (Biondi et al., 2001; Wiles et al., 1998; Gedalof and Smith, 2001). Similarly, Haston and Michaelsen (1994) found a 20-50 periodicity in Californian coastal tree rings going back 600 years. Perhaps most significantly, both Chao (2000) and Minobe (2000) found a 15-20 and 33-year cycle (respectively) on North Pacific SST since 1900.

A prominent 50-70 year cycle is also evident in some records. Both Chao and Minobe, in their aforementioned SST analysis, found indications of a cyclicity in this range. Additionally, this cycle has been seen over approximately the last 200 years in tree ring records and historical data from both North America (Minobe, 1997; Biondi et al., 2001; MacDonald and Case, 2005) and China (Shen et al., 2006). Cyclicity at this scale becomes weak or spurious prior to 1800 (Biondi et al., 2001; MacDonald and Case, 2005; Shen et al., 2006), although Shen et al. (2006) found a significant 75-115 year peak in eastern China previous to 1850, which they suggest may be caused by a Gleissberg cycle solar forcing.

2.1.2. Canada-Wide

2.1.2.1. Mainland Nunavut

The earliest paleoclimate investigations in this region involved using charcoal in paleosols as indicators of past forest fires, as well as paleosol morphology as an indicator of a transition between forest and tundra, in the Ennadai and Dubawnt Lake regions approximately 370 km W of the western shore of Hudson Bay (Bryson et al., 1965; Sorenson et al., 1971). These studies provided hints at movements in tree line and thus, climate changes in this region through the Holocene. Radiocarbon dating of the charcoal allowed for some rough estimates of the timing of tree line movement, and suggested a major tree line transgression of at least 280 km north of current tree line around 5500 yr BP, followed by a southward transgression around 3500 yr BP, and a series of smaller northward and southward transgressions up to present. These movements were hypothesized to be caused by changes in the position of the Arctic air mass front. The results of these studies were largely corroborated with further investigations of pollen analysis on peat profiles from the same area (Nichols, 1970; Kay, 1979).

2.1.2.2. Northeast Pacific Margin

Substantial research has been conducted on the northwestern coastal region of North America, within Alaska, Yukon and northern British Columbia. Much of this area was at the western edge of the Laurentide ice sheet during glacial maxima and therefore experienced deglaciation around 13000-12000 yr BP (Dyke, 2004), significantly earlier than most other regions of Canada. Various studies indicate significant climate changes occurring at both 7500 and 4000 yr BP, allowing the paleoclimate history of the northeast Pacific Margin to be divided into three parts: early Holocene (12000-7500 yr BP), middle Holocene (7500-4000 yr BP) and late Holocene (4000 yr BP-present).

The early Holocene paleoclimate was most likely warmer than today (Heusser et al., 1985), in addition to being highly arid prior to 12500 cal yr BP (Abbott et al., 2000). Wetter conditions began in interior Alaska around 13000-12000 cal BP (Edwards and Barker, 1994; Abbott et al., 2000, Mann et al., 2002), and intensified and spread to Yukon and the Mackenzie Delta region around 11000-9000 cal BP, in conjunction with an advancement of the tree line at this time (Ritchie, 1984; Spear, 1993; Abbott et al., 2000; Anderson et al., 2005).

A shift in climate at around 7500 yr BP marks the beginning of the middle Holocene. Lake level reconstructions and pollen changes indicate a colder (Lauriol et al., 2009) and drier climate (Heusser et al., 1985; Anderson et al., 2005). A reduction in snow accumulation in the alpine zone during this time also hints at a drier climate (Farnell et al., 2004). This climate shift resulted in a southward migration of the tree line (Ritchie, 1984; Spear, 1993). While a drier climate is evident in most research, it should be noted that Pienitz et al. (2000) and Lauriol et al. (2009) actually found the opposite to be true in central Yukon.

The late Holocene began around 4000 yr BP, with a shift to cooler, wetter conditions which are similar to those we find today. This transition appears to have occurred more or less congruently across Alaska, Yukon and the Mackenzie Delta, as indicated by various proxies such as ^{18}O (Anderson et al., 2007; Clegg and Hu, 2010), pollen, geochemistry and carbon/nitrogen measurements (Abbott et al., 2000; Anderson et al., 2005). It should be noted that some studies, such as Lauriol et al. (2009), found this climate transition to be towards cooler and drier conditions. This transition was accompanied by a shift in tree line to a more southward location (Spear, 1993).

Lastly, a number of records indicate a clear 20th century excursion in ^{18}O which indicates an extreme period of recent aridity (Anderson et al., 2007; Clegg and Hu, 2010).

2.1.2.3. High Arctic

The high arctic of Canada has seen the greatest number of Holocene climate studies using lake sediments, due to the fact that this region experiences a high sensitivity to climate variations and is thus ideal for observing such changes. The great majority of studies use diatom analysis, as this proxy has proven to be a clear and highly sensitive indicator of climate in this environment (Smol, 1983). Smaller numbers of other proxies such as pollen and chironomids are also present.

The early Holocene appears to have been significantly warmer than today. This is aptly demonstrated by the melt layers of an ice core from Agassiz Ice Cap on NW Ellesmere Island, which indicates a peak warmth around 12000-11000 cal yr BP, and elevated but slowly cooling temperatures up to around 6500 cal yr BP (Fisher and Koerner, 2003). This early warm phase is corroborated by a number of lake sediment studies (Briner et al., 2006; Finkelstein and Gajewski, 2008), although most of these lake studies do not extend to the earliest Holocene period. A large number of these studies do suggest a warmer period prior to around 4000 cal yr BP, followed by a sudden cooling trend generally lasting up to present (Smol, 1983; Zabenskie and Gajewski, 2007; Finkelstein and Gajewski, 2008; Rolland et al., 2008; Adams and Finkelstein, 2010). Additionally, many of these studies also see evidence of a Medieval Warm Period generally occurring around 1000-600 cal yr BP and a Little Ice Age occurring around 800-150 cal yr BP (Wolfe, 2002; Finkelstein and Gajewski, 2007; Podritske and Gajewski, 2007; Peros and Gajewski, 2009; Rolland et al., 2009; Adams and Finkelstein, 2010). A 20^{th} century warming period is also abundantly clear in many records (Wolfe, 2002; Adams and Finkelstein, 2010; Perren et al., 2003; Douglas et al., 1994; Michelluti et al., 2003; Zabenskie and Gajewski, 2007; Finkelstein and Gajewski, 2007; Finkelstein and Gajewski, 2008; Peros and Gajewski, 2009; Podritske and Gajewski, 2007; Lim et al., 2008).

A synthesis of climate records throughout Canada for the Holocene period shows a consistent story for the whole region. At its greatest extent at 18000 yr BP, the Laurentide Ice Sheet (LIS) covered all of Canada except for parts of Yukon (Dyke, 2004). The LIS began to recede due to higher summer insolation resulting from increasingly optimal alignment of precessional Milankovitch forcing (Berger and Loutre, 1991). By 11000 yr BP much of western Canada was deglaciated and experiencing some of the warmest temperatures ever seen during the Holocene. This period, known as the Holocene Thermal Maximum (HTM), would last until around 5000-4000 yr BP, although the later part of this period experienced cooling temperatures due to a weakening precessional forcing (Berger and Loutre, 1991). In central and eastern Canada, where the LIS was present up to 10000-8000 yr BP, the HTM was delayed due to the cooling effect of the ice sheet (Kaufman et al., 2004), which may have maintained the boundary of the Arctic air mass at a more southerly location (Bryson et al., 1965). These regions did not experience warming until around 6000-5000 yr BP, far later than western Canada. Finally, in all regions of Canada, the Neoglacial period occurred around 4000-3000 yr BP, resulting in a rapid and significant reduction in temperature. This climate remained to the present day, although minor fluctuations such as the Medieval Warm Period and the Little Ice Age are evident in some records from Arctic Canada. Lastly, a significant 20th century increase in temperature and aridity is seen in climate records across Canada, especially the arctic.

2.2. The Carbon Cycle

^{13}C has been used worldwide as a tracer of variations in the carbon cycle within lakes and their catchment. The isotopic signature of organic carbon in lakes can undergo distinct changes as aspects of the carbon cycle shift in response to climate. Factors influencing these isotopic variations depend on whether the source of organic matter is aquatic or terrestrial. Aquatic

sources of organic carbon accumulate in lake bottom sediments from sinking organic matter derived from photosynthetic algae and macrophytes, while terrestrial organic matter accumulates in lake bottom sediments from the catchment after being flushed into the lake through surface runoff or wind processes. It is crucial to determine the relative inputs of each of these components in order to properly understand the underlying causes of isotopic variation. Traditionally, organic matter origins have been quantified by the ratio of %C to %N in the sediment (C/N ratio). Aquatic vegetation contains a greater amount of nitrogen than terrestrial vegetation, so the C/N ratio of organic sediments derived from aquatic matter is generally much lower (<10) than sediments derived from terrestrial matter (>20; Meyers, 1994). Therefore, the C/N ratio can give a good quantitative estimate of the amount of algal vs. terrestrial input into a lake system, and has proven to be highly useful for this purpose in previous studies.

The relative and absolute contributions of aquatic and terrestrial organic matter in lake sediments can be affected by a variety of within-lake and catchment processes. Wolfe et al. (1999) showed that the C/N profile of a lake near the treeline in Siberia appears to have been mainly affected by changes from within the lake catchment. Specifically, the C/N ratio was higher during forest conditions than tundra conditions, due to the relatively increased biomass and wetter conditions of the forest environment. Alternatively, C/N ratio can also be an indicator of largely within-lake processes. Briner et al. (2006) found that on Baffin Island, where little terrestrial vegetation is present, variations in C/N ratio are likely due exclusively to variations in populations of different aquatic species. Brenner et al. (1999) and Frost et al. (2002) showed that C/N ratio can be an indicator of nutrient and trophic levels within the lake.

Numerous studies have also shown that varying lake levels can affect the C/N ratio. In these cases, during shallow periods, the lake is smaller and thus more susceptible to the influence of

catchment vegetation, while at times of deeper lake level, the lake is larger and aquatic vegetation has a greater influence on the sediments (Krishnamurthy et al., 1986; Haberzettl et al., 2005; Morrill et al., 2006; Conroy et al., 2008).

It has also been shown that variations in the C/N ratio can at least partially be the result of diagenesis. In particular, preferential decomposition of the nitrogen component of organic matter can result in an increased C/N ratio in those sections of the profile which have undergone the greatest decomposition (Stevenson and Cheng, 1971; Sampei and Matsumoto, 2001).

Once the source of organic sedimentation has been determined, $\delta^{13}C$ values within the sediments can further decipher the carbon cycle history of the lake and its catchment. In aquatically derived sediments, photosynthetic algae extract carbon from the dissolved inorganic carbon (DIC) pool of the lake into its organic structure. The resultant $\delta^{13}C$ values of aquatically sourced organic carbon closely reflect that of the DIC pool. The DIC pool itself has traditionally been considered to be most greatly affected by photosynthesis and respiration (McKenzie, 1985). Photosynthetic algae preferentially take in the lighter ^{12}C isotope from the DIC pool, and as such can actually deplete this pool of ^{12}C. Greater photosynthetic productivity will enhance this process, resulting in a DIC pool more enriched in ^{13}C, which will then be reflected in the organic carbon. Such productivity-driven ^{13}C enrichments are proposed as a cause for some of the $\delta^{13}C$ variation seen in Queens Lake (MacDonald et al., 1993) and Toronto Lake (Wolfe et al., 1996). In these lakes, enrichment in ^{13}C is associated with increased organic content and tree line advancement, suggesting that increased productivity is caused by warmer and wetter climate conditions. However, both MacDonald et al. (1993) and Wolfe et al. (1996) have found that the main component of $\delta^{13}C$ variation can be due to factors other than productivity.

Changes in lake meromixis can also often affect levels of productivity. For example, Schelske and Hodell (1991) and Hodell and Schelske (1998) found that $\delta^{13}C$ values in Lake Ontario increased dramatically during summer, which they attributed to productivity-driven enrichment in the DIC pool of the epilimnion during summer lake stratification. $\delta^{13}C$ values dropped dramatically in early summer and fall, however, due to mixing with the ^{13}C-depleted DIC pool of the hyperlimnion. However, O'Reilly et al. (2003) found the opposite effect for Lake Tanganyika in Africa. Recorded measurements at the lake going back to 1950 show an increase in temperature and a reduction in wind speed, both of which should cause an increase in lake stratification. Meanwhile, sediments of the lake record a $\delta^{13}C$ depletion during this time. It is hypothesized that lake mixing allows the upwelling of nutrients important to photosynthetic algae, so an increase in lake stratification reduces nutrient availability and in turn productivity, resulting in a $\delta^{13}C$ depletion.

Acting in opposition to photosynthesis is respiration, in which bacteria will oxidize organic matter within the lake or in lake bottom sediments, releasing CO_2 back into the DIC pool (Clark and Fritz, 1997). In aerobic environments, this process takes place using oxygen as the oxidizing agent to reduce organic matter and produce CO_2. This process preferentially fractionates ^{12}C, thereby enriching the DIC pool in this lighter isotope. Even in environments without oxygen, often because it was used up during aerobic respiration, other electron acceptors, if present, can still act as the oxidizing agent for respiration. For example, respiration is proposed as the dominant factor affecting $\delta^{13}C$ values in Queens Lake (MacDonald et al., 1993). $\delta^{13}C$ values in the sediments of this lake average -24‰, which is significantly enriched compared to average values in similar environments (-27‰ or -28‰; Wolfe et al., 1996; Wolfe et al., 1999; Wolfe et al., 2003). This signature is likely caused by preferential extraction of ^{12}C from the sediments

during decomposition by respiring organisms. Additionally, $\delta^{13}C$ values decrease up the profile, likely caused by a DIC pool which is becoming increasingly ^{13}C-depleted due to the continual addition of ^{12}C-enriched CO_2 by respiring organisms. In anaerobic environments with no other oxidizing agent, respiration cannot occur; rather, organic matter is often decomposed by methanogenic bacteria through the process of reduction (Clark and Fritz, 1997). This reaction fractionates ^{12}C into CO_2 even more strongly than respiration, resulting in a depleted DIC pool and thus having an effect on accumulating organic matter sediment values. Galand et al. (2010) was able to discern not just methanogenesis, but the relative rate of different methanogenic pathways, using $\delta^{13}C$ values measured from peatlands in Finland.

Respiration often occurs in the hyperlimnion during lake stratification. In the Yukon, for example, summer lake stratification may cause both an enrichment of ^{13}C in the epilimnion due to photosynthesis, and a depletion of ^{13}C in the hyperlimnion due to respiration (Anderson et al., 2007). Before and after summer, lake mixing occurs which merges the DIC pool of both layers into a single pool with an intermediate value. This process results in enriched $\delta^{13}C$ values of deposited organic matter during mid-summer when stratification is present, and depleted values during early summer and fall when mixing occurs. This is similar to previously mentioned findings by Schelske and Hodell (1991) and Hodell and Schelske (1998).

While photosynthesis and respiration have traditionally been considered the dominant processes controlling the ^{13}C isotopic composition of lake sediment organic matter, Wolfe et al. (1996) were able to demonstrate that changing hydrological conditions were the primary factor affecting $\delta^{13}C$ values in Toronto Lake. They used changes in $\delta^{18}O$ of lake sediment cellulose to show that the lake has switched numerous times between hydrologically open (short lake water residence time) and closed (long lake water residence time). They also investigated both bulk and

cellulose ^{13}C, and illustrated that times of hydrologically open conditions were closely associated with depleted $\delta^{13}C$ values. It was suggested that enhanced precipitation during hydrologically open conditions resulted in a 'flushing' of ^{13}C-enriched lake water DIC with DIC from the catchment which was much more depleted in ^{13}C. DIC from the catchment is depleted in ^{13}C because it is derived from soil CO_2 through a weathering reaction with silicate or carbonate minerals (Aravena et al., 1992; Clark and Fritz, 1997). This soil CO_2 is ultimately derived from catchment vegetation, which is also depleted in ^{13}C, having preferentially fractionated ^{12}C from the atmosphere during photosynthesis (Clark and Fritz, 1997). While DIC derived from carbonate weathering may substantially enrich DIC $\delta^{13}C$ values due to fractionation, DIC from catchments in the Canadian Shield tend to be almost exclusively derived from silicate weathering, and this silicate weathering process only enriches DIC $\delta^{13}C$ values by about 1‰. However, during times of hydrologically closed conditions, input of this ^{13}C-depleted DIC from the catchment is reduced, and the primary source of DIC is direct CO_2 exchange of the lake with the atmosphere. Relative to catchment DIC, the atmospheric source is far more enriched in ^{13}C because there is no process of fractionation through photosynthesis. Additionally, hydrologically closed conditions increase the residence time of available lake water DIC, allowing more time for algae to fractionate out the lighter ^{12}C isotope. The combined result is a much more enriched DIC pool in the lake during times of a hydrologically closed basin.

The association between organic matter $\delta^{13}C$ and hydrological conditions was further demonstrated by Wolfe et al. (1999) and Wolfe et al. (2003) at sites near the tree line in Siberia, with similar causes being proposed. These studies also suggest that ^{13}C tends to be more depleted in forested catchments as opposed to tundra catchments, due to higher vegetation mass and therefore greater soil decomposition within the catchment. This effect is often coupled with

and accentuates the effect on $\delta^{13}C$ from hydrological changes, due to the fact that a forested environment is generally associated with a wetter climate than a tundra environment. Aside from Wolfe et al. (1996; 1999; 2003), studies from other regions have also found this hydrological effect on $\delta^{13}C$ (Li and Ku, 1997; MacDonald et al., 2008).

$\delta^{13}C$ compositions in terrestrially-derived organic sedimentation are determined by the isotopic composition of the source vegetation within the catchment. While average values for catchment vegetation generally remain consistent, drastic changes in certain types of vegetation can significantly alter this value. For example, Talbot and Livingstone (1989) found $\delta^{13}C$ variations in organic lake sediments from Lake Victoria in East Africa, which they partially attributed to changes in the amounts of C3 and C4 plants in the catchment. Because C4 plants use a different carbon fixation pathway during photosynthesis than C3 plants do, they acquire a much more enriched $\delta^{13}C$ composition (-16‰ to -10‰) than C3 plants (-33‰ to -24‰). However, C4 plants are generally only found in hot and dry environments, so would be unlikely to have been present in the current study area at any time during the Holocene.

A more likely scenario in the current study area would be an influence in $\delta^{13}C$ values from macrophyte plants. This is because macrophytic plants tend to have more enriched $\delta^{13}C$ values than either phytoplankton or terrestrial vegetation, due to active uptake of ^{13}C-enriched HCO_3 from the DIC pool rather than CO_2 (Sand-Jensen and Borum, 1991). HCO_3 is more enriched in ^{13}C than CO_2 because the exchange reaction between the two species has a fractionation which favors ^{13}C in HCO_3. As an example, Krishnamurthy et al. (1986) suggested that changes in macrophyte content for Karewa Lake in India may have been affecting the $\delta^{13}C$ profile of the organic lake sediments.

2.3. The Nitrogen Cycle

The nitrogen cycle is much more complicated than the carbon cycle, and as such, environmental interpretations of lake sediment $\delta^{15}N$ records have proven to be difficult to decipher. Additionally, changes in nitrogen values have not been extensively studied and natural variations are therefore poorly understood. There are usually a multitude of possible causes for variations in $\delta^{15}N$ values; however, if other proxies can eliminate certain scenarios, then ^{15}N can be a powerful tool in determining precise environmental processes occurring in the lake.

Much like the carbon cycle, organic nitrogen in lake sediment can be derived from either terrestrial or lacustrine sources. However, because terrestrial plants have much less nitrogen content than aquatic plants, $\delta^{15}N$ values of direct terrestrial organic nitrogen input to lake sediments are not often a major contributor to overall sediment $\delta^{15}N$ values (Talbot, 2001). However, Letolle (1980) does show that $\delta^{15}N$ values for terrestrial material is generally lower than for aquatic plants, and Muzuka et al. (2004) and Watanabe et al. (2004) at least partially attributed a $\delta^{15}N$ depletion to an increase in catchment vegetation input for lakes they studied. Lacustrine deposits are sourced from aquatic plants and cyanobacteria, whose $\delta^{15}N$ values are dependent upon that of the dissolved inorganic nitrogen (DIN) and dissolved organic nitrogen (DON) within the lake. External inputs to lake water DIN and DON include both the catchment and the atmosphere, and variations in these inputs are partially responsible for changes in lake water DIN and DON $\delta^{15}N$ values.

From the catchment, surface runoff or groundwater delivers DIN in the form of nitrate, and to a lesser degree, ammonium, while DON is delivered in the form of organic compounds. These inorganic and organic compounds are extracted during decomposition of plant material and soil. This source generally contributes ^{15}N with δ values ranging from around 0 to +10‰ (Kendall,

1998), depending upon the type of plants in the catchment and the level of soil decomposition (greater decomposition produces more enriched $\delta^{15}N$ values). Wolfe et al. (1999; 2003) suggested that changing soil decomposition rates were primary factors in variations of $\delta^{15}N$ for lakes in the Siberian tundra, especially during the transition from a forest to tundra environment.

From the atmosphere, nitrogen can be deposited directly into the lake as DIN and DON through precipitation, or as N_2 through atmospheric exchange with lake water. Atmospheric $\delta^{15}N$ values for DIN and DON range from -6 to +6‰ (Kendall, 1998), and N_2 values are, by definition, 0‰. This N_2 is taken up by cyanobacteria through nitrogen fixation with little fractionation, so $\delta^{15}N$ values for these cyanobacteria are generally very close to 0‰ as well (Heaton, 1986).

While these external inputs can certainly affect lake water DIN and DON values, internal lake processes can have a strong effect as well. Much like the carbon cycle, aquatic plants assimilate nitrogen from the lake water DIN and DON pool, and increased productivity can enrich ^{15}N due to preferred fractionation of ^{14}N out of this pool. Numerous studies attribute ^{15}N enrichment within lake profiles to this process (Beuning et al., 1997).

However, other studies have also shown that when nitrate is not the limiting nutrient, ^{15}N extracted by aquatic plants from the DIC and DOC tends to be depleted due to increased fractionation; however, once algae populations have bloomed to the point that nitrate is limiting, $\delta^{15}N$ values quickly become enriched due to an enrichment of the DIC pool (Francois et al., 1996; Hodell and Schelske, 1998; Pilskaln, 2004). This trend, particularly the enrichment spike, is often seen in recent sediments near human-populated areas due to eutrophication of the lake caused by input of fertilizers or sewage (Hodell and Schelske, 1998).

Additional internal lake processes which can strongly affect $\delta^{15}N$ values often occur in anoxic conditions, such as the hypolimnion of a stratified lake, and can significantly alter the

geochemistry of the lake. Denitrification, for example, preferentially fractionates ^{14}N out of nitrate during reduction into N_2 under anoxic conditions, resulting in ^{15}N-enriched nitrate in the DIN pool. Alternatively, ammonium can build up in the hypolimnion due to a lack of aerobic plants for ammonium assimilation. Chu et al. (2009) suggest that ammonium buildup can cause both a ^{15}N depletion due to increased ammonium assimilation fractionation into organic matter during seasonal mixing events, and a ^{15}N enrichment due to an enrichment of the DIN pool from the abundance of ^{15}N-enriched ammonium. This is a good example of the complex nature of the nitrogen cycle and its tendency to oftentimes "go either way" in terms of $\delta^{15}N$ changes.

Ammonia volatilization is an additional process which can further affect $\delta^{15}N$ values. This process preferentially fractionates ^{14}N out of ammonium during conversion into ammonia, resulting in ^{15}N-enriched ammonium in the DIN pool. This process often occurs in alkaline lakes, such as Lake Bosumtwi, which was interpreted to be alkaline during part of its history due to high $\delta^{15}N$ values combined with the formation of calcite and dolomite (Talbot and Johannessen, 1992).

Both denitrification and ammonia volatilization tend to produce lake sediment $\delta^{15}N$ profiles which vary greatly, often with sharp changes in value. Lake Bosumtwi (Talbot and Johannessen, 1992) is, again, a great example of this. In general, a profile which does not contain sharp $\delta^{15}N$ excursions is an indication of a nitrogen-limited lake without anoxic or high pH conditions, in which the output $\delta^{15}N$ values reflect the input $\delta^{15}N$ values (Leng, 2006).

Outside of changes in lake water DIN and DON, there are a few other factors which can affect sediment $\delta^{15}N$ values. For example, an increase in cyanobacteria abundance can deplete sediment ^{15}N, because cyanobacteria tend to be depleted in ^{15}N themselves relative to algae, due to limited fractionation during nitrogen fixation of atmospheric N_2. $\delta^{15}N$ variations in numerous

lakes have been attributed to this process (Talbot and Johannessen , 1992; Gu et al., 1996; Mukuza et al., 2004).

Also, due to the volatile nature of nitrogen-bearing compounds, diagenesis may also affect sediment $\delta^{15}N$ values, causing enrichment due to preferential removal of ^{14}N. However, it is unclear whether this issue is significant in many cases (Spiker and Hatcher, 1984; Velinsky et al., 1991; McArthur et al., 1992; Meyers, 1994; Hassan et al., 1997).

3. Regional Setting

3.1. Study Area

Although the entire project covers much of the Northwest Territories, the current isotope study covers only the portion which is located within the Precambrian Shield region (fig. 1). The study includes paleolimnological investigations of two lakes, Danny`s Lake and Horseshoe Lake. Danny`s Lake is located 40 km SW of the tree line, at (63°28.547 N, 112°32.25 W), and Horseshoe Lake is located 40 km NW of the tree line, at (64˚17.381 N, 110˚03.701 W).

3.2. Climate

The study area spans the tree line, over which four ecoclimatic regions are traversed (from south to north: high boreal, low subarctic, high subarctic, and low arctic; Strong et al., 1989). Due to the large environmental differences, as well as the fact that the tree line roughly coincides with the southern extent of the Arctic air mass (Bryson et al., 1965), climate conditions can be expected to vary extensively over this range.

Due to a scarcity of weather stations, climate data for the study area is limited. In the high boreal ecoclimatic region there is extensive climate data at Yellowknife (62°27'46” N, 114°26'25" W), and north of this location there is a weather station in the low arctic ecoclimatic region at

Contwoyto Lake (65°29'00" N, 110°22'00" W). A comparison of instrumental records at these two weather stations illustrates that mean annual temperature at Yellowknife was greater than at Contwoyto (fig. 2a); precipitation values, however, do not appear to be significantly different between the two stations (fig. 2b). Much of the temperature difference likely occurs at the Arctic air mass boundary near the forest-tundra transition zone (Bryson et al., 1965).

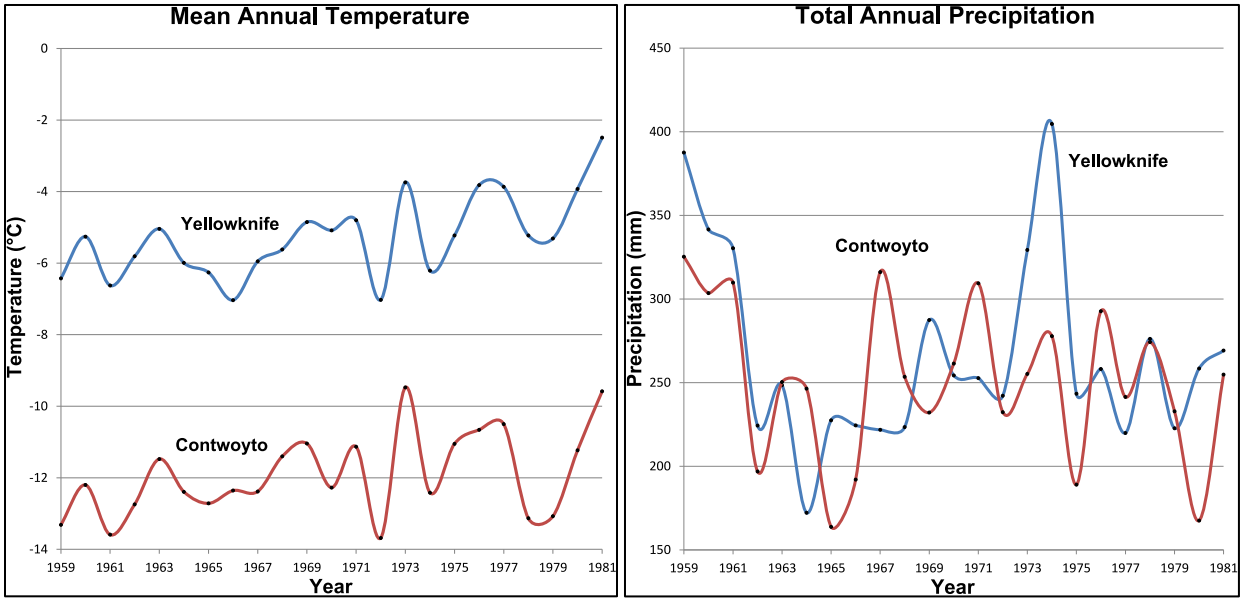

a) **b)**

Figure 2. Comparison of 1959-1981 a) mean annual temperature and b) total annual precipitation at the Yellowknife A and Contwoyto weather stations. 1959-1981 are the only years during which both weather stations were operating. *Data from Environment Canada.*

3.3. Geology

The study area is located within the Slave Province of the Precambrian Shield. This section of Archean crust is characterized by a depositional and volcanic history that has been overprinted by polyphase deformation and intruded by granitoid plutons (Bleeker, 2002). The major rock units include basement gneisses (4.00-2.95 Ga), metavolcanic and metasedimentary (turbidite) rocks (2.74-2.61 Ga), and widespread gneissic–granitoid plutons (2.64-2.60 Ga; Padgham and Fyson, 1992; Helmstaedt, 2009). This Precambrian basement is largely exposed due to the

removal of most of the overlying rock and soil during the Wisconsinan Glaciation which receded from the area approximately 9,000 yr BP (Dyke, 2004). Areas not exposed are often covered with glacial sediment. Glacial features such as eskers and boulder erratics are also strewn sporadically across the landscape.

3.4. Vegetation

The four ecoclimatic regions which exist in the study area each have their own variety of vegetation (Strong et al., 1989). The high boreal region is composed of a continuous forest of black spruce, jack pine, and some paper birch, with an understory of feathermoss, cranberry, blueberry, Labrador tea, lichen and peat moss. The boundary to the low subarctic region is marked by a replacement of continuous forest by open stands of black spruce, with an understory of dwarf birch, Labrador tea, lichen and peat moss. The high subarctic ecoclimatic region is distinguished by more stunted trees which grow more sparsely. Finally, the low arctic region occurs once no trees grow taller than understory level. Black spruce is no longer present, but rather, there is a continuous covering of dwarf birch, willow, Labrador tea, dryas, vaccinium, and peat moss.

3.5. Danny's Lake

Danny's Lake (63°28.547 N, 112°32.25 W; fig. 3) lies near the northern edge of the high boreal ecoclimatic region of the Northwest Territories, just 40 km SW of the low subarctic ecoclimatic region (forest-tundra transition zone). The climate is likely similar to that at the Yellowknife weather station, due to sharing the same ecoclimatic region as well as its relatively close proximity (150 km). The lake is surrounded by relatively flat, gentle hills of Precambrian Shield rock, covered with sparse trees and shrubs.

A recent forest fire has burned most of the vegetation at the lake site and its surroundings, resulting in a much more sparsely treed catchment. Young spruce and pine trees are beginning to emerge to replace the old vegetation.

Figure 3. Danny's Lake as seen by helicopter, looking northeast. *Photo by Andrew Macumber.*

3.5.1. Lake Properties and Dynamics

Danny's Lake is fairly small, covering an area of 20 ha, with a maximum depth of 10 m. The catchment size for the lake is 400 ha, with one small input stream draining a single upstream lake of comparable size (fig. 4). Groundwater flow is likely negligible due to the abundance of bedrock and extensive discontinuous permafrost in the region (50-90%; Natural Resources Canada, 1993). Therefore, surface runoff should account for the vast majority of water input to the lake. Instrumental data from the Yellowknife weather station is most likely to accurately reflect the climate of Danny's Lake, due to its relative proximity from Danny's Lake as well as

the fact that it shares the same ecoclimatic region. Data from this station from 1943 through 2006 provides an average total yearly rainfall of 154.7 mm, and an average total yearly snowfall of 138.0 cm (equivalent to 138.0 mm when converted to liquid), resulting in a total yearly precipitation of 292.7 mm. However, rainfall would generally only occur periodically during the 5 months of spring/summer/fall (May-October), while most of the snowfall would accumulate through the winter and flow through the lake during the short melt season (generally less than a month). Average discharge could therefore be expected to be much larger during spring melt than at any other time of year. Spring melt is therefore likely to be the dominant factor controlling input of sediment from the catchment into the lake, especially considering that the vast majority of this melt will enter the lake as surface runoff due to the overall lack of viable soil.

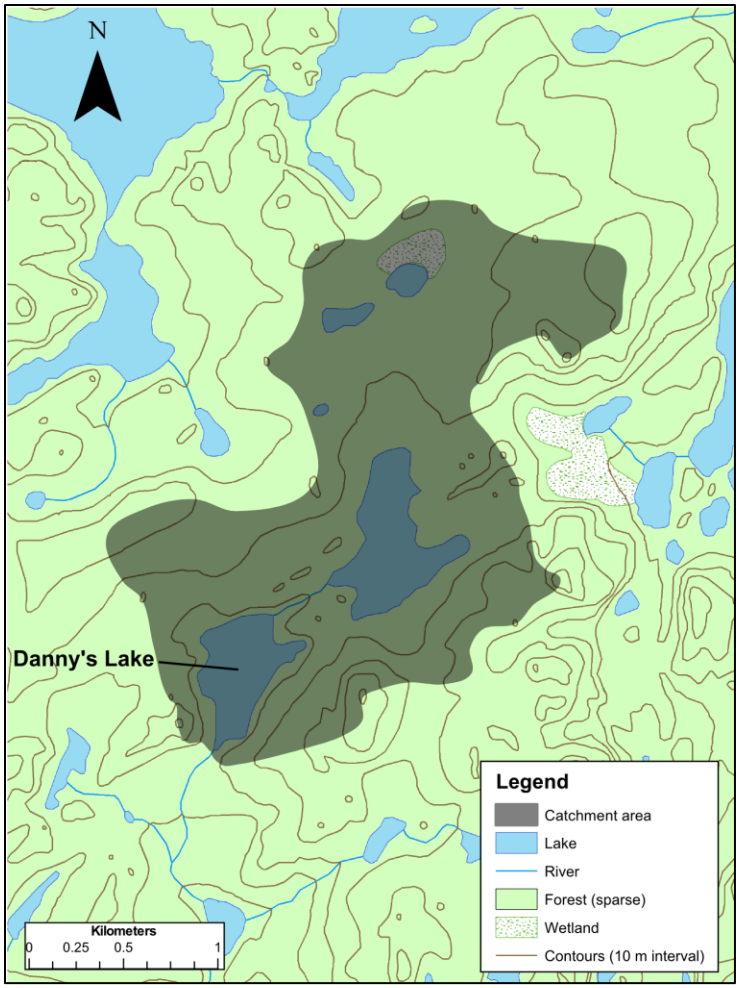

Figure 4. Danny's Lake catchment. Danny's Lake covers an area of 20 ha, and its catchment covers an area of 400 ha. The output stream is located at the southwest corner of Danny's Lake.

Bathymetry data indicates that Danny's Lake has an average slope of 8% and a maximum depth of 10 m (fig. 5). From these values, as well as the surface area of the lake (20 ha), an estimated total lake volume of 667000 m^3 can be calculated. A comparison of this volume to the total water volume flowing through the lake can provide an estimate of the water residence time for the lake. Given the area of the catchment and the average total yearly precipitation falling into the catchment, the total volume of yearly precipitation is 1.17 million m^3/year. However, not all of this volume will reach the lake, as some will be lost to evapotranspiration and this must be

taken into consideration. A measurement of evapotranspiration was taken by Spence and Rouse (2002) at a lake located just 50 km west of Yellowknife and within the same ecoclimatic region. They found a total yearly evapotranspiration rate of 237.38 mm/year. However, this rate may not be representative of the average yearly rate, as it was determined from just a single year (1999) and a partial record from the same lake the next year showed a significantly lower rate of evapotranspiration. Alternatively, Fernandes et al. (2007) calculated evapotranspiration rates over 40 years at locations across Canada using hourly surface climate data. They split their data into numerous regions throughout Canada, with Danny's Lake falling under the Mackenzie District region. While this region is extensive, most of it resides in the same ecoclimatic region as Danny's Lake. The average yearly evapotranspiration rate in this region was found to be 227.1 mm/year, similar to that of Spence and Rouse (2002). However, because it is a 40 year average value, it is more robust and may provide a more accurate estimate of the evapotranspiration rate at Danny's Lake. Using this value, we can estimate the volume of water in the catchment which is lost to evapotranspiration per year. Considering the size of the Danny's Lake catchment (minus the lake size itself, as any precipitation falling directly into the lake would be a direct contributor to lake input), we find that 863,000 m^3/year of water is lost to evapotranspiration. Subtracting this value from the total yearly volume of precipitation falling into the Danny's Lake catchment, we find that a total of 308,000 m^3/year of water from the catchment will reach Danny's Lake. Given this volume, and our calculated volume of Danny's Lake, we find that the water residence time is approximately 2 years. However, it is worth noting that isotopic studies of the region estimate that only 20-30% of precipitation in the Danny's Lake region returns to the atmosphere through evapotranspiration (Gibson and Edwards, 2002). If true, this would imply a much greater input of water to Danny's Lake and a

water residence time of slightly less than a year. However, this isotopic method appears to be highly imprecise (Gibson, 2001). Nevertheless, the evaporation rate estimate given by Fernandez et al. (2007) may be high, and therefore the previous water residence time of 2 years can be considered to be in the upper range of possible values. The estimated range of values for water residence time suggests that the lake water is largely catchment-dominated, and properties of the water should reflect values derived from this source.

Indeed, measured properties of lake water indicate that the current system is dominated by catchment input. Dissolved Inorganic Carbon (DIC) values gathered during the PANWT project (unpublished) were -12.72‰ in the winter of 2010, and ranged from -9.84‰ (lake surface) to -8.43‰ (lake bottom) in the summer of 2011. These values are depleted from the atmospheric value and suggest influence from catchment input.

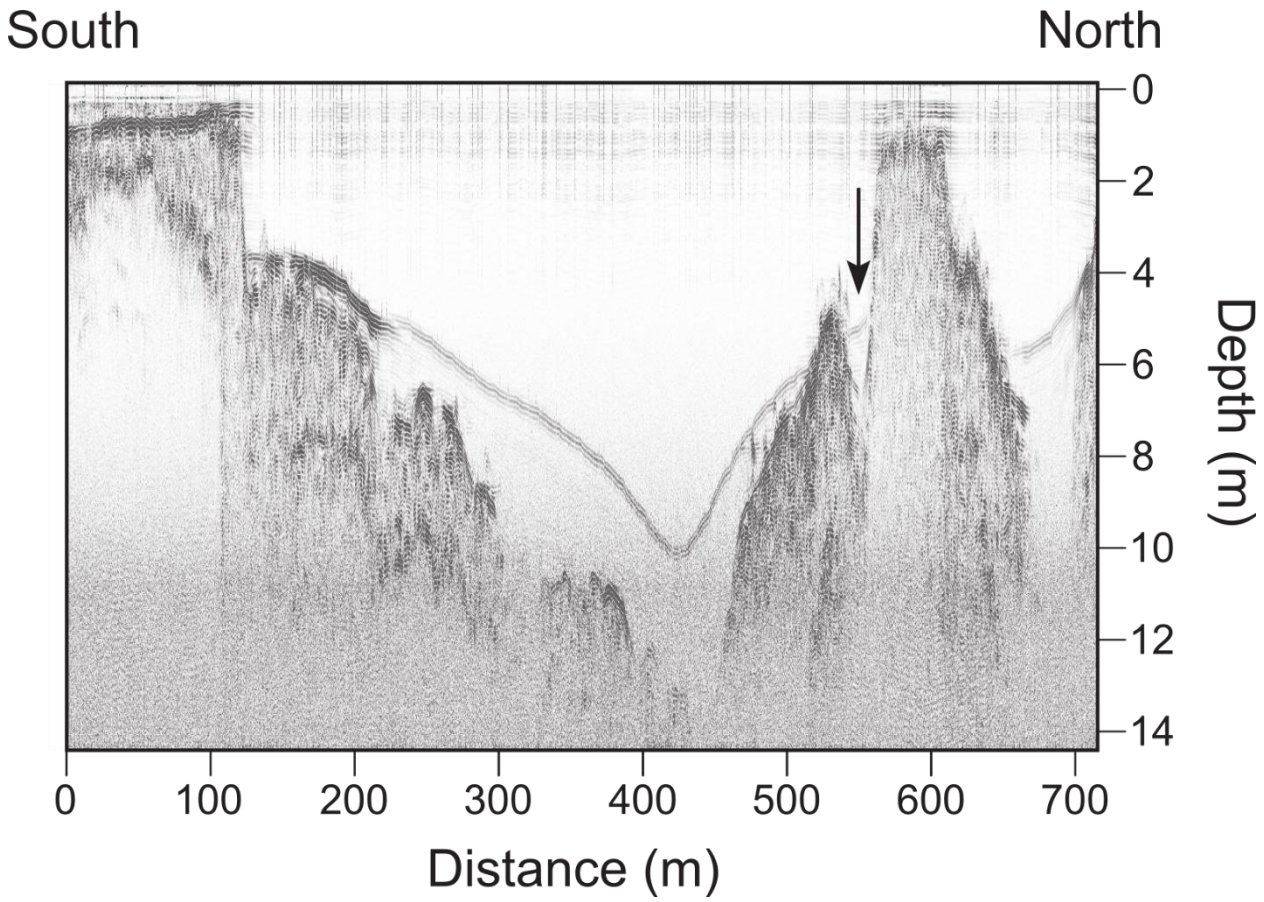

Figure 5. Danny's Lake bathymetric profile. The arrow indicates the location the freeze-core sample was taken from.

3.6. Horseshoe Lake

Horseshoe Lake (64˚17.381 N, 110˚03.701 W; fig. 6) lies within the low arctic ecoclimatic region of the Northwest Territories, 40 km NE of the high subarctic ecoclimatic region and 150 km NE of Danny's Lake. The site also lies within the same ecoclimatic region (low arctic) and just 50 km SE of the Contwoyto weather station, so likely shares a similar climate. The surrounding topography is very flat, consisting of glacial till covered in minor small shrubs and mosses which only partially cover the landscape. As the site is within the tundra, there are no

trees present. Frost-wedge polygonal patterning is evident in the areas surrounding the lake. Additionally, an esker runs into the lake from the northwest.

Figure 6. Horseshoe Lake as seen by helicopter, looking northeast. Photo by Andrew Macumber.

3.6.1. Lake Properties and Dynamics

Horseshoe Lake is much larger than Danny's Lake, covering an area of 560 ha with a maximum depth greater than 5 m. The sample site is located within a small bay at the southwest corner of the lake, and this only connects to the main portion of the lake by a small channel. However, this site must be well-connected to the rest of the lake in terms of water flow, because the only outlet for the lake is located within this bay. The lake's catchment is 2270 ha, which is much larger than Danny's lake and includes numerous input streams with small upstream lakes (fig. 7).

Because permafrost is continuous in this region (Natural Resources Canada, 1993), there is little to no groundwater flow. However, due to the larger catchment, surface water throughflow is much greater overall than at Danny's Lake. Data from the Contwoyto weather station, extending from 1959 through 1981, indicates an average yearly total rainfall of 129.8 mm, and an average yearly total snowfall of 121.0 cm (121.0 mm when converted to liquid), with a total yearly precipitation of 250.8 mm. Much like Danny's Lake, most of the snowfall will melt over a very short period of time during spring, resulting in a much higher average discharge than that from the rainfall. Spring melt is therefore most likely the dominant influence of catchment input to the lake.

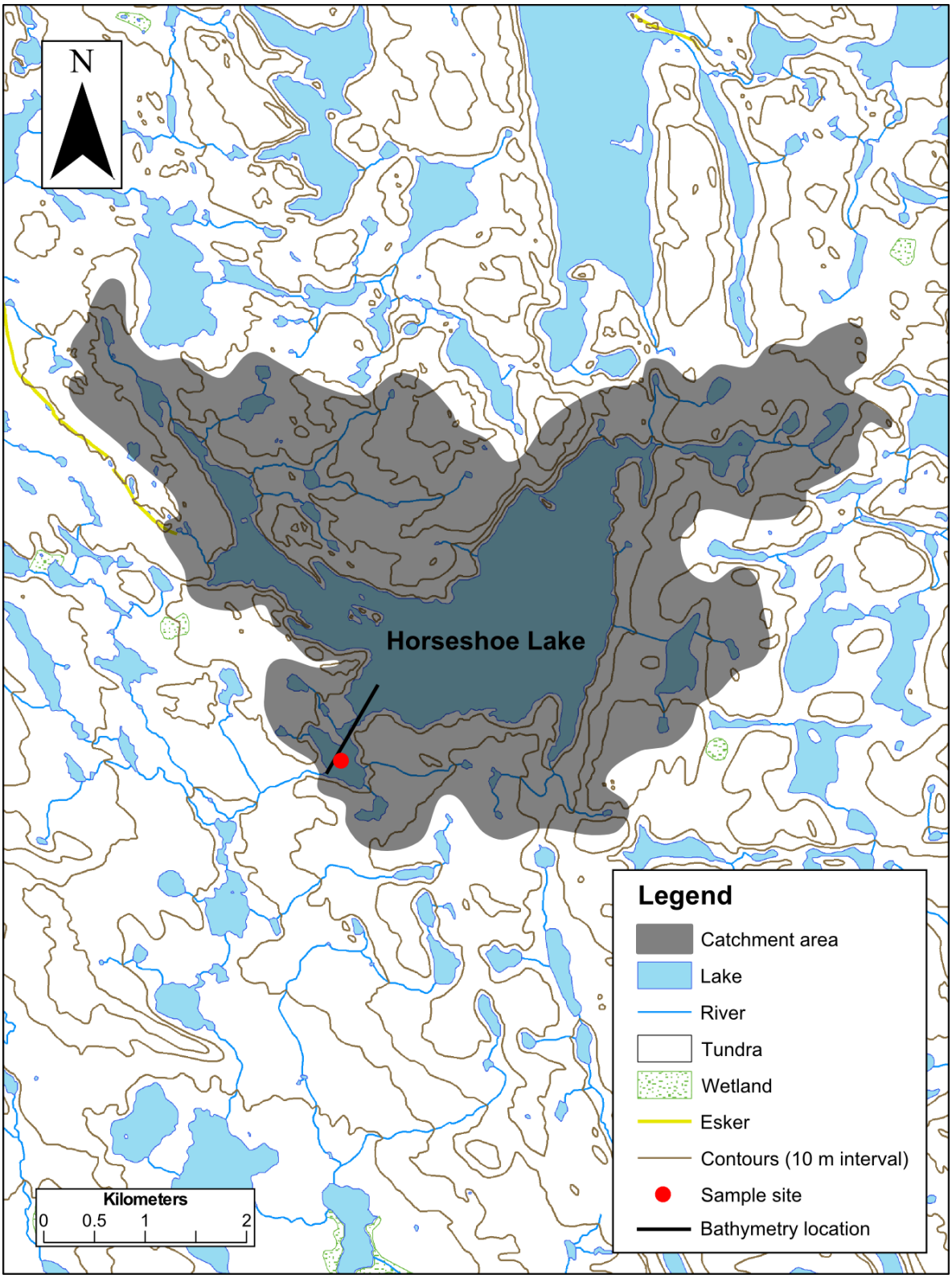

Figure 7. Horseshoe Lake catchment. Horseshoe Lake covers an area of 560 ha, and its catchment covers an area of 2270 ha. The core site is located in a small bay in the southwest corner of the lake, out of which the output stream drains in a southwesterly direction.

Determining lake volume for Horseshoe Lake is more difficult than for Danny's Lake due to the unusual crescent shape of the lake and the fact that bathymetry data only covers a portion of this crescent. However, bathymetric data indicates that the lake has steep sides and a generally flat bottom with an average depth of 3.5 m. Topographic data indicates that the shoreline is steep around the entire lake, suggesting that the portion of the crescent not covered by bathymetric data is likely similar in character to the rest of the lake. We can therefore estimate the lake size by assuming an average depth of 3.5 m over the entire lake. The sampling site bay can be calculated separately, as it is geographically isolated from the main portion of the lake and bathymetric data shows it only has a depth of 3 m (fig. 8). Using this method of estimation, the volume of water occupying Horseshoe Lake is calculated to be 19.4 million m^3.

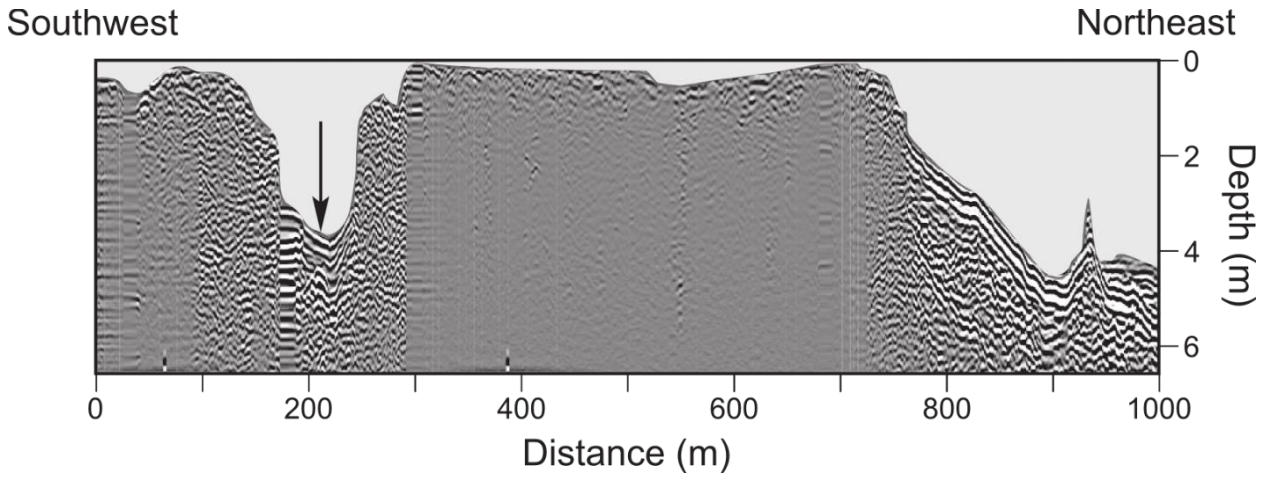

Figure 8. Horseshoe Lake bathymetric profile. The arrow indicates the location the freeze-core sample was taken from.

Considering the total yearly precipitation and catchment size, the average total yearly water volume entering the catchment would be approximately 5.7 million m^3. From this, evapotranspiration from the catchment must be taken into consideration. Using the same reference as was used for Danny's Lake to estimate evapotranspiration rates (Fernandes et al.,

2007), we can estimate evapotranspiration rates in the Arctic tundra to be 104.6 mm/year. When considering catchment size (minus lake size, since any precipitation falling in the lake is directly contributing to lake input), a total volume of approximately 1.8 million m^3/year of water is lost to evapotranspiration. Subtracting this from the total volume entering the catchment, the total water volume flowing through the Horseshoe Lake system is 3.9 million m^3/year. Considering the calculated lake volume, the water residence time in the lake is approximately 5 years. Using the isotopic method of Gibson and Edwards (2002), we could expect a loss through evapotranspiration of 5-10% of precipitation input to the catchment. Using this estimate, the water residence time would be approximately 3-4 years. In either case, the water residence time is significantly greater than that of Danny's Lake, and as such this lake can be expected to be significantly less catchment-dominated.

Indeed, measured properties of lake water suggest that the current system is less dominated by catchment input than Danny's Lake. Lake water DIC $\delta^{13}C$ values ranged from -11.64‰ (lake surface) to -12.25‰ (lake bottom) in the winter of 2010, and ranged from -6.44‰ (lake surface) to -8.79‰ (lake bottom) in the summer of 2011. These values are more enriched than those in Danny's Lake, and suggest that Horseshoe Lake is more greatly dominated by lake processes rather than catchment processes.

4. Methodology

4.1. Lake selection

Lakes for sample collection within the study area were chosen along a latitudinal gradient throughout Precambrian Shield of the Northwest Territories, from as far north as the border with Nunavut northeast of Yellowknife, to as far south as the northern shoreline of Great Slave Lake southeast of Yellowknife (fig. 1). Lakes chosen were along the TCWR, due to ease of access, as

well as our specific interest in how the TCWR is affected by climate change. Small lakes with minor inflow/outflow systems were avoided to maximize the possibility of a long and stable climate archive, and to ensure lakes were deep enough not to freeze completely to the sediment-water interface in winter (as this would disrupt the sediment profile). Additional lakes were selected for sampling away from the road by helicopter, in order to provide a continuous latitudinal gradient of lake sites.

4.2. Fieldwork

4.2.1. Winter Field Work

During the winter of 2010, a truck equipped with a rear-mounted auger was employed along the TCWR, and was used to drill a hole through the ice on lakes selected for sampling (fig. 9a). Sites were chosen at least 3 m away from the shoreline in order to reduce shore effects such as erosion (Galloway et al., 2010). A fish finder and sounding line were used to measure lake depth, to ensure the site was not so deep (>8 m) as to promote summer lake stratification which would expose the sediments to anoxic conditions, while also ensuring that the site was not shallow enough for winter ice to disturb the sediments. Water samples were then taken from the top of the water column using plastic bottles which were triple-rinsed with local lake water, and from near lake bottom using a kimmerer (fig. 9d) lowered down the hole. The kimmerer is designed to trap deep water through a spring-loaded mechanism which, when released by a weight hitting the kimmerer after sliding down the line, causes the kimmerer's compartment to close shut. The kimmerer, with its trapped water, was then hauled to the surface, where the water was poured into a plastic bottle which has been triple-rinsed by local lake water. Additional water properties (pH, dissolved oxygen, temperature and conductivity) were also measured on-site per meter depth, using a YSI multi-meter probe.

4.2.1.1. Core Collection

Cores were acquired from sampling sites using a tripod and winch system (fig. 9b), which allowed the core barrel to be lowered down the hole and into the sediment at the bottom. Sediment collected from the glew corer (fig. 9c) could only penetrate approximately 30 cm into the sediment, and acquired material was divided into top, middle and bottom sections for further use as near-surface sediment samples. The freeze corer (fig. 9b) can acquire sediments in excess of 1 m depth. It has two flat, rectangular metal faces on the outside, and an ethanol and dry ice mixture inside the core barrel which keeps the metal faces exceptionally cold and allows for extremely quick freezing of sediment onto their surface. This allows sediments to be extracted with minimal disturbance, providing a very high-resolution profile. Because there are two metal faces on the core barrel, two sediment profile 'faces' can often be obtained from a single core extraction.

4.2.2. Summer Field Work

In addition to winter field work, sampling was also conducted during the summers of 2009 and 2011. In 2009, lakes were sampled along the road east and west of Yellowknife, using a zodiac to gain access to the lakes. In 2011, lakes along the TCWR were re-sampled for summer water and sediment conditions, using a helicopter to gain access. New lakes were also sampled by helicopter in areas unreachable by ice road in winter, in order to ensure a continuous latitudinal gradient of sample sites. Top and bottom water samples and on-site water property measurements were obtained in the same manner as winter sampling. Surface sediment samples were taken using an Eckman Grab (fig. 9e). An Eckman Grab is a metal container whose bottom is composed of 'jaws' which are held open by a spring-loaded mechanism. After the Eckman Grab was dropped in the sediment, a weight was dropped down an attached line to release the

spring mechanism and cause the jaws to snap shut, capturing the sediment near the top of the sediment-water interface. The Eckman Grab was then hauled to the surface, where the top 1 cm of sediment was scooped into a plastic container using a spoon.

a) Truck with rear-mounted auger used for drilling holes in the ice along the Tibbitt to Contwoyo Winter Road. *Photo by Jennifer Galloway.*

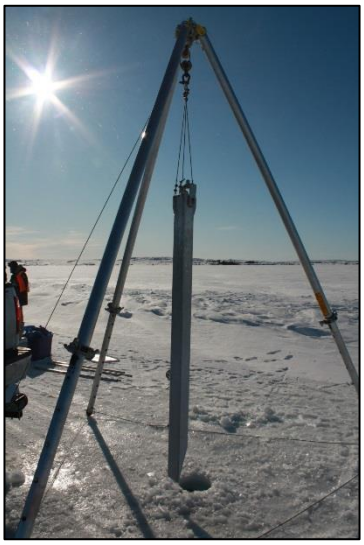

b) Freeze core barrel with tripod and winch system used for lowering it through the drilled hole in the ice. *Photo by Jennifer Galloway.*

c) Glew core barrel with sediments extracted from the top 30 cm of lake-bottom sediment. *Photo by Jennifer Galloway.*

d) Off-lake demonstration of how the kimmerer would be used on the lake. *Photo by Carley Crann.*

e) Off-lake demonstration of how the Eckman Grab would be used on the lake. *Photo by Carley Crann.*

Figure 9. Field work during the winter of 2010 (a-c) and the summer of 2011 (d-e).

4.3. Modern Lake Survey

A modern lake survey was completed using environmental data from 73 lakes throughout the PANWT project area (Appendix). The lakes used in this survey are highlighted in the study area map (fig. 1). Data used includes lake bottom sediment trace element and isotope (carbon and nitrogen) data, as well as lake water property data. Lake water property data was measured in the field during sample collection, using a YSI multi-meter probe, and both trace element and isotope data for lake bottom sediments were obtained from eckman grab and glew core samples (see 4.2.1. Winter Field Work, and 4.2.2. Summer Field Work). Sediment trace elements were analysed at the Geological Survey of Canada using the aqua regia method, while carbon and nitrogen isotopes were analysed using the IRMS in the Hatch Isotope Laboratory at the University of Ottawa. The preparation procedure for the isotopic samples was identical to that for the down-core analysis of Danny's Lake and Horseshoe Lake – the samples were dried and crushed into a powder before the appropriate amount was carefully weighed and put into tin capsules for analysis.

4.3.1.1. Statistical Analysis

The data was first screened to remove variables with more than 15% of sample values being unknown (missing or above or below detection limits). For remaining variables, all values below the detection limit were arbitrarily given values of half the detection limit, as suggested by Clarke (1998), and values above the detection limit were given values equal to the detection limit. All missing values were given a null value. Next, values for all variables were converted to the same units where possible (ie. all sediment trace element concentration data was changed to parts per million (ppm)).

Next, samples were divided up into groups based on geographical and climatological region. The study area map (fig. 1) was used to divide samples into those located in the boreal forest region, the tundra region, and the transition zone between the two. In addition to these environmental groupings, an additional group was made from all R09 samples to test for a possible anthropogenic effect of being near an all-season road.

Transformations were then applied to the dataset. First, compositional data was opened by applying a geometric mean transformation, in which each sample variable value was divided by the geometric mean of its compositional components. Second, a Box-Cox transformation was applied to each variable to normalize the distribution. To determine the appropriate λ values for the Box-Cox transformations of each variable, a Box-Cox test was applied to each variable (Appendix). Because a Box-Cox transformation requires values to be positive, each $\delta^{13}C$ value was increased by 40 prior to the transformation.

Outliers were then identified using Tukey boxplots (Appendix).

In order to ensure accuracy in multivariate data analysis, each variable was centered about the variable mean, and scaled by dividing each value by the variable MAD. Second, the number of variables used was reduced as per requirements for PCA. To determine which variables were the least informative and could therefore be removed, relationships between the variables were investigated using a Kendall tau rank correlation and Ward's method of hierarchical cluster analysis of variables (Appendix). Groupings were determined, from which, in most cases, a single variable was chosen to represent each group for multivariate analysis.

Once the dataset was prepared for multivariate analysis, Ward's method of hierarchical cluster analysis was performed on the samples, as well as PCA and a Kruskal-Wallis analysis of variance (Appendix).

4.4. Down-Core Isotope Analysis

All freeze cores were kept frozen and delivered to Ottawa for storage and processing in the Patterson Research Laboratory at Carleton University. The Danny's Lake core was chosen due to its location just south of the tree line as well as the fact that the core contains two faces (Face 1 and Face 2) from which material could be taken. The Horseshoe Lake core was selected as a second lake for isotope analysis in order to provide a comparison with Danny's Lake isotope results. Its location just north of the tree line is optimal because it allows the study of a lake which is currently dominated by a much different environment than Danny's Lake (tundra as opposed to boreal forest), yet which is also near enough Danny's Lake to potentially experience similar climate variations through time.

Both cores were sliced at 1 mm intervals through the entire core using a custom designed sledge microtome (Macumber et al., 2011; fig. 10). The microtome uses a ceramic blade connected to a crank and bolt system for precise mm to sub-mm slicing of the still-frozen core. Of these slices, one slice per cm (1 cm resolution) was selected at evenly spaced intervals for bulk carbon and nitrogen isotopic analysis through the core in both the Horseshoe Lake core and Face 2 of the Danny's Lake core. Such a 1 cm resolution through-core analysis provides a well-resolved overview of variations in carbon and nitrogen isotopes over the majority of the Holocene. Additionally, samples from the top of Danny's Lake core Face 1 (0-140 mm depth) were selected for high-resolution analysis at a 3 mm resolution. This analysis was completed in order to gain a more detailed understanding of climate variations for the recent past. Further samples were also selected for high-resolution isotope analyses at four slices per mm (2.5 mm resolution) at evenly spaced intervals in two sections of Danny's Lake core Face 2 (524-680 mm depth and 864-1010 mm depth). The upper (524-680 mm depth) section was chosen for high-resolution analysis due

to the stability of isotope values for this time period in the whole-core (1 cm resolution) record, as a comparison to the isotope values from the top high-resolution section. The lower (864-1010 mm depth) section was chosen for high-resolution analysis in order to gain a detailed understanding of a time period of significant and sudden variation in all isotopic proxies within the whole-core (1 cm resolution) record.

Due to the fact that most of the material from the top of Danny's Lake core Face 2 was used for analysis of other proxies, it was required to conduct the high-resolution analysis of the top section of the core from Face 1. The isotope records of Face 1 and Face 2 were merged under the assumption that the age of any determined depth for Face 2 is identical to the age of the equivalent determined depth for Face 1. For this assumption to be valid, the determined sediment-water interface for both faces must be identical, and all slicing must be identical between the two faces. Because the sediment-water interface is a sharp transition in both faces, and the interface most likely occurs at the same level in both faces due to their extremely close proximity, the determined position of the sediment-water interface is probably very similar between the two faces. While the slicing through the core in both faces is most likely very similar, over the length of the core there may be some minor shifting in determination of depth between them. However, over the short 14 cm length of the top of the core, it is unlikely that the slices between both faces are significantly offset from one another. Therefore, while there may be some minor depth offset between the isotope records of both faces, this offset is not likely to be substantial.

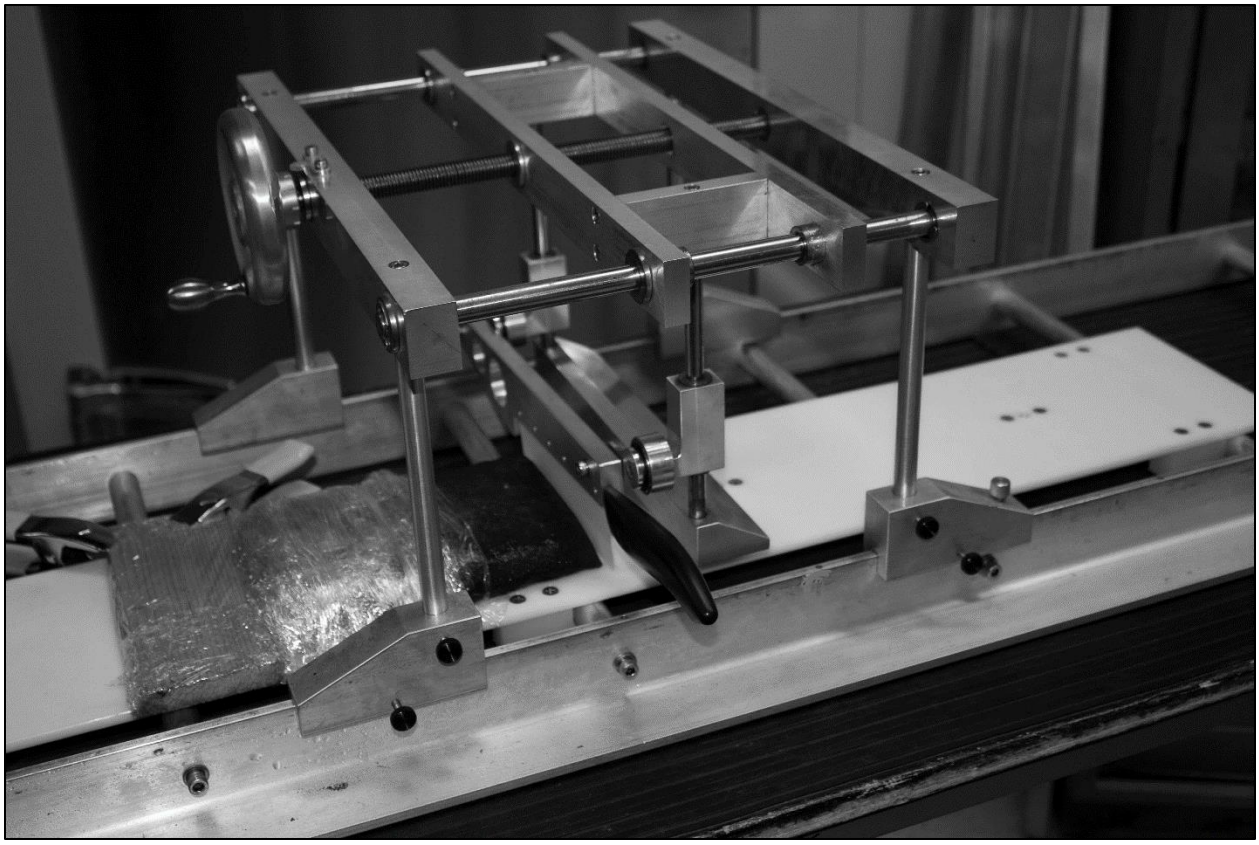

Figure 10. Sledge Microtome. This instrument was designed specifically for the Ice Road Project in order to slice cores at resolutions of 1 mm or less. *See Macumber et al. (2011).*

In addition to samples selected for isotopic analysis, 28 approximately evenly spaced samples through Danny's Lake core Face 2 and 8 approximately evenly spaced samples through Horseshoe Lake core were selected for preliminary bulk carbon and nitrogen concentration analysis. This preliminary analysis was required because the amount of sample material required for bulk carbon and nitrogen isotopic analysis using an Isotope Ratio Mass Spectrometer (IRMS) is dependent upon the ratio of mass amount of carbon to nitrogen in the sample.

Prior to any analysis, all isotopic and preliminary samples were dried in an oven at 60ºC over a three day period or until entirely dry. They were then crushed into a powder using a spatula, or a mortar and pestle in cases in which the sediment residue was particularly hard. Crushed sample

material was then mixed for homogeneity. Appropriate sample amounts were then transferred into small tin capsules, as well as an equal weight measure of tungsten oxide which was used as a combusting agent. The tin capsules containing this material were then rolled into a tight ball for use in the Elemental Analyser (EA) and Isotope Ratio Mass Spectrometer (IRMS) machines at the Hatch Isotope Laboratory in the University of Ottawa. The EA combusts sample material with oxygen at 1800ºC, converting it to various gas molecules such as CO_2 and N_2. These molecules are then passed through a gas chromatography column to separate them, after which the amount of each gas is determined using a thermocouple detector. If the original weight of sample material is known, as well as the atomic weight of carbon and nitrogen and an estimate of the number of gas molecules of each type read by the thermocouple detector, then a concentration for carbon and nitrogen in the sample can be calculated. If isotopic analysis is required, these gases are then vented to the IRMS, where they are ionized and shot through a tube with a magnet that bends the path of the ions. Ions will experience a differential in degree of bending depending on differences in weight, allowing the path of differently weighted ions to separate. Because different isotopes are different weights, these different isotopes separate from one another and can be read by ion detectors which determine the relative amounts of each isotope passing through the magnet. For transport between and through the EA and IRMS, a continuous flow system is used with a helium carrier. This equipment analyzes samples in 'runs', in which a group of samples is analyzed in sequence along with a number of standards for calibration purposes. Each run requires these standards, allowing for re-calibration of each run. These standards include nicotiamide, ammonium sulphate+sucrose, and caffeine. Additionally, glutamic acid is used as an internal standard not used for calibration, but rather to test the accuracy of calibrated values. For the EA, analytical precision is consistently +/-0.1% for both

carbon and nitrogen concentrations, while for the IRMS, analytical precision is based on a comparison of calibrated measurement of the glutamic acid standard vs. the known value for the standard. Usually this precision is greater than 0.2‰. For my own study, a total of eight runs were completed: a Danny's preliminary run, a Danny's whole-core low-resolution run, a Danny's top high-resolution run, a Danny's middle high-resolution run, two Danny's bottom low-resolution runs, a Horseshoe preliminary run, and a Horseshoe whole-core run.

The Danny's Lake preliminary run included 28 samples through the Danny's Lake core (no duplicates), plus standards. 2-4 mg of material was weighed out for each sample. This analysis only used the EA, as a method of roughly determining the carbon/nitrogen concentration in the samples.

The Danny's Lake whole-core low-resolution run included 85 samples (no duplicates) plus standards. Based on results of the Danny's Lake preliminary run, 17-24 mg of material was weighed out for each sample, except for rare cases in which substantially less material was weighed out (as little as 11 mg) due to a lack of material. Both the EA and IRMS were used for analysis. The analytical precision of the IRMS was +/-0.07‰ for $\delta^{13}C$ and +/-0.03‰ for $\delta^{15}N$.

The Danny's Lake top high-resolution run included 46 samples (no duplicates) plus standards. Based on the Danny's Lake preliminary run, 17-24 mg of material was weighed out for each sample, although in some cases less was used due to a lack of material (as little as 6 mg). While these smaller amounts are not optimal, they are still within the window of acceptable weights to use for sample material. Both the EA and IRMS were used for analysis. The analytical precision of the IRMS was +/-0.03‰ for $\delta^{13}C$ and +/-0.02‰ for $\delta^{15}N$.

The Danny's Lake middle high-resolution run included 59 samples (including 2 duplicates) plus standards. Based on the Danny's Lake preliminary run, 10-16 mg of material was weighed out for each sample. Both the EA and IRMS were used for analysis. The analytical precision of the IRMS was +/-0.03‰ for $\delta^{13}C$ and +/-0.04‰ for $\delta^{15}N$. However, it should be noted that the greatest difference between duplicates was slightly outside most of these precision values. Specifically, the greatest difference was 0.05‰ for $\delta^{13}C$, 0.06‰ for $\delta^{15}N$, and 0.31% for carbon concentration.

The Danny's Lake bottom high-resolution samples were split into two runs. The first run included 18 samples (no duplicates) from the upper (more recent) part of the section, plus standards. Based on the Danny's Lake preliminary run, 27-32 mg of material was weighed out for each sample. Both the EA and IRMS were used for analysis of both runs. For the first run, the analytical precision of the IRMS was +/-0.02‰ for $\delta^{13}C$ and +/-0.02‰ for $\delta^{15}N$. The second run included 39 samples (no duplicates) from the lower (less recent) part of the section, plus standards. Based on the Danny's Lake preliminary run, 10-14 mg of material was weighed out for most samples, although a few samples required as much as 29 mg. For this run, the analytical precision of the IRMS was +/-0.02‰ for $\delta^{13}C$ and +/-0.04‰ for $\delta^{15}N$.

The Horseshoe Lake preliminary run included 8 samples through the Horseshoe Lake core, plus standards. 2-4 mg of material was weighed out for each sample. This analysis only used the EA, as a method of roughly determining the carbon/nitrogen concentration in the samples.

The Horseshoe Lake whole-core run included 84 samples (no duplicates) plus standards. Based on results of the Danny's Lake preliminary run, a large variety of sample sizes were required through the core. Sample sizes used range from 9 to 42 mg of material. Both the EA and IRMS

were used for analysis. The analytical precision of the IRMS was +/-0.12‰ for $\delta^{13}C$ and +/-0.07‰ for $\delta^{15}N$.

Standard procedure calls for an acid leach previous to any organic carbon isotope analysis in order to remove unwanted calcium carbonate which could negatively affect results (Brodie et al., 2011a). However, studies indicate that acid leaching can affect isotope values and jeopardize results (Froelich, 1980; Bunn et al., 1995; Yamamuro and Kayanne, 1995; King et al., 1998; Lohse et al., 2000; Schubert and Nielsen, 2000; Ryba and Burgess, 2002; Kennedy et al., 2005; Schmidt and Gleixner, 2005; Galy et al., 2007; Fernandes and Krull, 2008; Brodie, 2011; Brodie et al., 2011a; 2011b). Additionally, waters within the Canadian Shield have been shown to contain extremely low quantities of dissolved inorganic carbon due to their derivation almost entirely from silicate rather than carbonate rocks (Stainton, 1973). In light of this fact, as well as the consideration that the Canadian Shield is a poor source of inorganic carbon material, the need to perform an acid leach for this study was questioned.

To verify that little inorganic carbon is present in the sediments of Danny's Lake, three samples of material from various depths of the Danny's Lake glew core, which reaches to 30 cm below the sediment-water interface, were analyzed using an off-line carbonate extraction. The procedure involves addition of hydrochloric acid to the sample material under vacuum conditions. The acid reacts with inorganic carbon to form a gas, which is delivered through vacuum tubes to a precise barometric sensor for determination of the amount of gas produced. Results of this procedure verify that the quantity of inorganic carbon in the sediment of Danny's Lake is insignificant (<1%), and therefore no leaching method is required. While Horseshoe Lake was not tested for inorganic carbon content using an off-line carbonate extraction, it was

assumed that this lake is also poor in inorganic carbon due to the similarity of environmental and geographic conditions (Precambrian Shield) of this lake with Danny's Lake.

4.5. Radiocarbon Dating and Age-Depth Modeling

Macrofossils were absent in the core so bulk sediment samples were chosen for accelerator mass spectrometry (AMS) ^{14}C dating at the ^{14}CHRONO Centre at Queen's University, Belfast. All samples underwent a standard hydrochloric acid wash to remove carbonate material. Radiocarbon ages were calibrated using Calib software version 6.1.0 (Stuiver and Reimer, 1993) and the IntCal09 calibration curve (Reimer et al., 2009).

4.5.1.1. Danny's Lake Age Model

A Bayesian age-depth model was constructed in Bacon for Danny's Lake (fig. 11), based on 25 radiocarbon dates obtained from the core (Table 1). The age modeling procedure for Bacon is similar to that outlined in Blaauw and Christen (2005), but more numerous and shorter sections are used to generate a more flexible chronology (Blaauw and Christen, 2011). The suggested memory properties for lake sediment cores were used with a "strength" of 20 and a mean of 0.1. An accumulation mean of 80 yr/cm was used based on a summary of accumulation rates for this region by Crann et al. (in prep.). The accumulation shape was set to 20, which is very high; however, setting the parameter at this level reduced the noise associated with likely outliers.

Since bulk sediment samples at high latitudes commonly incorporate old carbon (e.g. Abbott and Stafford, 1996), a freshwater reservoir effect (FRE) was calculated based on the projected age of the sediment-water interface from an age-depth model constructed in Clam (Crann et al., in prep.). The Clam model was constructed using a smooth spline with the smoothing parameter set to 0.7 and seven outliers removed using the general outlier model (Bronk Ramsey, 2009a) in OxCal version 4.1 (Bronk Ramsey, 2009b). The calculation of the FRE is based on the

assumption that the sediment-water interface should yield an age close to the year the core was collected. Based on the high-quality preservation and lack of disturbance of Danny's Lake core, the assumption that the sediment-water interface of the core is recent is most likely accurate. The FRE was subtracted from uncalibrated radiocarbon dates before Bayesian age-depth modelling was undertaken.

Table 1. Danny's Lake radiocarbon dates, including a 430 year freshwater reservoir effect adjustment. Bolded samples indicate those removed as outliers.

		^{14}C age BP (1σ)				
Lab ID (UBA-)	Depth (cm)	Uncorrected		Corrected ΔR=430		Corr. cal BP (2σ)
17359	5.7	693	± 21	263	± 21	284-424
17360	10.2	855	± 23	425	± 23	462-519
16543	15.0	1329	± 23	899	± 23	740-908
17361	21.9	1617	± 25	1187	± 25	1055-1177
17431	27.8	1659	± 21	1229	± 21	1072-1257
16544	32.6	1916	± 25	1486	± 25	1315-1408
20377	33.5	2071	± 24	1641	± 24	1419-1611
20378	34.2	2159	± 24	1729	± 24	1566-1703
17929	34.5	2257	± 26	1827	± 26	1700-1825
20376	35.3	2073	± 28	1643	± 28	1417-1614
20375	36.8	2248	± 25	1818	± 25	1697-1822
17432	37.6	2659	± 32	2229	± 32	2152-2335
20374	38.4	2392	± 25	1962	± 25	1865-1953
20373	39.3	2448	± 33	2018	± 33	1885-2059
17930	40.4	2549	± 26	2119	± 26	2002-2152
20371	41.4	2554	± 28	2124	± 28	2002-2154
20372	43.3	4863	± 29	4433	± 29	4877-5276
16545	45.0	2912	± 24	2482	± 24	2459-2717
16546	56.9	3604	± 25	3174	± 25	3361-3446
16547	70.1	5039	± 51	4609	± 51	5057-5471
16548	85.1	5834	± 29	5404	± 29	6180-6286
17931	89.5	6231	± 34	5801	± 34	6496-6674
16439	95.5	8112	± 32	7682	± 32	8412-8541
17932	99.1	7623	± 38	7193	± 38	7940-8111
16440	113.6	7450	± 30	7020	± 30	7792-7935

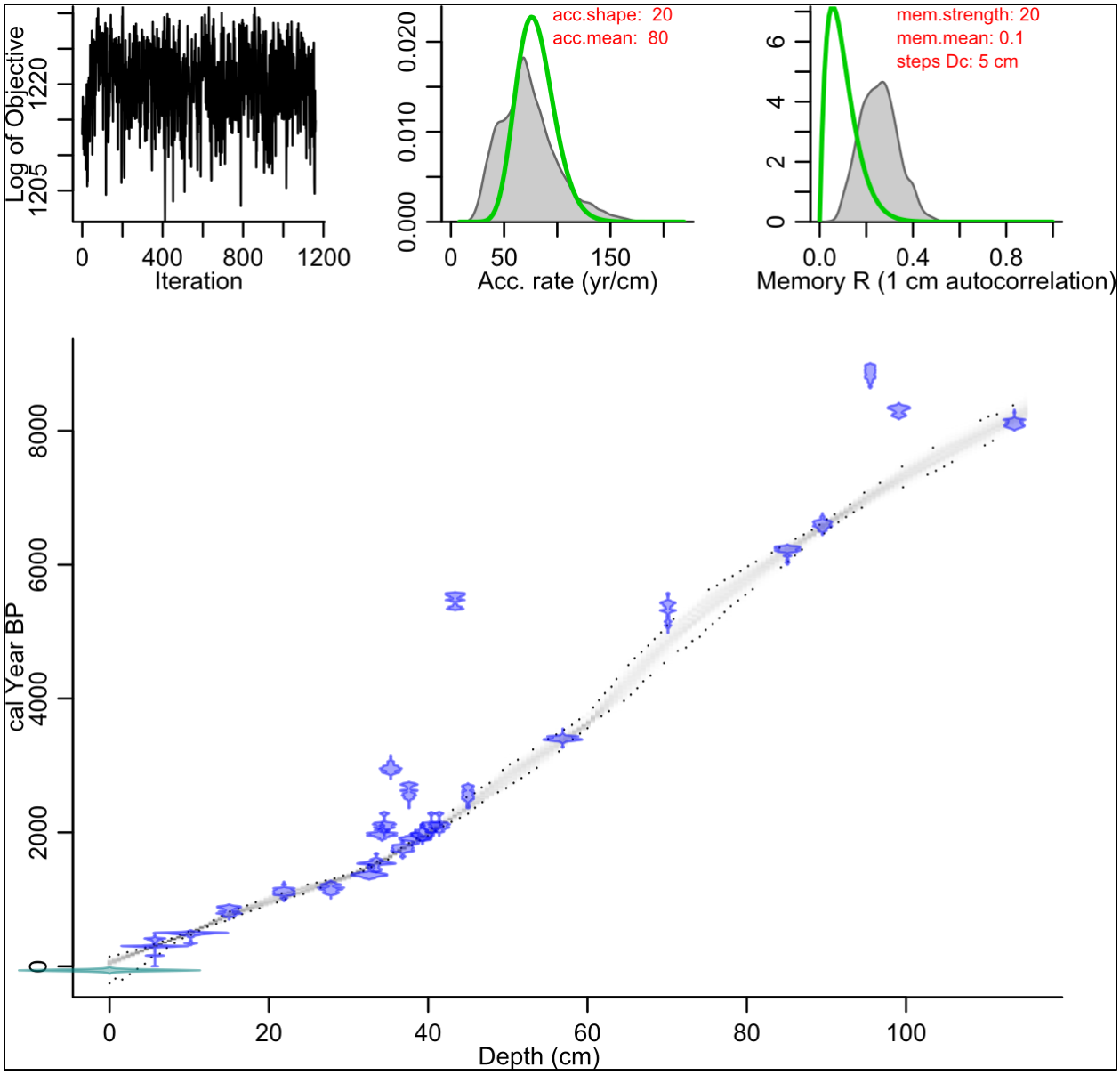

Figure 11. Danny's Lake age model, from Crann et al. (in prep). Created using Bacon (Blaauw and Christen, 2011).

4.5.1.2. Horseshoe Lake Age Model

Ten bulk organic samples were extracted from the Horseshoe Lake core for radiocarbon analysis, none of which were found to be outliers (Table 2). A smooth spline age model with a smoothing parameter of 0.3 was constructed using the classical age-depth modeling software Clam (fig. 12;

Blaauw, 2010; Crann et al., in prep). For this core, the sediment-water interface coincides with a recent age, indicating that there is no FRE for this lake. Bayesian age-depth modelling with Bacon was not undertaken at this time because there are no outliers in the model and because the way Clam handles the sharp fluctuations in accumulation rate is preferred (Crann et al., in prep).

Table 2. Horseshoe Lake radiocarbon dates. There was no freshwater reservoir effect, and no samples were determined to be outliers.

Lab ID (UBA-)	Depth range (cm)	^{14}C age (BP) ± 1σ	Cal BP ± 2σ
17350	9–9.5	178 ± 25	(-2)–291
17163	18–18.5	1148 ± 42	967–1172
17351	28–28.5	2763 ± 22	2785–2924
17352	38–38.5	3343 ± 23	3481–3639
19973	43.2	3776 ± 36	3992–4281
17938	46–46.5	4885 ± 27	5589–5653
17165	55–55.5	5916 ± 58	6628–6897
17937	68–68.5	6723 ± 29	7516–7656
17166	80–80.5	7488 ± 40	8199–8383
17167	106–106.5	8011 ± 43	8718–9014

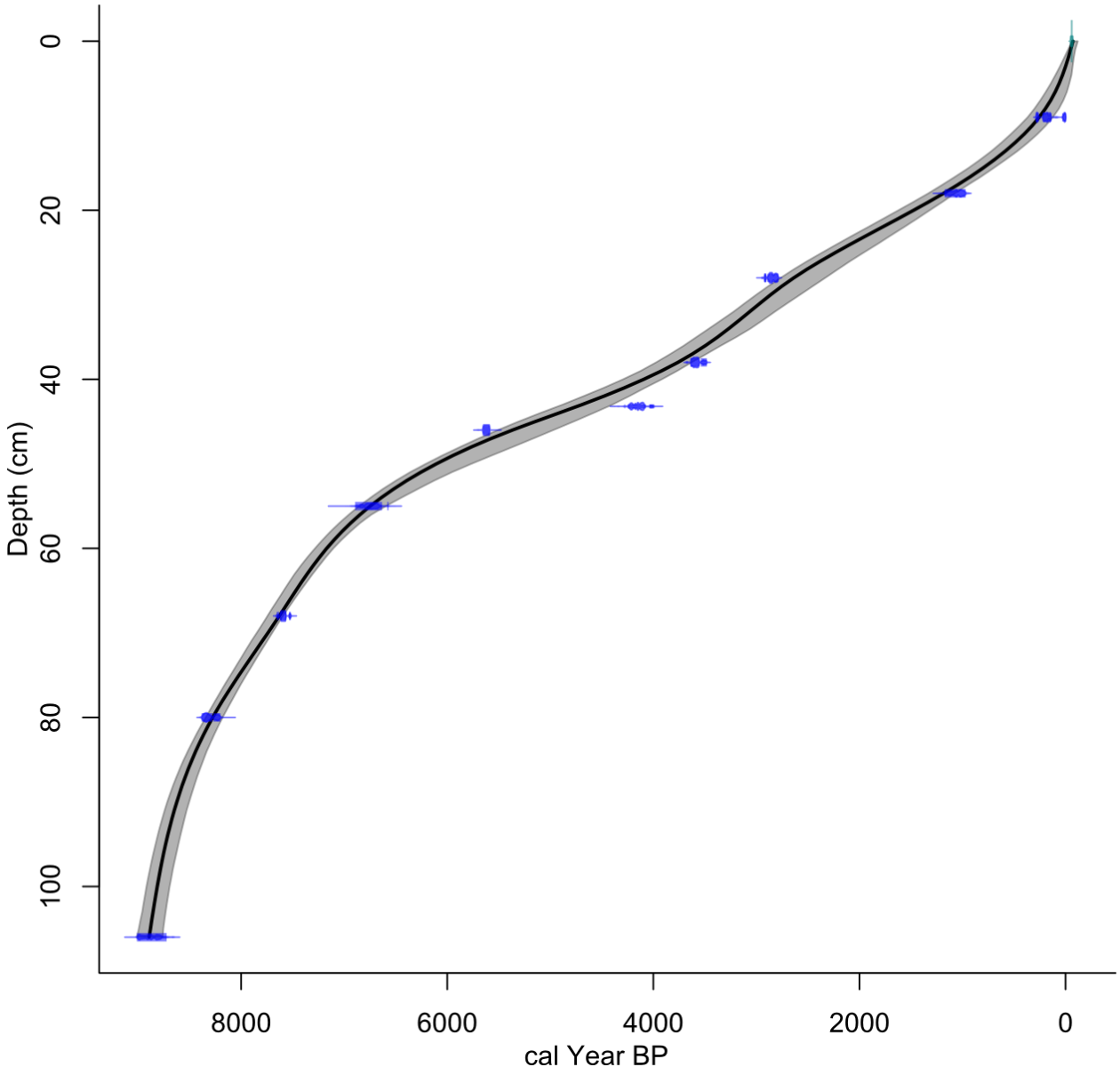

Figure 12. Horseshoe Lake age model, from Crann et al. (in prep). Created using Clam (Blaauw, 2010). The grey region represents the 95% confidence interval.

5. Results

5.1. Modern Lake Survey

Tukey boxplots of the variables are useful both to check the distribution and to detect outliers (Appendix). A strong right-skew is apparent in most of the variables, and as such a Box-Cox

transformation was applied. Outliers were also apparent in the boxplots (Appendix), four of which were identified as true outliers and removed.

Kendall's tau rank correlation as well as Ward's method of hierarchical cluster analysis on variables (Appendix) illuminated some correlations among variables which were used to create groupings. Determined groupings include: (Ti, Li, K, Pb, Fe, Al, Mn, As, Mg), (Cu, Cd, Zn, Ni), (%C, %N, C/N ratio, Ca, S), (Na, conductivity, pH), and (^{13}C, ^{15}N, dissolved oxygen (DO)). From these, nine variables chosen due to limitations on the number of variables allowed in multivariate analysis. The variables chosen include ^{13}C, ^{15}N, %C, conductivity, Ca, S, Ti, Cu, and Hg. These variables were used to perform Ward's method of hierarchical cluster analysis for samples and PCA (Appendix).

Cluster analysis of variables (Appendix) appears to cluster the samples in loose agreement with their predefined groupings (Boreal Forest, Arctic Tundra, Transition Zone and R09). The analysis generally orders samples with R09 on the left, followed by Arctic, then Transition Zone, and finally Boreal Forest on the right. With the exception of the R09 group, the trend appears to be one of more northerly sites to the left, with more southerly sites to the right. This is visualized with a scatterplot of Ward's cluster sample ordering vs. latitude (Appendix). The graph shows a clear trend in overall latitudinal changes from left to right.

Principle Components Analysis (PCA) was also performed on the dataset in order to provide more insight into the groupings and their driving influences. Principle Component (PC) 1 contains 48% of the variance, PC 2 contains 18% of the variance, and the remaining components contain 11% or less of the variance (Appendix). Therefore, most of the variance can be explained by the first two components. The diagram of PC 1 vs. PC 2 shows a clustering of the predefined groups. Among these groups, there is almost no overlap between the Arctic and

Boreal Forest groups, while the Transition Zone group sits between these two groups and significantly overlaps both. The differences between these three groups are almost entirely within PC 1. PC 1 shows a strong loading for %C, S, and Ca, a slightly weaker loading for Hg and ^{15}N, and a moderate loading for ^{13}C. Ti and Cu show very little correlation with PC 1 (Appendix).

The R09 group clusters away from the other groups, with little overlap with these other groups. However, there is not a great deal of difference between R09 and any of the other groups in terms of PC 1, due to a large variance of sample positions along PC 1 for R09. Rather, R09 separates out from the other groups almost entirely along PC 2. PC 2 shows an extremely strong loading for Cu, a strong loading for conductivity, a strong but weaker loading for ^{13}C, and a moderate loading for Ti, Hg, ^{15}N and C. Ca and S show very little correlation with PC 2 (Appendix).

The final step was to statistically determine how different the groups are from one another. For each variable, the set of values from each group were tested against every other group using the Kruskal-Wallis test to determine whether the groups were significantly different from one another (Appendix). p(same) values of less than 0.05 indicate that two groups of values are significantly different enough from one another that they can be considered to originate from different populations. Results indicate that, while variables differ in their level of differences between the groups, every group appears for the most part to be significantly different from every other group. The Arctic Tundra, Boreal Forest and R09 groups show the greatest level of differences between each other, while the Transition Zone group shows fewer differences from the other groups.

5.2. Danny's Lake

5.2.1. Chronology

Based on the age model for Danny's Lake (fig. 11), the age of the lake is just over 8000 cal yr BP. The average accumulation rate through the whole core is 72 yr/cm, although is varies a great deal throughout the core. The deposition rate is 45 yr/cm shortly before 8000 cal yr BP, after which it incrementally decreases to a rate of 110 yr/cm by 5000 cal yr BP. After 5000 cal yr BP the accumulation rate increased again, up to 40 yr/cm by 1500 cal yr BP, followed by a slowing to 80 yr/cm by 700 cal yr BP.

Based on the projected age of the sediment-water interface from the age-depth model, a Freshwater Reservoir Effect (FRE) of 430 years was calculated for Danny's Lake. An FRE appears to be common for many lake sediment cores collected during the Ice Road Project. An FRE can be caused by a variety of sources, such as: (1) input of carbon from macrophytes, which does not readily exchange CO_2 with the atmosphere; (2) input of "dead" ^{14}C from bedrock; or (3) the in-wash of old organic material from the catchment (Crann et al., in prep). $\delta^{13}C$ values obtained during radiocarbon dating are not unusually enriched, suggesting that influence from macrophytes is not likely to be an issue. We also know that the old carbon is not likely coming from the bedrock as Danny's Lake is sitting in a weathering-resistant granitic terrain. Therefore, the most likely cause of the FRE at Danny's Lake is the in-wash of old organic material during the spring melt (Crann et al., in prep). This carbon can enter the lake through soil erosion or as catchment DIC in groundwater and surface runoff (Abbott and Stafford, 1996; Geyh et al., 1998; Blaauw et al., 2011). In Danny's Lake, input to lake water DIC has been shown to be catchment-dominated (see section 3.6.1), so catchment DIC is therefore a very plausible source of old carbon into the lake. This may be particularly relevant in high-latitude locations such as the

Northwest Territories, as cool average temperatures and the presence of permafrost could slow the rate of soil decomposition in comparison to areas further south. The FRE is assumed to be consistent through the history of Danny's Lake, and an age offset was applied evenly through the entire core to account for this effect. The assumption that the FRE has been consistent through time may not be valid (Barnekow et al., 1998; Geyh et al., 1998; Grimm et al., 2009; Blaauw et al., 2011). However, determination of precise changes in the FRE offset through time is difficult to achieve without alternative sources of material for radiocarbon dating such as varves, plant macrofossils or tephra. Therefore, assuming a constant FRE, while not preferable, is the best possible option to apply to the age model with the information given.

5.2.2. Sedimentology

Danny's Lake Core (fig. 13), which extends from surface to 114.2 cm depth, is composed entirely of organic-rich mud. There are no observable features such as laminations or visible grains in any part of the core. The core is dark brown in colour near the top, with a gradual transition to light brown up to 91.2 cm depth. At this depth, there is a sharp colour change back to a dark brown colour which persists to the bottom of the core. Water content near the top of the core is extremely high, approaching 90% at the very top.

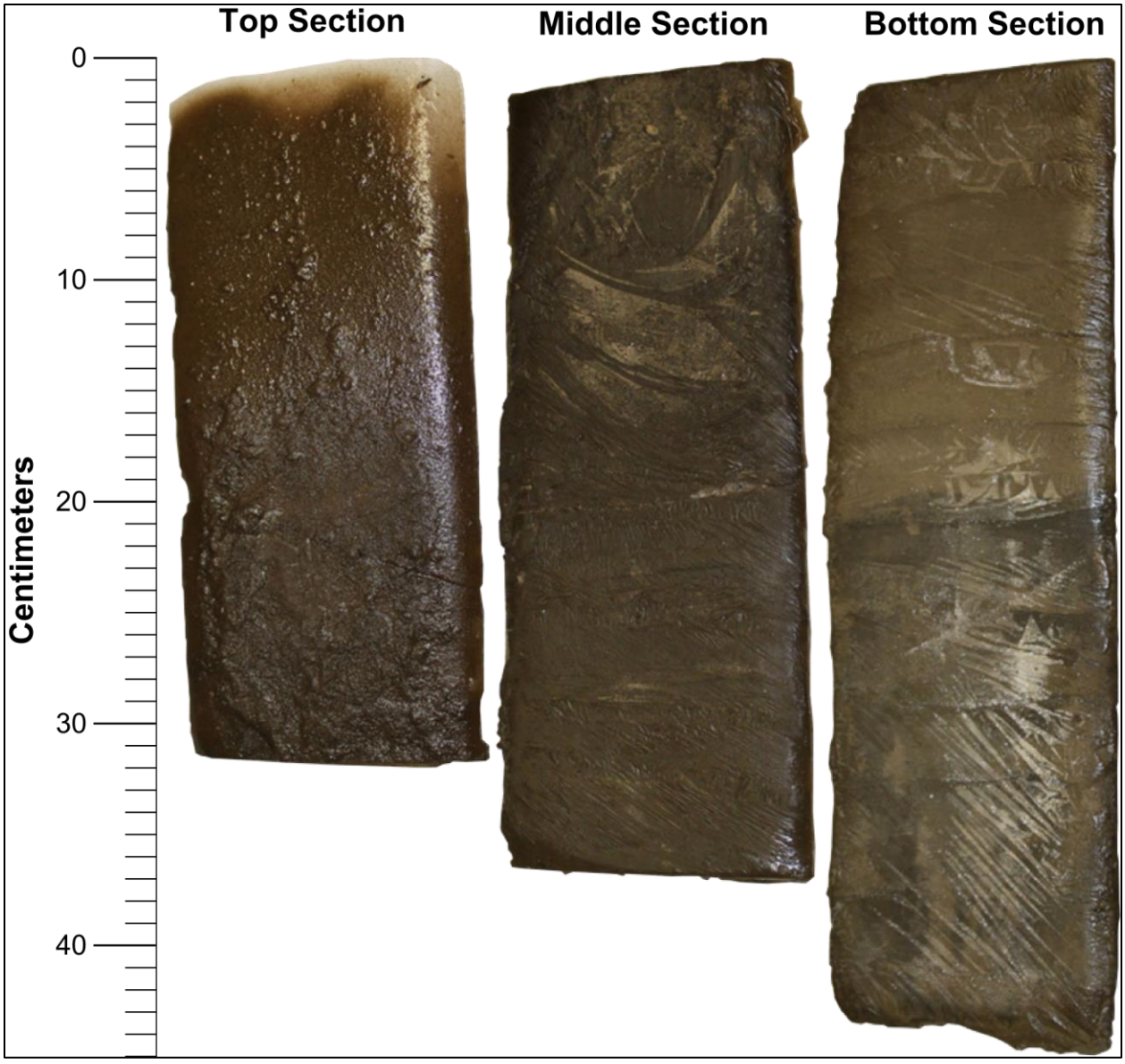

Figure 13. Danny's Lake core. Photo by Andrew Macumber.

5.2.3. Whole-Core Isotopic Analysis at 1 cm Resolution

Whole-core isotopic analysis was conducted through Face 2 of the core at a 1 cm resolution, from the bottom of the core (114.2 cm) to near the top (up to 14.2 cm). The very top of the core was not analyzed in Face 2 along with the rest due to a lack of available sediment. However, the very top of the core was analyzed for Face 1 (see section 6.2.5).

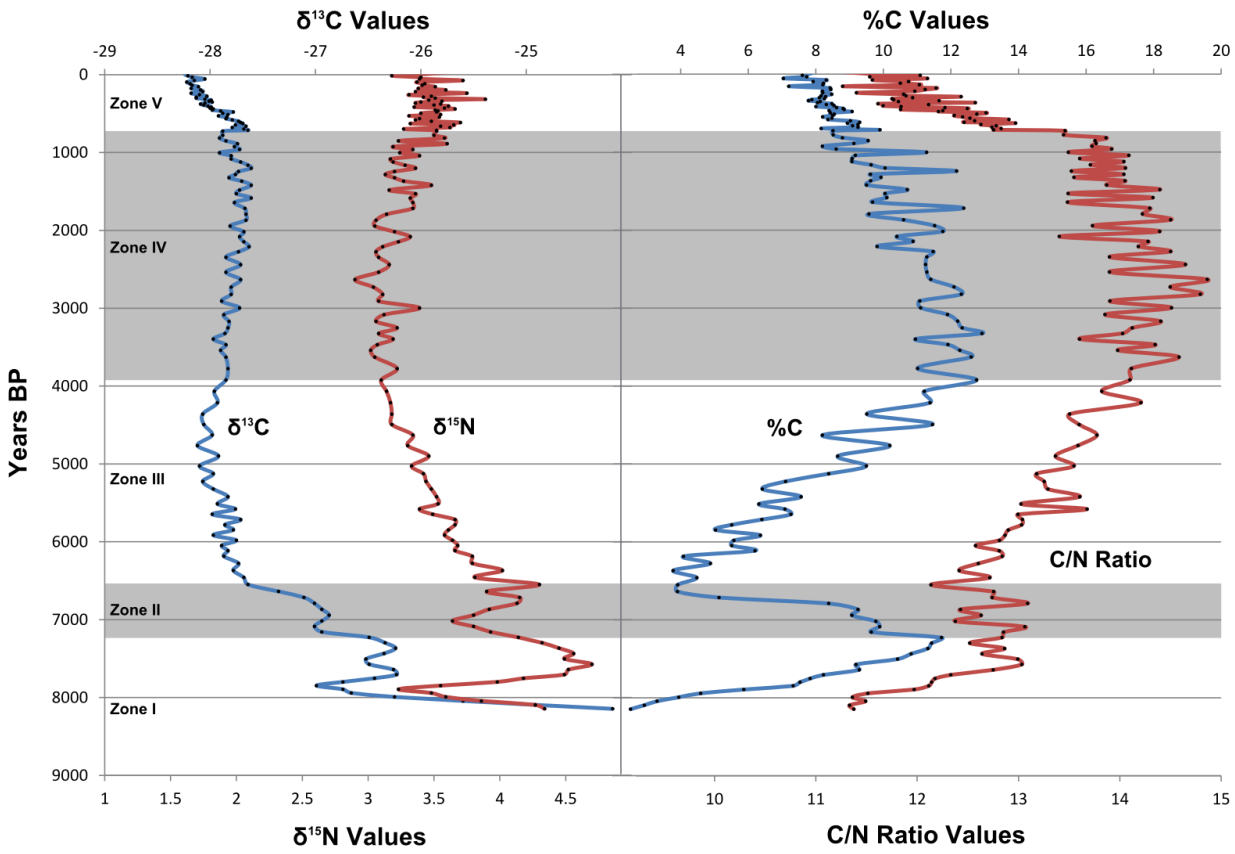

Figure 14. Danny's Lake whole-core isotopic analysis at 1 cm resolution (3 mm resolution from 714 BP to present).

From 8145 – 7300 cal yr BP there large, sharp variations in isotopic values across the board. Both $\delta^{13}C$ and $\delta^{15}N$ begin at the very bottom of the core with enriched values (-24.2‰ and 4.3‰, respectively) which quickly plummet to -27‰ ($\delta^{13}C$) and 3.2‰ ($\delta^{15}N$). This is followed quickly by another enrichment spike in both isotopes, up to -26.3‰ and 4.7‰, respectively. This spike is matched closely with a large increase in %C, %N, and C/N ratio (2.5% to 11.7%, 0.2% to 0.9%, and 11.3 to 13.0, respectively).

From 7300 – 6700 cal yr BP, there is a strong decline in $\delta^{13}C$ (to -27.6‰), %C (to 3.9%), and %N (to 0.3%), as well as a drop in $\delta^{15}N$ (to 3.6‰) followed by a rebound (to 4.3‰). The largest and most sudden drop, by far, is around 6700 cal yr BP. %C and %N, in particular, experience

an extremely sharp reduction at this point, of 5.3% and 0.4%, respectively. This point also coincides with the sharp colour change seen in the core.

Immediately after the colour change, isotopic trends are much more gradual and appear more stable than before. In addition, smaller-scale cyclicity is apparent among all proxies, which is not previously apparent. These characteristics appear to be persistent through the remainder of the core.

Beginning at 6700 cal yr BP, %C and %N begin a gradual increase up to 12.7% and 0.9%, respectively. C/N ratio also increases, from 12 to 14.5. $\delta^{13}C$ and $\delta^{15}N$ both experience a gradual depletion trend, although $\delta^{13}C$ only changes by about 0.5‰, which is not a highly significant amount.

At around 4000 cal yr BP, another change occurs among the trends of all proxies. However, these changes are not as sharp, and the timing less consistent, than at 6700 cal yr BP. Changes include an end to the increasing trend in %C, %N, and C/N ratio, with each of these levelling off or even slightly decreasing. Both $\delta^{13}C$ and $\delta^{15}N$ undergo an enrichment trend, although neither proxy changes value by a very significant amount, at only around 0.5‰.

5.2.4. Top Section High Resolution (3 mm) Isotopic Analysis (714 to -48 cal yr BP; 14.0-0.3 cm; averaging 16.7 yr/3 mm)

5.2.4.1. Top Section Profile

The top section profile (fig. 15) shows an overall gradually decreasing trend for C/N ratio (13.0 to 11.1), $\delta^{13}C$ (-27.6‰ to -28.2‰), and %C (9.9% to 7.0%) up to present. The reduction in C/N is particularly rapid from 714-150 cal yr BP, after which it appears to level off. %N and $\delta^{15}N$ remain stable throughout at around 0.65% and 3.5‰, respectively. At the very top of the core, a

small excursion is evident in most proxies – an enrichment in $\delta^{13}C$ and $\delta^{15}N$, an increase in organic matter, and a reduction in C/N.

In addition to the overall trends, each proxy displays high-frequency smaller-scale fluctuations. These fluctuations are only from 0.1‰-0.2‰ for $\delta^{13}C$ and $\delta^{15}N$, and may not represent a real signal beyond error. However, fluctuations for C/N ratio and %C are from 0.5-1, and are likely significant.

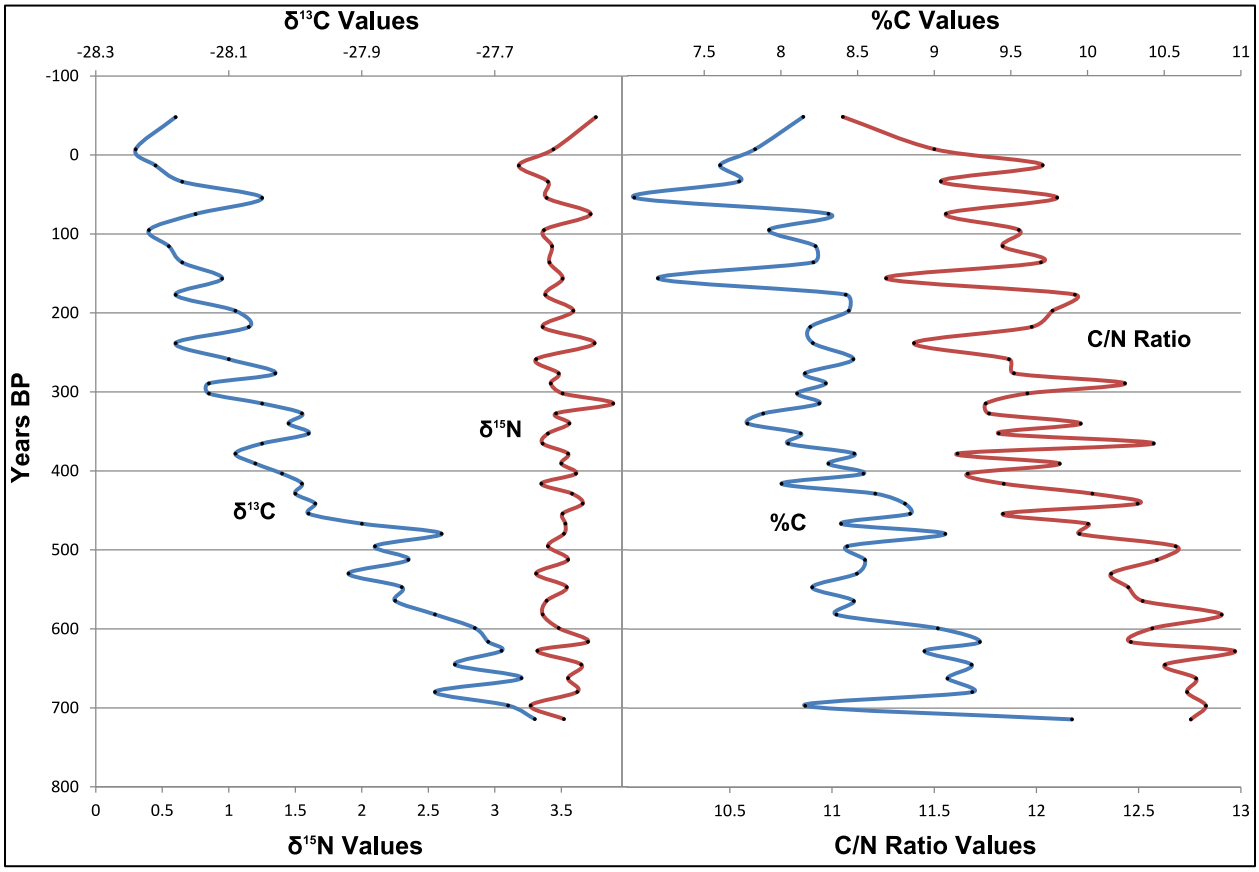

Figure 15. Danny's Lake top section high resolution (3 mm) isotopic analysis.

5.2.4.2. Top Section Spectral, Wavelet and Cross-Wavelet Analysis

To test the significance of these small-scale fluctuations, spectral analysis was completed on the C/N ratio and %C for the top section (fig. 16). $\delta^{13}C$ and $\delta^{15}N$ are not considered here because

the cyclical variations seen in their values are too small to be considered significant (maximum cycle variations of approximately 0.15‰ for $\delta^{13}C$ and 0.40‰ for $\delta^{15}N$). With a sampling resolution of 16.7 years, the minimum cycle frequency which can be detected is twice that amount, or 33.4 years, based on the Nyquist number (Shannon, 1949). Results indicate a clear 39-year cycle in the C/N ratio, at above 99% significance. %C also shows this cycle, at above 95% significance. In addition, a 71-78 year cycle is seen in the C/N ratio at greater than 95% significance.

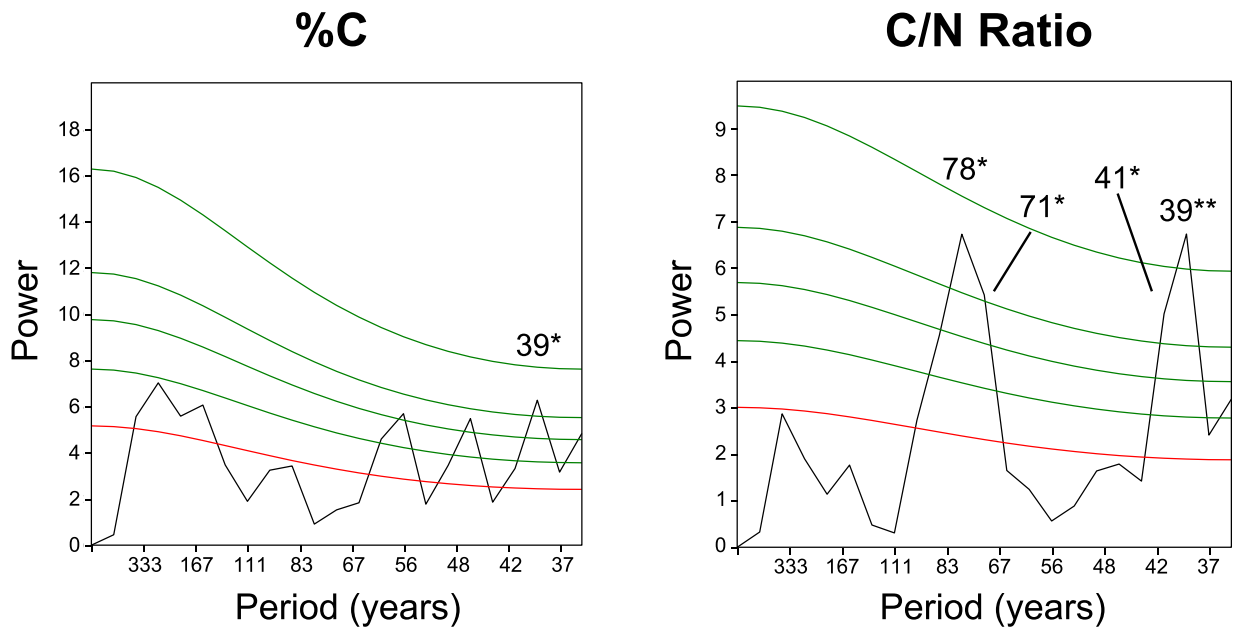

Figure 16. Danny's Lake top section spectral analysis for %C and C/N Ratio. Peaks reaching above the highest green line are greater than 99% significant and are marked with (**). Peaks reaching above the second-highest green line but below the highest are between 95%-99% significant, and marked with (*).

Wavelet analysis (fig. 17) delineates a 39-41 year cyclicity in both C/N ratio and %C which is seen on and off throughout the record, as well as a cycle at 71-87 years which is seen strongly in the C/N wavelet from 550-100 cal yr BP, and in the %C wavelet from 400-50 cal yr BP. There is also a possible 156 year cycle detected among both proxies through the entire record. Additionally, the %C wavelet shows possible inconsistent 46 year and 56-60 year cycles.

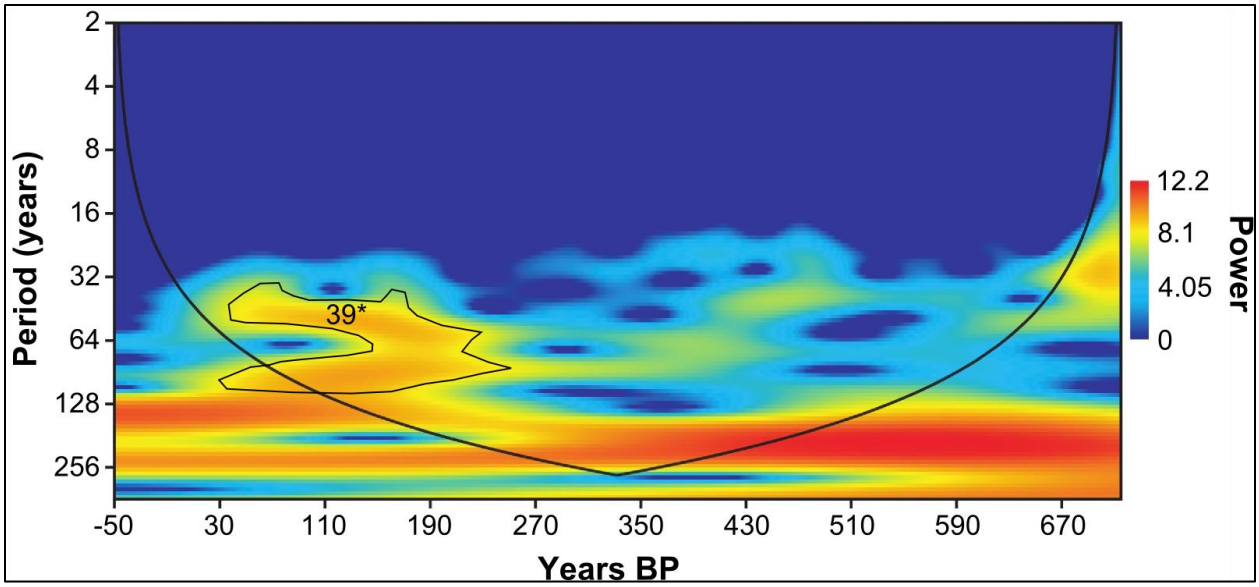

a)

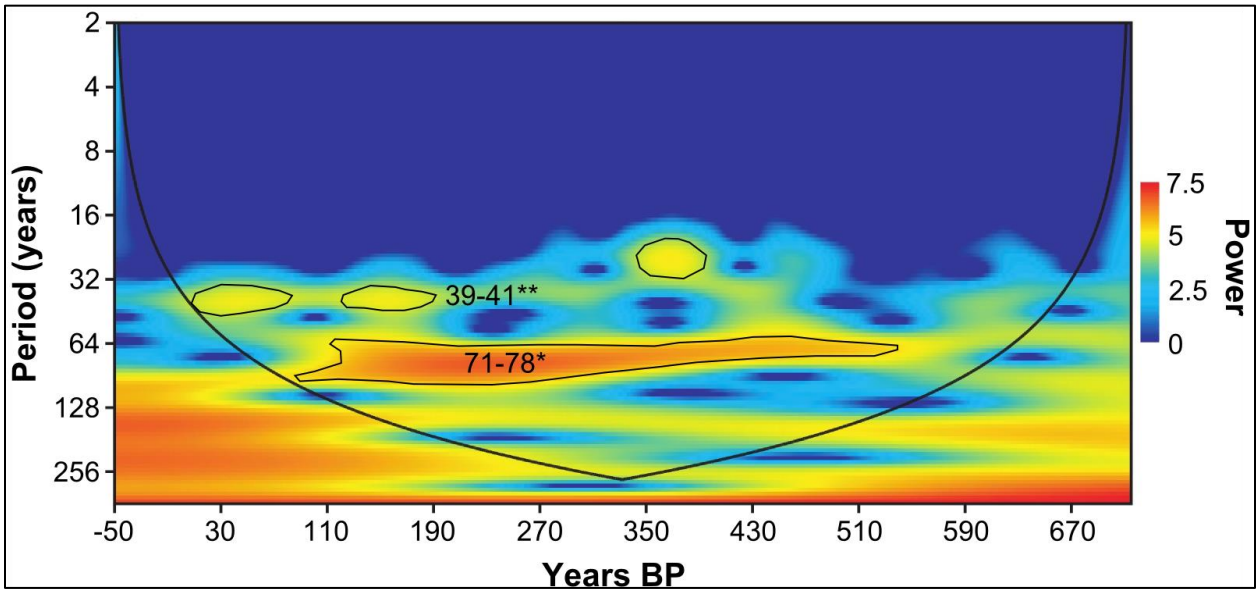

b)

Figure 17. Danny's Lake top section wavelet analysis for a) %C, and b) C/N Ratio. Regions with strong power are highlighted and areas of strong power correlating to spectrally significant periods are labelled with the significant period (** = greater than 99% significance, * = greater than 95% significance).

Cross-wavelets were used to compare C/N and %C with the tree-ring based PDO records of both MacDonald and Case (2005; fig. 18a) in North America and Shen et al. (2006; fig. 19a) in China, as well as total solar irradiance as measured using ^{10}Be in ice cores by Steinhilber et al. (2009; fig. 20a). Both C/N and %C showed similar results in their comparison with these records.

Comparison with the PDO record of MacDonald and Case (2005) shows a strong but inconsistent correlation at the 60-80 year cyclicity (fig. 18b, c). Comparison with the PDO record of Shen et al. (2006) shows a very strong correlation at the 75-115 year cyclicity from 450-150 cal yr BP, followed by another very strong correlation at the 50-70 year cyclicity from 100 cal yr BP-present (fig. 19b, c). Comparison with the total solar irradiance record of Steinhilber et al. (2009) shows a possible weak correlation at a frequency of 50-70 years from 500-350 cal yr BP and 200-100 cal yr BP, as well as a stronger correlation at a frequency of 70-110 years from 250-0 cal yr BP (fig. 20b, c).

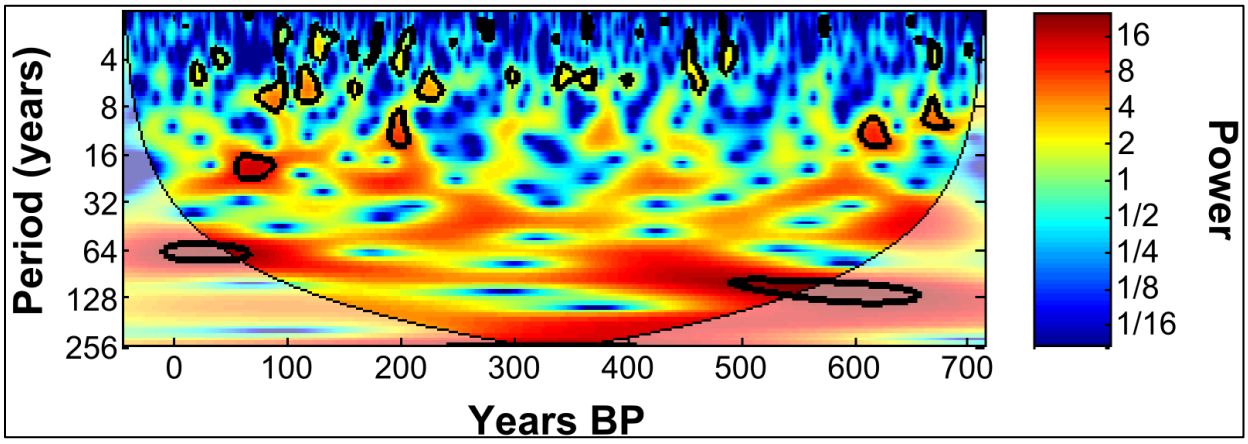

a)

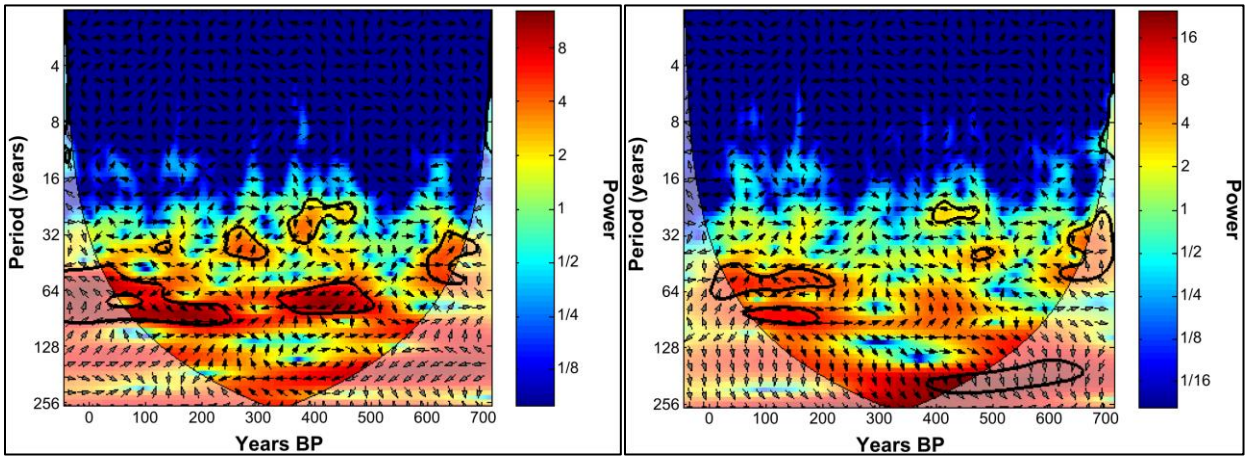

b) c)

Figure 18. a) Wavelet of the tree ring-based PDO record taken from MacDonald and Case (2005). b) Cross-wavelet comparing the record of MacDonald and Case (2005) with the C/N record of Danny's Lake top section. c) Cross-wavelet comparing the record of MacDonald and Case (2005) with the %C record of Danny's Lake top section.

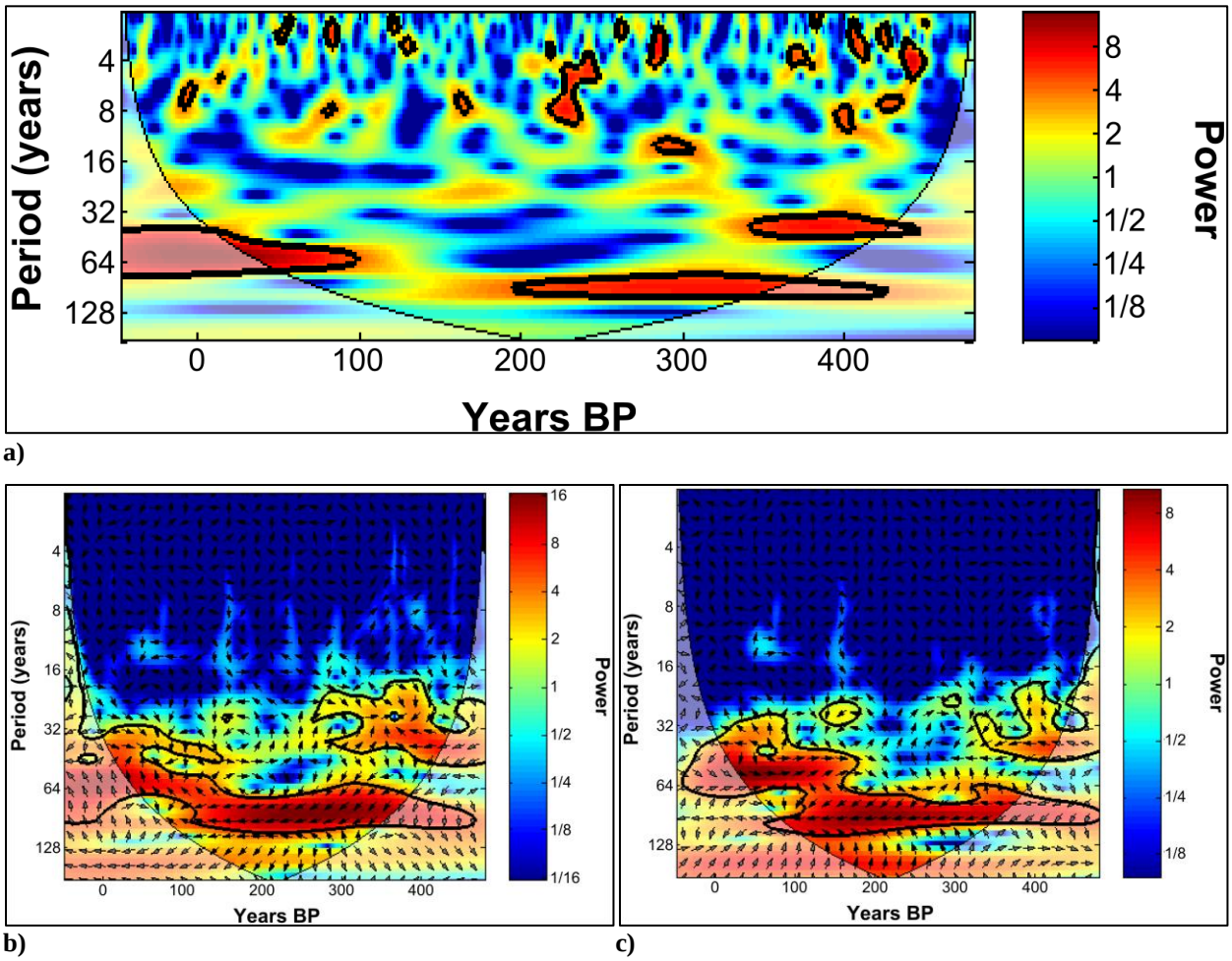

Figure 19. a) Wavelet of the tree ring-based PDO record taken from Shen et al. (2006). b) Cross-wavelet comparing the record of Shen et al. (2006) with the C/N record of Danny's Lake top section. c) Cross-wavelet comparing the record of Shen et al. (2006) with the %C record of Danny's Lake top section.

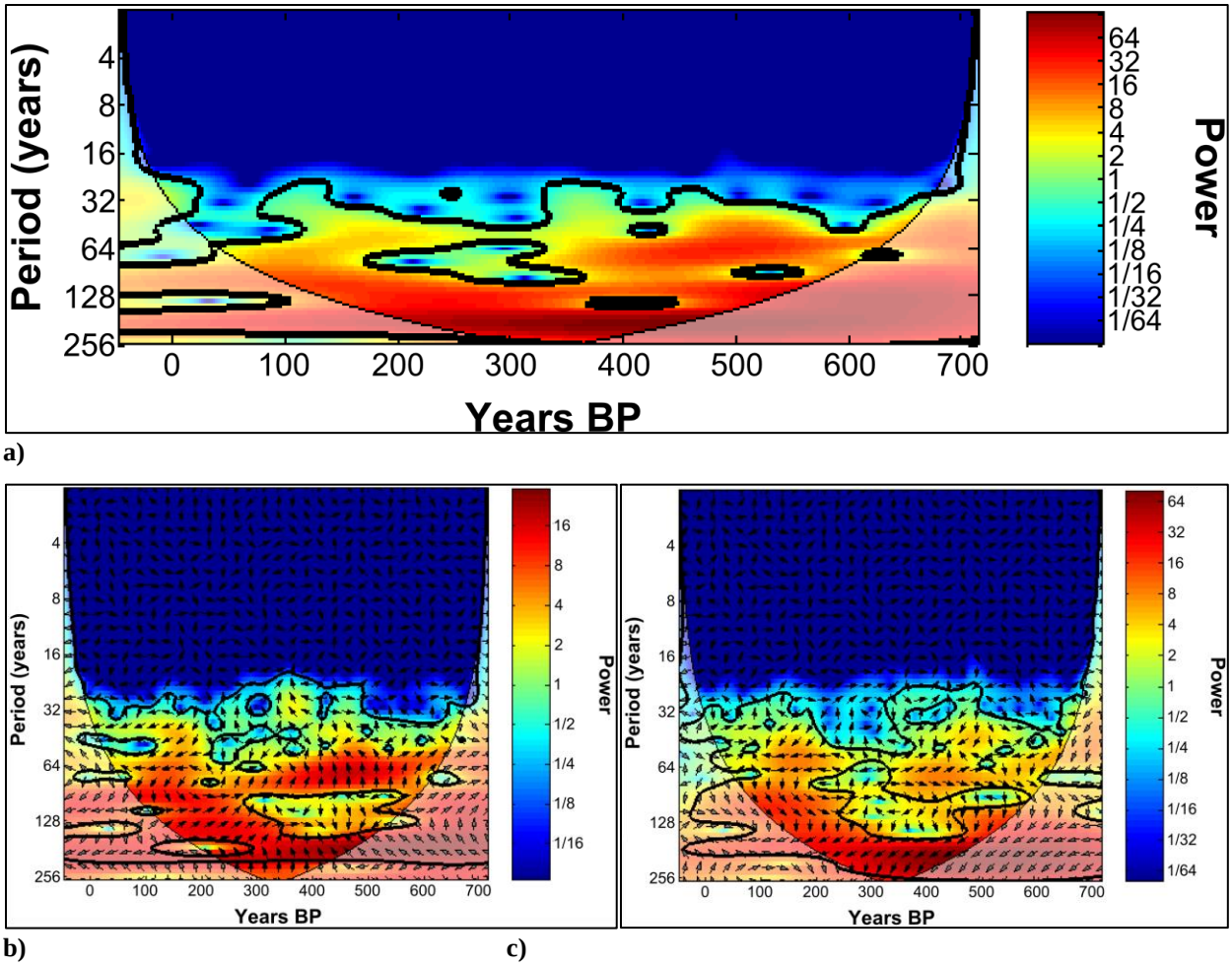

Figure 20. a) Wavelet of the Total Solar Irradiance record taken from Steinhilber et al. (2009). b) Cross-wavelet comparing the record of Steinhilber et al. (2009) with the C/N record of Danny's Lake top section. c) Cross-wavelet comparing the record of Steinhilber et al. (2009) with the %C record of Danny's Lake top section.

The arrows present on the cross-wavelets indicate whether correlations seen in the cross-wavelet are in phase, out of phase, or lagged in phase. Due to the error in the age model of Danny's Lake, there is not enough precision in the phase relationships of the cross-wavelets to take consideration of them with any degree of confidence. However, arrows which all point in the same direction within a particular region of a cross-wavelet are indicative of a consistent phase relationship at a particular frequency. This consistency in phase relationship is unlikely to be present in regions with little or no correlation. Because it is possible for cross-wavelets to display high-correlation colours (dark red regions) in cases when no actual correlation is present,

the pattern in the arrows acts as an important verification of high-correlation regions in the cross-wavelet (Grindsted et al., 2004). All of the cross-wavelets presented in this study appear to show strong consistency in arrow direction within dark red regions, suggesting that these dark red regions represent real correlations.

5.2.5. Middle Section High Resolution (2.5 mm) Isotopic Analysis (4737-3014 cal yr BP; 68.0-52.4 cm; averaging 27.6 years per 2.5 mm)

The middle section was analyzed at high resolution in order to compare recent short-term cyclicity with that from an earlier time period, as well as to gain insight to the 4000 cal yr BP transition period. While the long-term trends are consistent with the whole-core low-resolution section, actual values appear to be offset for each of the proxies. This offset is most likely due to slight difference in calibration of the standards between runs of the IRMS (the high-resolution middle section was analyzed during a different run than the whole-core low-resolution section). It is important to note that this offset only occurs between samples of different runs, and not among samples of the same run. Also, the offset is small and within error, and should not be considered as a discrepancy between runs. However, this offset is noticeable when combining the low-resolution and high-resolution profiles, creating the artificial appearance of spikes in the data. For this reason, the low-resolution and high-resolution sections have been kept separate.

5.2.5.1. Middle Section Profile

The middle section profile (fig. 21) displays an overall very minor increasing trend in $\delta^{13}C$ (-27.9‰ to -27.7‰), as well as C/N ratio (13.3 to 14.5), %C (7.6% to 15.0%), and %N (0.6% to 1.1%). $\delta^{15}N$ is consistent at around 2.9‰, with no overall change.

Much like the top section, the middle section displays small-scale variations throughout, although these variations generally appear more random and less cyclical than in the top section.

Additionally, again much like the top section, the high-frequency fluctuations in $\delta^{13}C$ and $\delta^{15}N$ vary a maximum of 0.1‰, which may not be significant beyond error. However, the high-frequency fluctuations seen in %C, %N and C/N ratio vary by around 1-3, which is likely significant.

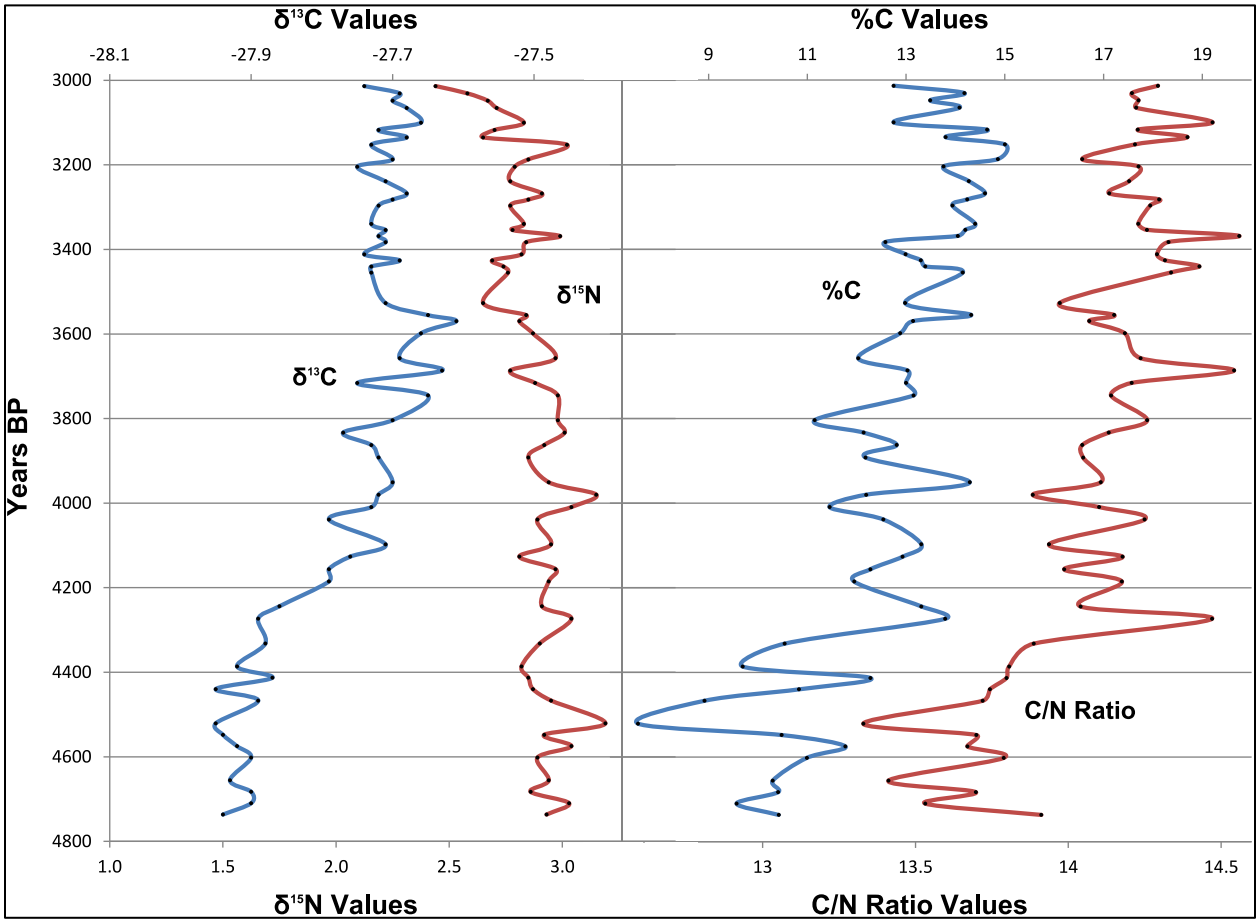

Figure 21. Danny's Lake middle section high resolution (2 mm) isotopic analysis.

5.2.5.2. Middle Section Spectral, Wavelet and Cross-Wavelet Analysis

To test the significance of these high-frequency fluctuations, spectral analysis was completed on C/N and %C in this section (fig. 22). Again, $\delta^{13}C$ and $\delta^{15}N$ were excluded because cyclical

variations in the results are not significant. C/N showed a 115-year cycle and %C showed a 101-year cycle, both with greater than 95% significance.

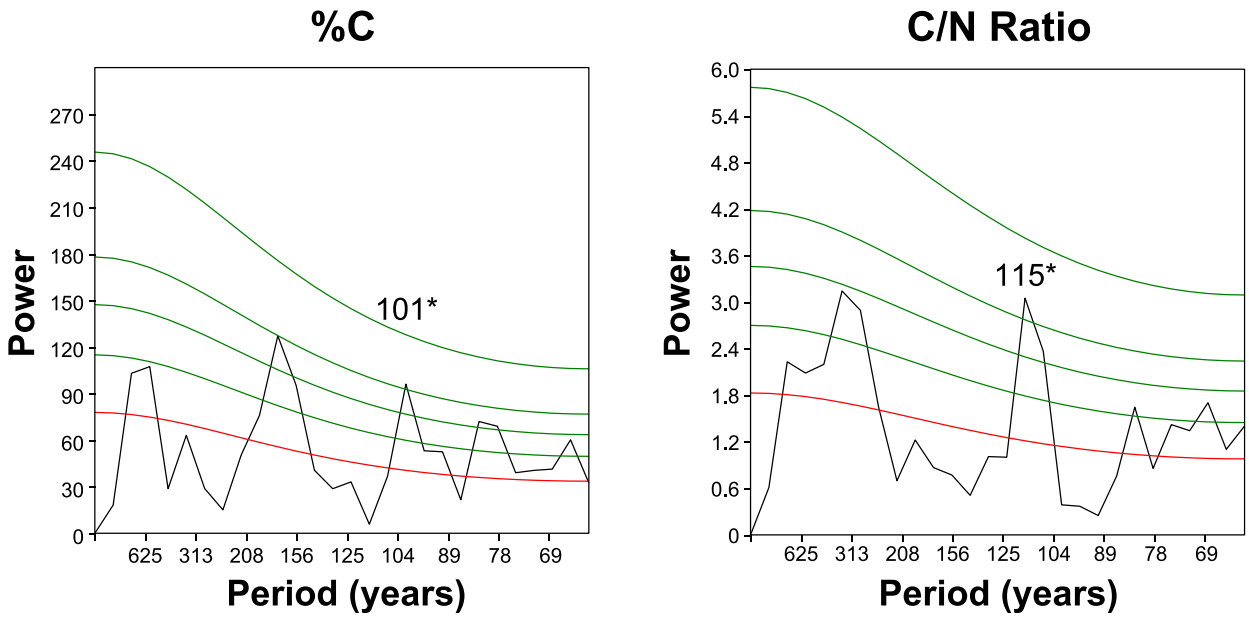

Figure 22. Danny's Lake middle section spectral analysis for %C and C/N Ratio. Peaks reaching above the highest green line are greater than 99% significant and are marked with (**). Peaks reaching above the second-highest green line but below the highest are between 95%-99% significant, and marked with (*).

Wavelet analysis for the middle section (fig. 23) displays weak on-and-off 101 year cycles in %C and 115 year cycles in C/N. Additionally, there appears to be a 157-172 year cycle in %C from around 4800-3600 cal yr BP. The C/N ratio also contains a small and weaker similar cyclicity during the same time period.

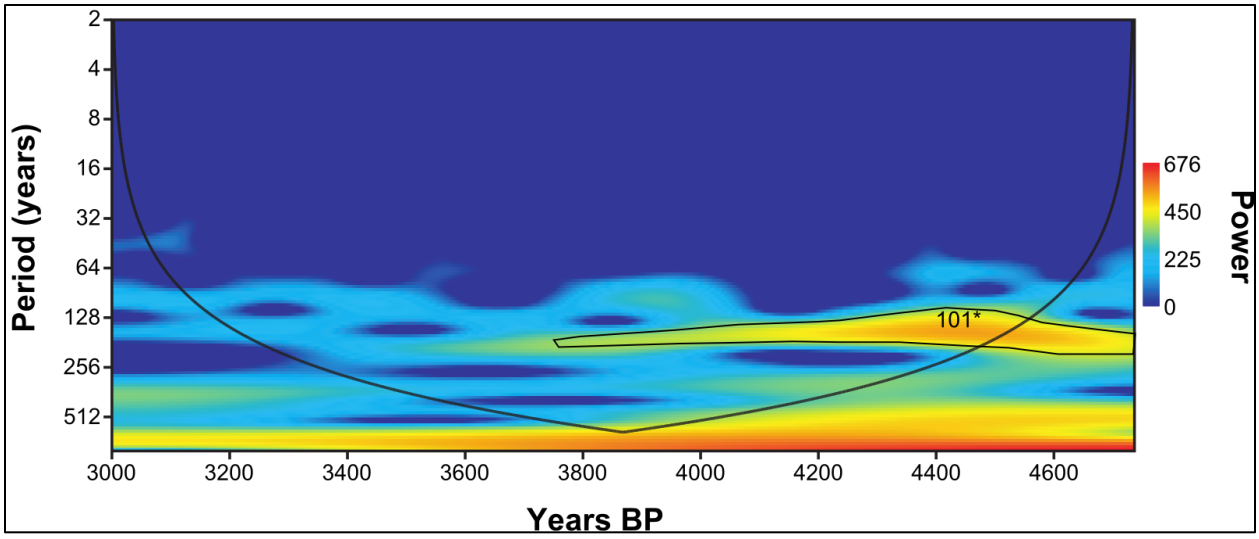

a)

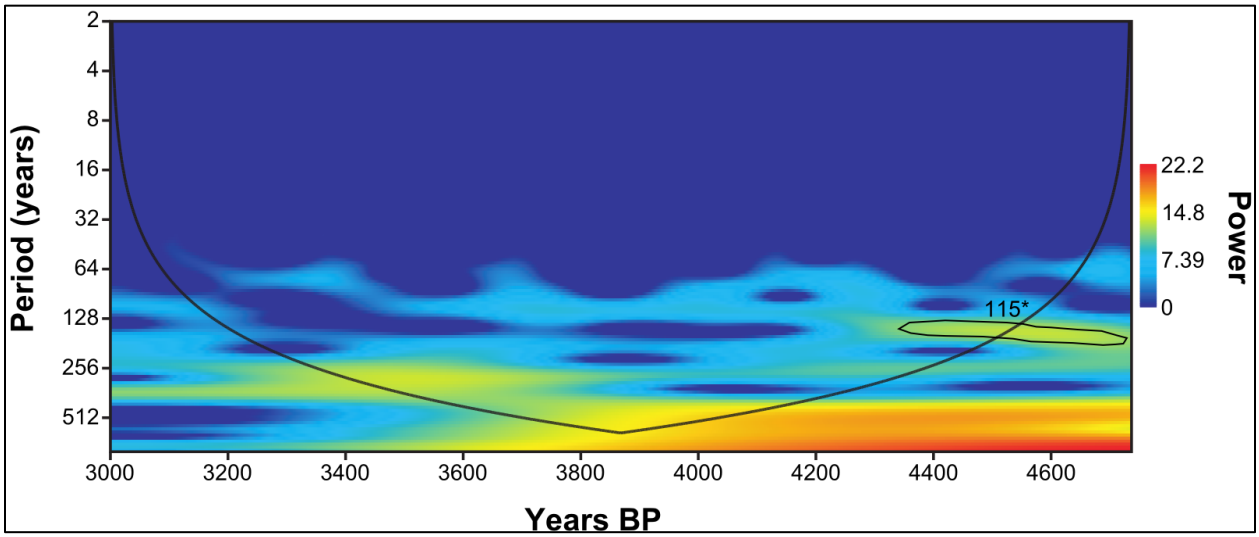

b)

Figure 23. Danny's Lake middle section wavelet analysis for a) C/N Ratio, and b) %C. Regions with strong power are highlighted and areas of strong power correlating to spectrally significant periods are labelled with the significant period (** = greater than 99% significance, * = greater than 95% significance).

Cross-wavelet analysis was used to compare %C with the total solar irradiance record of Steinhilber et al. (2009; fig. 24a), but not with any PDO record, as there is no PDO record available for this time period. The comparison with total solar irradiance does not show any major correlations, except for possible weak and inconsistent correlations at 120-140 years and 250-270 years (fig. 24b).

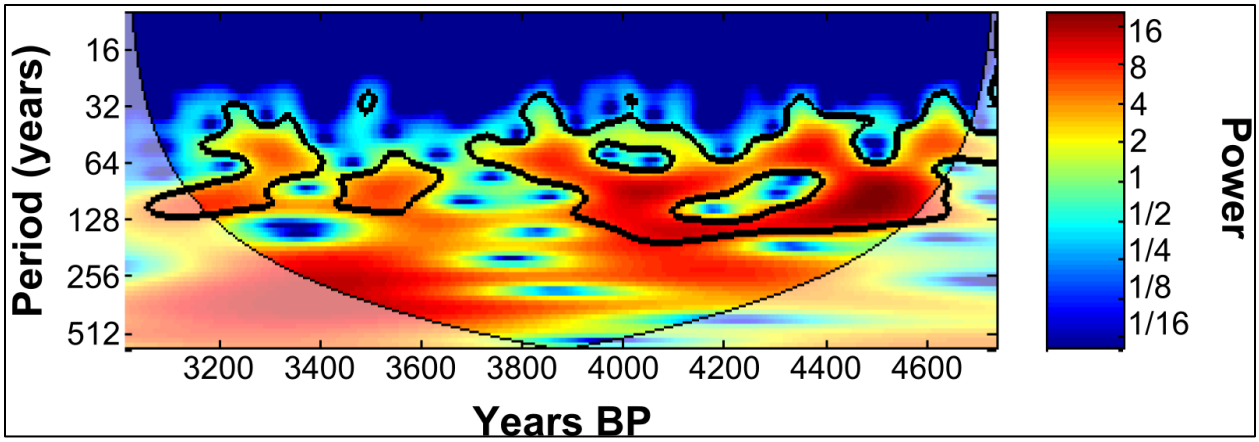

a)

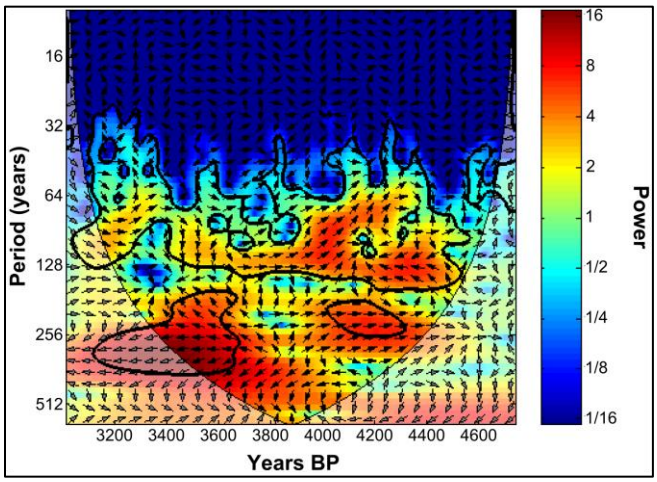

b)

Figure 24. a) Wavelet of the Total Solar Irradiance record taken from Steinhilber et al. (2009). b) Cross-wavelet comparing the record of Steinhilber et al. (2009) with the %C record of Danny's Lake middle section.

5.2.6. Bottom Section High Resolution (2.5 mm) Isotopic Analysis (7421-6295 cal yr BP; 101.0-86.4 cm; averaging 19.3 yr/2.5 mm)

The bottom section was analyzed at high resolution in order to gain insight into Zone II from the whole-core low-resolution analysis, most importantly at the sharp boundary at 6700 cal yr BP. No spectral, wavelet or cross-wavelet analyses were completed, due to the highly variable and chaotic nature of the proxy values through the section.

5.2.6.1. Bottom Section Profile

A high-resolution view in this section (fig. 25) displays a clear transition into Zone II at 7269 cal yr BP. This transition is marked by an initial spike in ^{13}C and a negative spike in the C/N ratio. ^{13}C, %C, and %N shift to decreased values through the remainder of Zone II, in comparison to their values in Zone I (-26.2‰ to -26.9‰, 12.0% to 9.8%, and 0.9% to 0.7%, respectively). At the sharp transition marking the boundary between Zones II and III, all proxies display a decreasing trend, although some show a sudden drop while others show a more gradual change. %C and %N both show a similarly steep decline during the transition, with %C dropping from 10.1% to 4.7%, and %N from 0.8% to 0.4%, over a 122 year period. The C/N ratio drops even more rapidly, showing a drop from 13.8 to 12.8 (significantly greater than any of the surrounding C/N spikes) in just 61 years. Meanwhile, $\delta^{13}C$ and $\delta^{15}N$ decline much more gradually over the entire high-resolution section, with only a slight increase in rate of decline during the transition period.

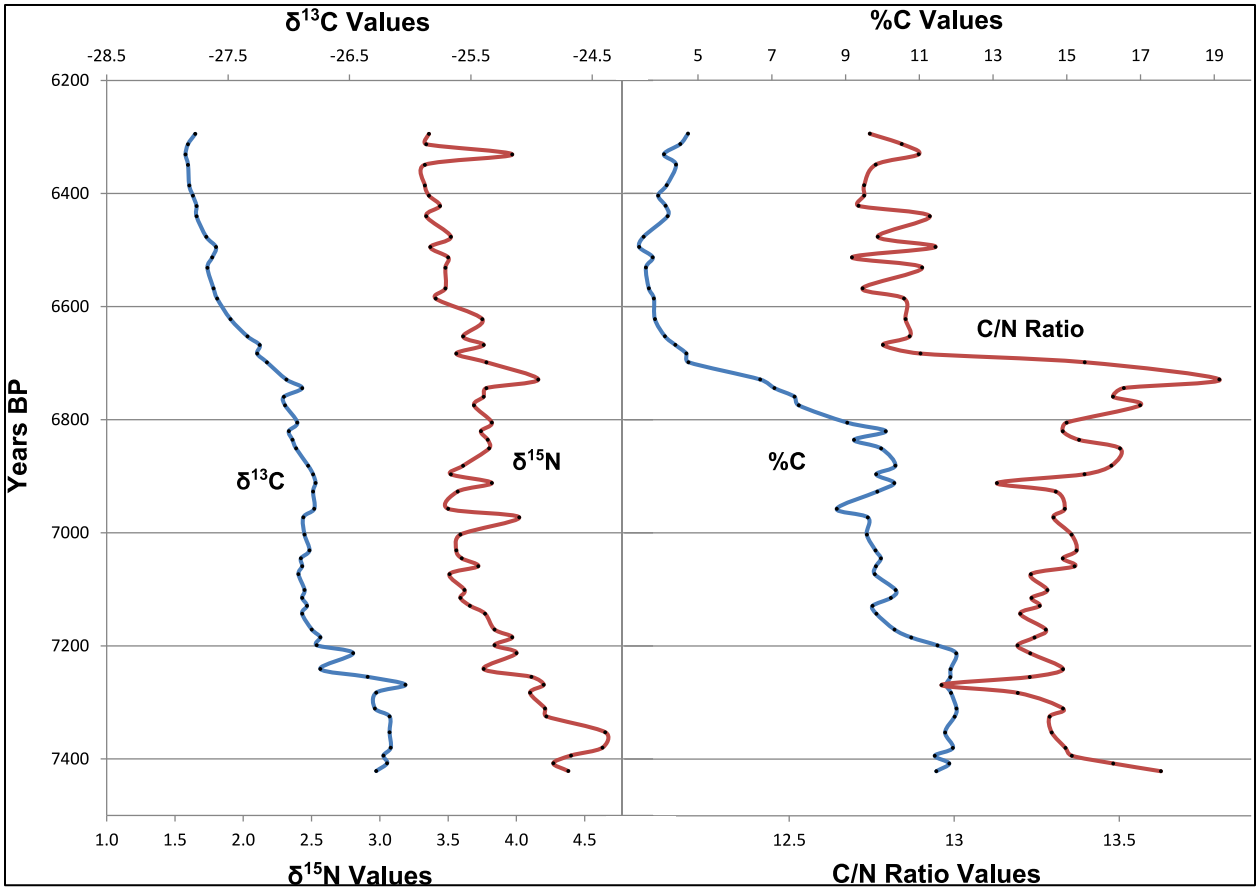

Figure 25. Danny's Lake bottom section high resolution (2 mm) isotopic analysis.

5.3. Horseshoe Lake Core

5.3.1. Chronology

Based on the age model, Horseshoe Lake extends to nearly 9000 cal yr BP, with an average accumulation rate of 85 yr/cm. However, much like Danny's Lake, Horseshoe Lake also has a highly variable accumulation rate over time. The accumulation rate was low (~20 yr/cm) between 8700-7500 cal yr BP, then increased to 225 yr/cm by 5000 cal yr BP. Above ~7500 cal yr BP the accumulation rate again gradually decreased to 100 yr/cm by 3000 cal yr BP, then increased to 150 yr/cm by 2000 cal yr BP and finally decreased again to 60 yr/cm at the top of the core.

5.3.2. Sedimentology

Horseshoe Lake core (fig. 26) extends from surface to a depth of 100.5 cm. It is composed primarily of silt and mud. Overall, the organic content appears to be less and the average grain size appears to be larger than at Danny's Lake. Much like Danny's Lake, this core contains no laminations or other textures. The colour grades from dark brown near the top to lighter brown towards the bottom, then grades into grey clay at the bottom.

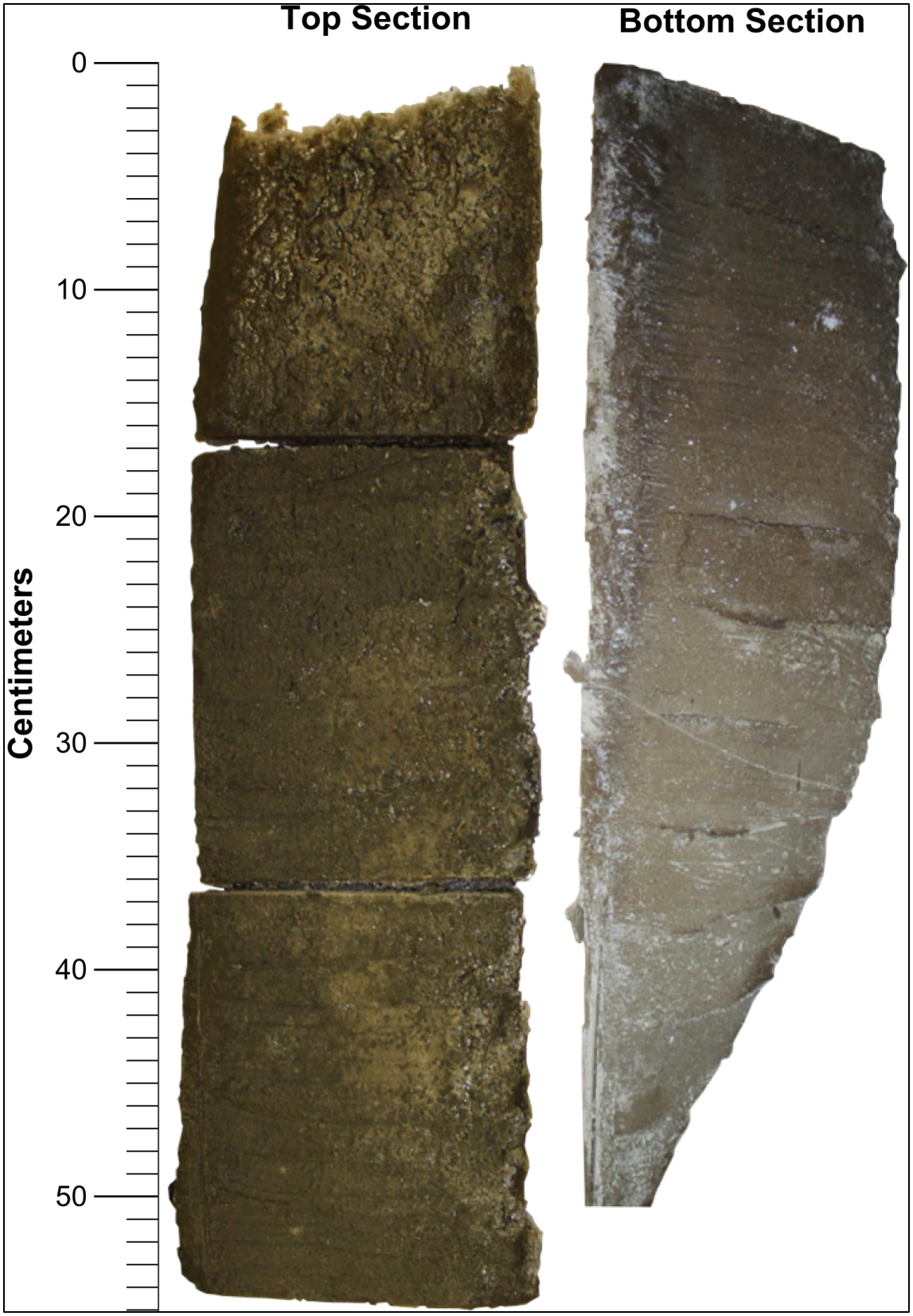

Figure 26. Horseshoe Lake core. *Photo by Andrew Macumber.*

5.3.3. Whole-Core Isotopic Analysis at 1 cm Resolution

Like Danny's Lake, the Horseshoe Lake core was analyzed from top to near bottom (down to 84 cm depth) at a 1 cm resolution (fig. 27). However, due to the low-quality results obtained from this profile, no high-resolution sections were analyzed.

From the bottom to the top of the core, C/N ratio, %C, and %N all show a very general increasing trend from bottom to top (11.5 to 14, 2.4% to 15.7%, and 0.2% to 1.1%, respectively). $\delta^{15}N$ remains relatively constant at around 2.25‰, with seemingly random fluctuations ranging from 1.7‰ to 2.9‰. $\delta^{13}C$ shows an enrichment trend from 8500 cal yr BP (core bottom) to 7200 cal yr BP (-22.3‰ to -21.3‰), followed by a depletion trend to 900 cal yr BP (down to -23.7‰), and then another enrichment trend to present (reaching -23.2‰). These values are far more enriched than those of Danny's Lake. In addition to the overall trends, there are smaller-scale variations, although they appear much more chaotic and less cyclic than those of Danny's Lake. The only consistent small-scale feature is a large positive spike in all proxies (with the exception of the C/N ratio, which has a negative spike) from 3180-2890 cal yr BP.

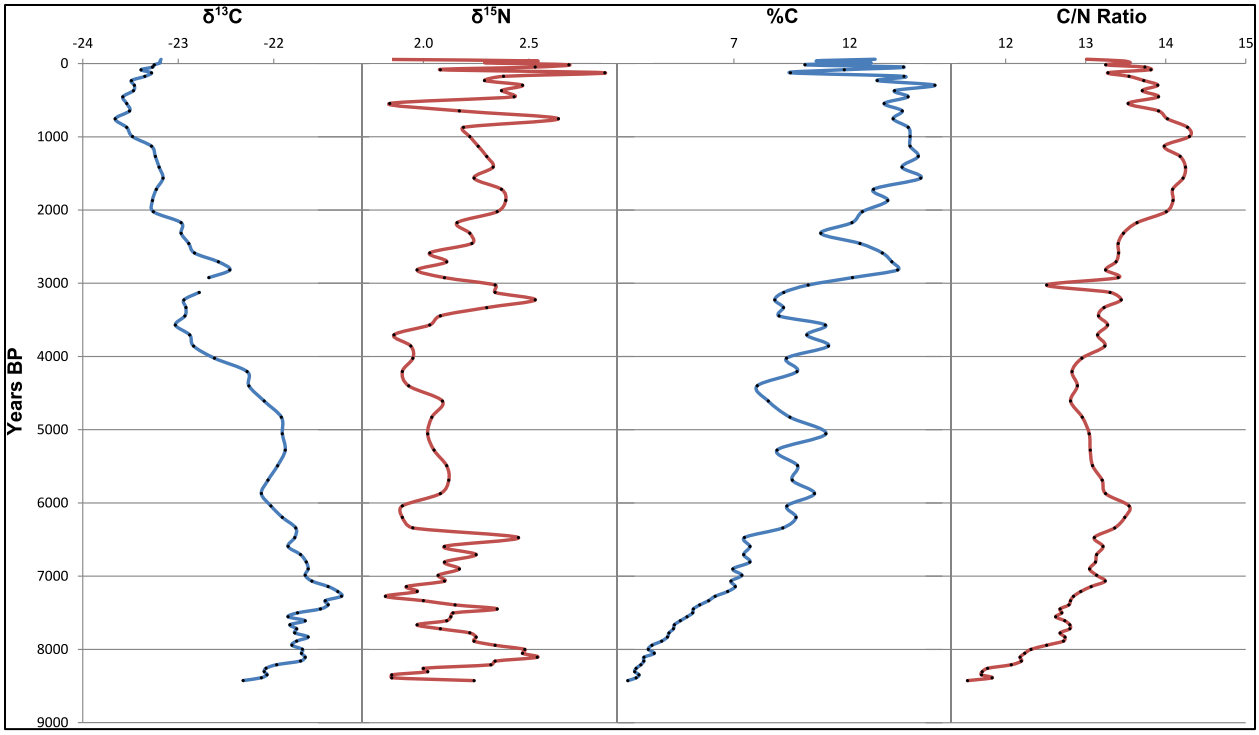

Figure 27. Horseshoe Lake whole-core isotopic analysis at 1 cm resolution.

6. Discussion

6.1. Modern Lake Survey

Sample data for the modern lake survey were divided into tundra, forest and transition zone groups based on major differences in environmental conditions between these environments. Differences in values of environmental parameters have been demonstrated by Ruhland and Smol (1998), who performed a survey of lakes throughout the north-central NWT and Nunavut and found higher ion concentrations, conductivity, alkalinity, and pH levels at boreal forest sites than at tundra sites. In addition to the three environmental groupings, a fourth grouping (R09) was created. This grouping was created to separate out all samples acquired from lakes located adjacent to an all-season road with high-frequency traffic (fig. 1), due to the possibility that dust or other anthropogenic pollutants affect these sites.

Numerous apparent outliers were determined using Tukey boxplots (Appendix). While most of these outliers may be attributable to the inherent right-skew of the data, there are four outliers which clearly stand out (one Ni, two Mn, and one Fe value), all of which belong to just two samples (R11-14-04 and R11-17-05). Values for these samples are found to be quite high for many of their variables, accounting for many of the other possible outliers seen in the boxplots. These samples are not near any known sources of contamination, nor are they near each other geographically, and they do not share an ecoclimatic region (one is in boreal forest while the other is in tundra). However, it is likely that local geology plays a strong role in altering the values of these outliers. In a similar lake survey, Ruhland and Smol (1998) found a group of tundra samples with anomalously high values for variables such as pH, conductivity, alkalinity, Mg and Ca. These anomalies were attributed to unique local bedrock and surficial geology surrounding those lakes. While there were enough of these anomalous samples in the Ruhland and Smol study to keep them and consider them a separate group, in our own study there are only two anomalous results and therefore they must be omitted.

Before the dataset could be investigated using multivariate analysis, the number of variables used for this analysis was reduced to nine. This was done because when dealing with multivariate analysis, the maximum number of variables which can reliably be used is dependent upon the sample size. In previous literature, this minimum sample-to-variable ratio ranges from 2:1 up to 20:1 (Everitt, 1975; Kunce et al., 1975; Cattell, 1978; Nunnally, 1978; Kline, 1979; Gorsuch, 1983; Marascuilor and Levin, 1983; Arrindell and van der Ende, 1985; Bryant and Yarnold, 1995; Hair et al., 1995; Velicer and Fava, 1998; MacCallum et al., 1999; Hogarty et al., 2005). However, ratios of 5:1 or less generally require large sample sizes. As such, a reasonable ratio of

approximately 8:1 was chosen for this study, which allows for 9 variables over the total of 71 samples and therefore requires some variables to be removed.

In order to reduce the number of variables used, groupings of similar (highly correlated) variables were created from which a single variable could be used as a representative of the group. Kendall's tau correlation in conjunction with Ward's method of hierarchical cluster analysis was used to determine correlations among variables in order to assist in the creation of goupings. Six groupings were determined:

Group A consists of the lithophile elements Ti, Li, and K, which have a very strong Kendall's tau correlation with each other, as well as many of the heavy metals (Pb, Fe, Al, Mn, As, Mg), which are also well correlated with each other and the lithophile group. All of these elements group together using cluster analysis as well. Heavy metals and lithophile elements are very often correlated with sediment grain size because these elements will readily bind to a surface, and small grains have a greater surface area than large grains. This correlation has been aptly demonstrated in previous literature (Horowitz and Elrick, 1987; Wang et al., 2006). While grain size data from the surface samples is not available to test this hypothesis, Group A is assumed to be most strongly affected by grain size due to findings from previous literature. Because these elements are all affected by the same process, just a single element from this group is required for multivariate analysis in order to avoid redundancy. Ti was chosen to represent Group A due to its extremely high correlation with other elements in the group as well as support from previous literature for the use of Ti as normalization factor for grain size (Horowitz, 1985).

Group B can be seen in the Kendall's tau correlation with the heavy metals Cu, Cd, Zn and Ni. These elements are also grouped separately with cluster analysis. These are mostly chalcophile elements which are often observed to increase through anthropogenic means (Singh et al., 1997;

Audry et al., 2004; Wu et al., 2007). Cu was chosen as the representative element for this group, as the Kendall tau correlation shows it to have the greatest correlation with the other elements from the group as well as the least correlation with other variables, suggesting that it may be the least affected by factors outside of that which directly affects Group B.

Group C includes %C, %N, C/N ratio, Ca, and S. These variables all show a strong Kendall's tau correlation with one another and group together with cluster analysis. It should not be surprising that %C and %N should group strongly together, as they are both dependent upon vegetation input. Because %C shows slightly greater correlation with other variables than %N does, it was chosen to represent both %C and %N for multivariate analysis. C/N ratio is obviously directly dependent upon %C and %N values, and can be removed. The reasons that Ca and S both correlate strongly with %C and %N are not so obvious, and therefore these elements are both of interest and should remain as part of the multivariate analysis.

Group D includes Na, conductivity and pH, all of which group strongly together in both the Kendall's tau correlation and the cluster analysis. Na is obviously a strong factor in determining conductivity, and conductivity and pH directly affect one another, so this grouping is not surprising. Because conductivity appears to show the strongest Kendall's tau correlation with the other two variables, it was chosen to represent this group.

Group E includes ^{13}C, ^{15}N and dissolved oxygen (DO), all of which group together using cluster analysis. Realistically, however, DO shows very little Kendall's tau correlation with any other variables and can be removed. While ^{13}C and ^{15}N correlate with each other moderately, they are both proxies of interest for this study and were chosen for use with multivariate analysis.

Group F includes water depth, U, Hg and P, all of which group together using cluster analysis. However, there is not a great Kendall's tau correlation of any of these variables with many

others. The exception is Hg, which appears to show moderate to good correlation with numerous other variables, including the isotopic proxies. Therefore, Hg is a variable of interest and was chosen to represent this final group.

Once the variables of interest were chosen, Principle Components Analysis (PCA) was conducted on the data. PCA indicates that the predefined groupings of Arctic Tundra, Transition Zone and Boreal Forest are most greatly affected by the variables C, S, and Ca, with strong loadings from Hg, ^{15}N, and ^{13}C as well. A weaker but significant loading is also seen with conductivity. The C loading is not surprising, as a forested catchment would deliver much higher terrestrial vegetation to the lake sediments than a tundra catchment would. In turn, this terrestrial organic matter input is likely to affect variations in ^{13}C and ^{15}N if the value of these isotopes from terrestrial vegetation is different from that of lake-derived vegetation. It is likely that variations in ^{13}C and ^{15}N values from Danny's Lake from 6700 cal yr BP to present are primarily due to variations in the amount of terrestrial organic matter input. This can be inferred from the importance of ^{13}C and ^{15}N shown between ecoclimatic regions with the PCA as well as the fact that the ^{13}C and ^{15}N profiles are anti-correlated with C/N ratio in Danny's Lake after 6700 cal yr BP.

The remaining significant loadings, seen in S, Ca, Hg, and conductivity, are also not surprising. Higher levels of Ca in boreal vs. tundra environments can be attributed to greater pH levels. As pH shows good correlation with and is part of the conductivity group, we can expect that the positive correlation of boreal forest with conductivity is also attributable to pH. The increase in conductivity is most likely due to the discontinuous permafrost conditions within the lake catchment, as opposed to the continuous permafrost conditions of the tundra. Discontinuous permafrost allows greater groundwater flow and therefore increased ion concentration and

conductivity of the lake water. pH is likely to be higher in boreal forest as opposed to tundra due to the fact that boreal forest environments tend to bring in dissolved inorganic carbon (DIC) to the lake as bicarbonate from the catchment, as opposed to CO_2 from the atmosphere. A CO_2-rich source of DIC in tundra lakes causes a reduction in pH values. A positive correlation between Hg concentrations and boreal forest may also be attributable to extraction from soils due to groundwater. These results are very similar to that of Ruhland and Smol (1998), who also found an increase in ion concentration, conductivity, pH, and Ca in boreal forest conditions. The positive correlation between boreal forest and S concentrations may be attributable to extraction from soils by groundwater, or perhaps due to greater ease of sulphate reduction by microbial activity in higher pH conditions.

PCA suggests that the R09 group is separate from the other groups, but for much different reasons than the separation between the Arctic/Transition/Boreal groups. Rather, the R09 group shows much lower Cu concentrations than the other groups, as well as greater conductivity and Ti. The increased conductivity is likely due to ions leaching into lakes from salting of the nearby road. Increased Ti may be suggestive of overall lower grain sizes within this group, as small grain sizes have been shown to strongly affect Ti and other heavy element concentrations (references). Reduced grain sizes may be due to small dust particles being introduced to the sediments from road activity. Alternatively, higher values of Ti and the other lithophile and heavy metal elements within Group A may be the result of anthropogenic influences from sources such as automobile exhaust. However, this possibility appears to be at odds with the fact that Group B heavy metal elements, represented by Cu, are in very low concentrations within the R09 group.

It is unclear why there is such a low concentration of Cu (and presumably Cd, Zn, and Ni, which also make up Group B) in the R09 group. These heavy metals are often associated with anthropogenic pollution, and therefore their low concentrations in the R09 group are somewhat surprising. It is possible that other anthropogenically altered variables, such as conductivity, pH, or dust levels, may be affecting Cu in non-obvious ways. Alternatively, the R09 group is geographically fairly clustered, allowing for the possibility that local geology may be affecting variables within the sediments in ways in which samples from other groups are unaffected.

Based on the strong separation of the R09 group from the other groups in ways which appear not to have much effect on those other groups with PCA, as well as the strong clustering of R09 samples with Ward's hierarchical cluster analysis, it appears likely that the R09 group is indeed a distinct and unique group. A scatterplot of Ward's cluster analysis ordering of samples plotted against latitude illustrates clearly that there is a strong latitudinal effect influencing the Arctic Tundra, Transition Zone, and Boreal Forest groups. This latitudinal effect is not present in the R09 group. This suggests that while the arctic tundra to boreal forest environmental transition is the strongest factor affecting the variables of most sites, sites beside the road are dominated by a totally different and not well understood process. It is likely that this process is related to anthropogenic effects.

6.2. Danny's Lake Core

Results of whole-core isotopic analysis of Danny's Lake core clear trends, as well as distinct timings of overall changes in trends for multiple isotopic proxies. These locations were marked as boundaries between zones. Four zones were delineated, and shall be labelled Zone I, Zone II, Zone III and Zone IV (fig. 14). Additionally, the top high-resolution section, which was analyzed separately, may be considered as Zone V.

In addition to isotopic analysis, grain size analysis (Macumber et al., in prep.) and pollen analysis (Sulphur et al., in prep.) were both completed through the core. Much of the paleoenvironmental interpretation of isotopic results relied heavily on comparison with both the grain size and pollen results, and as such both of these other proxies will be references regularly throughout the following discussion.

6.2.1. Zone I (8145-7300 cal yr BP; 114.2-100.2 cm)

The very bottom of the core, at just over 8000 cal yr BP, contains extremely low organic content, suggesting that the earliest stages of Danny's Lake may have existed in an environment with relatively few plants of either terrestrial or aquatic origin. Low C/N values indicate that the small amount of organic material present originated mostly from within the lake. Of the terrestrial component, pollen analysis reveals high proportions of *Betula* (birch) pollen, likely reflecting shrub-tundra in the catchment at this time. Low proportions of pollen from arboreal taxa, such as *Picea* (spruce), indicate that the lake catchment was not forested (Sulphur et al., in prep.). Such low-productivity catchment conditions should result in catchment-derived DIC with enriched $\delta^{13}C$ values, due to the likely presence of ^{13}C-enriched glacial clays and tills, as well as a relative lack of depletion through fractionation from vegetation. Indeed, the earliest $\delta^{13}C$ values are highly enriched in comparison to later values in Danny's Lake and other lakes in similar environments (Wolfe et al., 1996; 1999). This earliest stage of the lake most likely occurred during a time just after deglaciation occurred in the area, so a relative lack of arboreal vegetation probably represents a lag time in the establishment of climax vegetation communities in the region; although shrub tundra may also have been maintained by abundant fires and/or climate conditions (Sulphur et al., in prep.).

A drastic increase in organic material through this zone, as well as a large decrease in $\delta^{13}C$, suggests that vegetation did not take long to become established in the region. In fact, organic material content quickly reaches some of the highest levels seen through the core, indicating that vegetation quickly became very abundant. Pollen accumulation rates of Picea albertiana increase, likely reflecting the initial expansion of arboreal vegetation in the region (Sulphur et al., in prep.). The minor increase in C/N values during this time suggests a small increase in terrestrial vegetation input; however, C/N values plateau at around 12.6, suggesting a primarily aquatic source of organic material (Meyers and Ishiwatari, 1993; Meyers, 1994). The high organic matter input in combination with low terrestrial input suggests that lake productivity was very high at this time. This possibility is also supported by a $\delta^{13}C$ enrichment, which may have been at least partially caused by an abundance of algae in the lake during high-productivity conditions. At northern latitudes, productivity is usually related to temperature, because lower temperatures increase time of winter lake ice-cover and subsequently reduce the length of the productive summer season (Willemse and Törnqvist, 1999). Hence, higher productivity in Zone I is likely due to warm temperatures.

Grain sizes during this time are dominated by clay-sized fractions and few silt or sand-sized particles (Macumber et al., in prep). Certain studies suggest that larger grain sizes are indicative of drier conditions, due to either large changes in lake level for lakes with a steep-sided catchment (Menking, 1997), or a strong aeolian influence (ie. Wang et al., 2001). Other studies, however, suggest that smaller grain size reflects drier conditions, due to lower runoff energy from the catchment to the lake (Sun et al., 2002; Chen et al., 2004; Conroy et al., 2008). Because Danny's Lake does not have a steep-sided catchment, nor exists in an exceptionally windy area with access to abundant aeolian sediments, abundance and intensity of precipitation to the

catchment can be assumed to be the primary factor affecting grain size. In this case, the dominance of small, clay-sized particles during this time indicates a dry environment. If this is the case, then it must be recognized that such a dry environment, with a very low accumulation rate of sediments into the lake, may partially be responsible for the increased organic material, as organic sedimentation from algae may have been the primary source of sedimentation into the lake.

Isotopic data is also consistent with a dry climate. Low abundances of terrestrial vegetation and maintenance of shrub tundra could be expected in these conditions, for example, by frequent fires (Sulphur et al., in prep.), supporting the low C/N ratio seen during this time. Additionally, a dry climate is likely to result in closed hydrological conditions in Danny's Lake catchment, in which input and output of water to the lake is dominated by atmospheric processes (evaporation) rather than catchment processes (runoff or groundwater). Such conditions should be reflected in an enrichment of ^{13}C, as aptly demonstrated by Wolfe et al. (1996; 1999; 2003) in similar environments, and is clearly seen in Danny's Lake core during this time.

Isotopic, grain size, and pollen proxies all illustrate that the climate was both warm and dry from 8000-7300 cal yr BP. Such conditions are well-supported by previous literature (Heusser et al., 1985; Wolfe et al., 1996; Kaufman et al., 2004) and are probably caused by a higher summer insolation during the Early Holocene (Berger and Loutre, 1991).

6.2.2. Zone II (7300-6700 cal yr BP; 100.2-91.2 cm)

A transition to slightly wetter and possibly cooler conditions is the most likely explanation to account for the changes seen in Zone II. Specifically, the bottom high-resolution section shows a positive spike in $\delta^{13}C$ and a negative spike in C/N ratio at 7269 cal yr BP, which may be due to a nutrient-driven productivity spike caused by the initiation of wetter conditions. Following this,

slightly more depleted $\delta^{13}C$ values through the remainder of the zone are consistent with a depletion of DIC from increased flushing driven by more open hydrological conditions (Wolfe et al., 1996; 1999; 2003). Depleted $\delta^{13}C$ values could also be indicative of reduced productivity, which suggests the possibility of cooler conditions during this time. Reduced organic matter content as well as elevated C/N values support this notion. The dip in organic matter seen at this time may also be caused by a dilution of organic matter content by an increased mineral accumulation rate due to an increase in precipitation. Grain size increases in this zone, with an increased component of silt, supporting the notion of an increase in precipitation at this time (Macumber et al., in prep.). Pollen evidence suggests a delayed change which occurred at 95 cm depth, in which *Betula*-dominated shrub tundra gave way to boreal forest vegetation dominated by *Picea*. *Alnus* (alder) also became abundant at this time. This transition is interpreted to reflect the development of moister climate conditions (Sulphur et al., in prep.). A lack of immediate response of terrestrial vegetation to increased precipitation may simply be because the change was not great enough to significantly affect the terrestrial ecosystem. Alternatively, if the climate was cool during this time as suggested by $\delta^{13}C$, organic matter content and C/N ratio, then continuous permafrost may not have had a chance to melt and would have made it very difficult for more deeply-rooted forest vegetation to become established. Additionally, Huang et al. (2004) suggest that timing of tree line advancement from site to site may vary by hundreds of years based on varying amounts of local glacial till which could be used as soil. As the Danny's Lake region is largely surrounded by exposed Precambrian Shield, it is plausible that there would be a substantial delay in the advancement of forest to this area.

The end of Zone II at 6700 cal yr BP, marked by profound changes in all isotope proxies as well as a sudden change in colour of the sediment, is the most distinctive feature of the Danny's Lake

core. It is clear that a sudden, major event occurred at this time which, based on the later record, changed the dynamics of the lake permanently. The colour change is certainly due to the drastic change from organic-rich to clay-rich sediment. Many of the lakes which were cored for the PANWT project contain clay-rich sediments at the very bottom which transitioned suddenly to much more organic-rich sediments. The clay sediments in these cores most likely originate from glacial runoff, during a time when the glacier margin was still advanced enough that the lakes were proglacial. Once the glacier retreated beyond the extent of the catchment of these lakes, they immediately transitioned to non-proglacial lakes with organic-rich sediment. This type of transition from clay-rich to organic-rich, with a glacial mechanism, is well-documented in lakes near the margins of receding glaciers (Briner et al., 2010). However, this transition period in Danny's Lake core is unusual in two regards. First, the transition at Danny's Lake is opposite of other lakes observed in the PANWT project; that is, the transition in Danny's Lake is from organic-rich sediments to clay-rich sediments, rather than the other way around. This suggests that if the mechanism of the transition is glacial, then the glacier must have been advancing rather than receding, which is unlikely for this time period. Second, pollen data delineates a large transition just before the colour change, at 95 cm, with major and immediate changes in abundances of numerous pollen species which suggest a transition from shrub tundra to boreal forest in this region (Sulphur et al., in prep.). Such a close association of sudden pollen changes with the colour change in the core strongly suggests that the mechanism of the colour change transition may have been climatological rather than glacial.

Based on these pollen changes, the climate at this core depth is interpreted to have shifted from a dry to a wet climate (Sulphur et al., in prep.). With the introduction of forest to the Danny's Lake catchment, an increase in both organic material and C/N ratio may be expected. As an

example, Wolfe et al. (1999) found a sudden decrease in both organic material and C/N ratio following the transition from forest to tundra at a lake in Siberia. However, this pattern is not seen at Danny's Lake. Rather, the transition from tundra to forest is accompanied by a drastic reduction in organic matter as well as a decrease in C/N ratio, as opposed to the expected increase. However, these discrepancies may primarily be the result of a drastic increase in sediment accumulation rate rather than any actual change in organic matter input. Indeed, grain size data shows a large and sudden change at the transition zone from clay-dominated sediments to silt and sand-dominated sediments (Macumber et al., in prep.). This supports the view that the main cause of the transition at 6900 cal yr BP was a sudden major increase accumulation rate, caused by an increase in precipitation. A depletion in $\delta^{13}C$ also occurs at this transition, which may have resulted in a change to hydrologically open conditions in the catchment due to increased precipitation and a greater input of ^{13}C-depleted DIC from the catchment (Wolfe et al., 1996).

This transition period may be related to climate shifts observed for other lakes in the region. Most studies record a shift in climate at around 5000 yr BP, generally to wetter conditions as the dry Arctic air front moved north (Moser and MacDonald, 1990; Wolfe et al., 1996; Pienitz et al., 1999; Ruhland and Smol, 2005). While the timing in Danny's Lake is somewhat earlier than what may be expected based on previous studies, Huang et al. (2004) found that a tree line shift occurred at 6300 cal yr BP in UCLA Lake, just east of the study site. This timing is very similar to that at Danny's Lake, and may be attributable to similar local environmental conditions. For example, much like UCLA Lake, Danny's Lake is surrounded predominantly by bare Precambrian Shield rock, which may delay the growth of forest compared to areas around other nearby lakes that contain abundant glacial sediments (Huang et al., 2004). Realistically,

however, age models from previous studies in the area are not well-constrained, often containing as few as two to four age dates through the entire core (MacDonald et al., 1993; Wolfe et al., 1996; Pienitz et al., 1999; Ruhland and Smol, 2005; MacDonald et al., 2008). Additionally, none of these studies have taken into account a possible FRE, despite the abundant use of bulk organic sediment for age dates. As such, it may be realistic to expect age model errors on the order of 1000-2000 years for these studies. The Danny's Lake timing of 6900 cal yr BP for the advancement of the tree line may therefore correlate with, and be a more accurate date for, the later climate shift seen by previous researchers in nearby areas.

6.2.3. Zone III (6700-3900 cal yr BP; 91.2-62.2 cm)

After 6700 cal yr BP, a shift to isotopic values with less variation and more gradual trends suggests that the lake system became much more stable. Major shifts in climate or lake dynamics, such as fluctuations between open and closed hydrological systems or variations in stratification or pH, are unlikely to have occurred after this point, as these types of changes would most likely result in sharp variations in proxy values (Wolfe et al., 1996; Leng et al., 2006). However, gradual trends do suggest that changes were likely occurring, albeit at a much slower pace. An increasing trend in C/N ratio from 12 to 17 indicates that the lake sediments were changing from being dominated by aquatic vegetation to becoming primarily dominated by terrestrial vegetation. This trend is mirrored by an increasing trend in organic matter abundance, which suggests that the increasing dominance of terrestrial vegetation was caused primarily by an increasing supply of vegetation from the catchment, rather than a dwindling supply of aquatic vegetation. Such an increase in catchment vegetation input is likely the result of a buildup of vegetation in the catchment following the introduction of more favorable climate conditions for vegetation (increased moisture). This is the reasoning of Wolfe et al. (1999), who also found

increased C/N values in forest as opposed to tundra conditions. Peat, in particular, may have begun to accumulate slowly at this time (averaging 100 cm growth per 1000-2000 years; Clymo, 1991), and as it became thicker and more developed, a greater degree of input from this catchment vegetation source could be expected. *Sphagnum* (peat moss) and other moss spores begin to increase in the Danny's Lake pollen record near 75 cm (Sulphur et al., in prep.). Such a buildup of vegetation would also tend to hold on to any remaining minerogenic sediment in the catchment, reducing the input rate of these sediments to the lake and thereby acting as a secondary mechanism to increase relative organic matter abundance in the sediment.

Additional support for increased precipitation in this zone can be found in the grain size data. Average grain size at this time is significantly greater than it is prior to 6900 cal yr BP, with a relative reduction in clay and an increase in both silt and sand components. These results suggest that input energy to the lake was much greater, due to an increase in runoff and therefore precipitation (Macumber et al., in prep.). In Danny's Lake, such an increase in precipitation is especially prone to major increases in runoff, due to the low-soil, discontinuous permafrost setting. This increased runoff may also act as an additional cause of increased C/N values, due to the abundance of particulate terrestrial organic carbon this runoff provides to the lake (Kaushal and Binford, 1999).

Further evidence for a wet period in Zone III can be found in the pollen data, which corroborates a transition to a wet and forested period through Zone III. For example, peak accumulation rates of Picea mariana pollen occur near 87 cm, suggesting a time of maximum expansion of this taxa (Sulphur et al., in prep).

Additionally, $\delta^{13}C$ and $\delta^{15}N$ experience a gradual depletion, which is also what may be expected due to open hydrological conditions in the catchment during a wet period (Wolfe et al., 1996;

1999; 2003). However, the actual value of change in these trends is not large and may be insignificant. Because both of these proxies (especially $\delta^{15}N$) are anti-correlated with C/N through both Zone III and Zone IV, their variations may also simply be caused by changes in terrestrial vegetation input due to slightly depleted values in the terrestrially sourced organic carbon compared to the aquatically sourced component. Support for this possibility is shown through the correlation of ^{13}C and ^{15}N with boreal forest vs. tundra environments using multivariate statistics (see section 5.1). Additionally, previous research has shown that $\delta^{13}C$ values of living terrestrial material from boreal forest environments (-27.9‰; Junger and Planas, 1994) appears to be slightly more depleted than benthic lake algae (-26‰; France, 1995). France (1995) suggests that aquatic plants tend to have more enriched $\delta^{13}C$ values than terrestrial plants due to the more resistant diffusion gradient surrounding aquatic plants in water. $\delta^{13}C$ values for Danny's Lake agree well with these terrestrial and algal values, although are much closer to the terrestrial value, suggesting that organic material in Danny's Lake through Zones III and IV is primarily dominated by terrestrial input, with some algal input causing the trends. Palynomorphs of obligately aquatic plants (e.g., *Myriophyllum*) are indeed a rare constituent of the Danny's Lake pollen record (Sulphur et al., in prep.). A similar mechanism was employed as an explanation of $\delta^{13}C$ trends in a lake in southern Ontario (Aravena et al., 1992). Additionally, near the current study area, Wolfe et al. (1996) found that $\delta^{13}C$ values from the cellulose component of lake sediment organic matter, (attributed to an entirely aquatic source of organic carbon), was slightly enriched compared to bulk organic carbon (containing a component of terrestrial carbon input). A similar pattern in Danny's Lake would certainly account for the minor variations seen in $\delta^{13}C$.

A wet period from 6900-4000 cal yr BP is in general agreement with previous studies in the area (Moser and MacDonald, 1990; MacDonald et al., 1993; Wolfe et al., 1996; Pienitz et al., 1999; Huang et al., 2004; Ruhland and Smol, 2005). Most of these studies have found a wet period, with an advanced tree line, from around 5000-3000 yr BP. However there are variations in the timing of these transitions of up to 1000 years or more, which is most likely attributable to errors in age models in these studies, diachroneity associated with edaphic (site-specific) factors, or uncalibrated dates from the earlier studies. As previously mentioned, the timing of the transition periods seen at Danny's Lake is likely to be a more correct assessment of the timing of transition periods throughout the region, due to the larger number of radiocarbon dates as well as the incorporation of an FRE (see Crann et al., in prep.).

6.2.4. Zone IV (3900-726 cal yr BP; 62.2-14.2 cm)

At around 4000 cal yr BP, trends for all proxies undergo a shift once again. C/N ratio and organic content stabilize and even trend towards a slight reduction. This shift suggests that terrestrial vegetation input to the lake has stopped increasing and may be slightly decreasing. However, pollen and spore accumulation rates of arboreal taxa including Picea and Larix, as well as non-arboreal pollen and spores, increase at this time, suggesting an expansion of terrestrial vegetation. These shifts, as well as a reduction in inferred fire frequency and magnitude, suggest a shift to cooler temperatures at this core depth (Sulphur et al., in prep.). A reduction in organic carbon content from the catchment despite expanding arboreal taxa may be due to a reduction in precipitation. However, there is little change in grain size over this period, indicating that precipitation may not have changed significantly (Macumber et al., in prep.). Cooler temperatures, as suggested by pollen analysis, may also have been the cause of a reduction in organic carbon, due to a reduction in lake vegetation.

The timing of this shift coincides nicely with the general timing of a well-known climate shift to cooler conditions throughout the northern hemisphere (Smol, 1983; Zabenskie and Gajewski, 2007; Finkelstein and Gajewski, 2008; Rolland et al., 2008; Adams and Finkelstein, 2010). This shift is the boundary from the Early/Middle Holocene to the Late Holocene "neoglacial period". In the central Northwest Territories, records show that this shift occurs at 3000 yr BP and is accompanied by a southerly retreat of the tree line (Moser and MacDonald, 1990; Pienitz et al., 1999; Ruhland and Smol, 2005). MacDonald et al. (1993) found this shift to occur at 4000 yr BP, which matches the timing of the Danny's Lake record. All of these studies interpreted this shift in tree line to be caused by a shift to cooler and sometimes drier conditions.

6.2.5. Top High-Resolution Section (Zone V; 714 to -48 cal yr BP; 14.0-0.3 cm)

The top section was analyzed using material from Face 1 rather than Face 2 due to the majority of material from the top of Face 2 being used for the study of other proxies. The determined depths of the two faces are assumed to be identical, and therefore these faces may be directly correlated with one another. However, because this correlation technique may not be entirely precise, as well as the fact that Face 1 and Face 2 may differ somewhat even at matching depths (despite being side-by-side), it is advisable to treat the boundary between the whole-core lower-resolution section and the top high-resolution section with caution.

Isotopic values, for the most part, do not shift significantly at the Zone IV/Top High-Resolution Section boundary. A shift to more enriched $\delta^{13}C$ values is evident, although this shift is extremely small (0.24‰) and is likely due to small errors in correlating the tops of Face 1 and Face 2 of Danny's Lake core. The only somewhat significant shift which occurs at this boundary is with the C/N value, which drops by 0.7. Because this shift is exactly at the location of the

change from the whole-core lower-resolution section to the top high-resolution section, the shift is likely to be at least partially due to potential error as described above.

Some of the isotopic trends within the top high-resolution section are markedly different than those in the whole-core low-resolution section. These trends probably reflect a real environmental change from the previous section, because unlike the transition zone boundary, interpretation of these trends is independent of previous trends or values, and therefore most of the previously mentioned possible errors are unlikely to be a plausible concern. The trends which show significant change between these two sections include both $\delta^{13}C$ and C/N ratio. $\delta^{13}C$ undergoes a depletion trend, which may be caused by flushing of the DIC pool due to increased precipitation (Wolfe et al., 1996; 1999; 2003). Increased precipitation may be expected to increase catchment vegetation; however, C/N undergoes a depletion trend at this time, which, in combination with the continuing decreasing trend in organic matter, suggests a decrease in terrestrial vegetation. Additionally, pollen and spore accumulation rates, especially those of mosses, decline near 14 cm, suggesting a contraction of these populations. At the same time, an increase in Picea mariana suggests a possible increase in moisture (Sulphur et al., in prep.). It appears that a reduction in terrestrial vegetation may have occurred despite an increase in precipitation, likely due to cool temperatures. Cool temperatures may also partially be the cause of the $\delta^{13}C$ depletion, due to a reduction in lake productivity.

The possible reduction in temperature may be expected, as it coincides with the timing of the Little Ice Age (LIA), a well-established climate cooling pervasive throughout the northern hemisphere from around 650-150 cal yr BP (IPCC AR4 WG1). After 150 cal yr BP, the C/N ratio appears to more or less stabilize, which may be related to an increased abundance of vegetation in the catchment due to warming at the end of the LIA.

Interestingly, every isotope proxy appears to undergo an excursion at the very top of the core, beginning around 13 cal yr BP (1937 AD). The combined decrease in C/N ratio and increase in organic matter indicates a possible productivity spike during this time. This suggestion is supported by the enrichment in $\delta^{13}C$. A recent productivity spike would likely be due to increased temperatures seen in the recent instrumental climate record (IPCC AR4 WG1). However, there are not enough data points to ascertain a definitive trend.

6.2.6. Time Series Analysis

In addition to general trends, smaller-scale cyclical variations were apparent throughout the record. These were investigated in both the top and middle high-resolution sections of the core using time-series analysis. Only %C and C/N were considered for time-series analysis, because the amplitude of small-scale variation seen in $\delta^{13}C$ and $\delta^{15}N$ was too small to be considered significant. The bottom high-resolution section was not investigated using time-series analysis due to the extreme shifts in trends seen in this section.

6.2.6.1. Top High-Resolution Section (714 to -48 cal yr BP; 14.0-0.3 cm)

Spectral analysis verifies significant cyclicities at both 39-41 and 71-78 year frequencies in the top high-resolution record (fig. 16). Further analysis with wavelets illustrates that the 71-78 year cyclicity is strongly present from 600-100 cal yr BP, while the 39-41 year cyclicity is present inconsistenly throughout the record, but most strongly from 190-0 cal yr BP (fig. 17). Because our study region has been shown to be affected by the PDO (Bonsal et al., 2001; Labrecque et al., 2009; Pisaric et al., 2009), these cyclicities were tested for a possible relation to this climate phenomenon. This was done by comparing C/N and %C with the tree ring PDO records of MacDonald and Case (2005) and Shen et al. (2006) using cross-wavelet analysis. The record of MacDonald et al. (2005) was chosen because it was partially built using tree ring records from a

relatively nearby location (northern Alberta), and because the record spans the entirety of our own record. The record of Shen et al. (2006) was chosen because it is from China, whose distantly-located climates are unlikely to correlate with our own through any other mechanism than a PDO. The cross-wavelet analyses show that C/N and %C are well-correlated at a 70-80 year cyclicity with the records of both MacDonald and Case (2005) and Shen et al. (2006) from 500-100 cal yr BP, with a continuation of this correlation in the MacDonald and Case cross-wavelet all the way up to present. A second strong correlation is seen in both PDO cross-wavelets at a 50-70 year cyclicity from 100 cal yr BP-present. The appearance of 70-80 year and 50-70 year frequencies in both PDO cross-wavelets suggests that these cyclicities are primarily caused by the PDO. It should be noted that the 39-41 year cyclicity seen in the spectral analysis shows a weak and inconsistent correlation in the PDO cross-wavelets. This suggests that there may be a minor PDO relation to the 39-41 year cyclicity.

The timing of the 70-80 year cyclicity in the cross-wavelet of our own record and Shen's record may be related to the LIA, which occurred around 650-150 cal yr BP (IPCC AR4 WG1). Shen et al. (2006) have suggested that the 70-80 year cyclicity seen during this time may be associated with a Gleissberg cycle solar driver. To test this possibility, a cross-wavelet analysis was completed comparing C/N and %C with a total solar irradiance record measured using ^{10}Be from ice cores (fig. 20b, c; Steinhilber et al., 2009). This record was chosen due to its high resolution and continuous extent over all time periods covered by the top and middle high-resolution sections, including up to very recent times. There were no obvious correlations during the period of the LIA, except for a possible weak correlation at a frequency of 50-70 years from 500-350 cal yr BP and 200-100 cal yr BP. These results do not strongly support the possibility of a Gleissberg driver during the LIA. There is also very little evidence from other studies to support

the assertion of Shen et al. (2006) of a Gleissberg solar driver during this time. In fact, numerous studies find a general absence of significant cyclicity of any kind earlier than 200 cal yr BP (Biondi et al., 2001; MacDonald and Case, 2005).

The shift at 100 cal yr BP to the smaller-frequency 50-70 year cyclicity, seen in the cross-wavelets of our record with both Shen et al. (2006) and MacDonald and Case (2005), is similar to the emergence of a 50-70 year cyclicity seen over the last 200 years in other PDO studies of North America as well (Minobe, 1997; Biondi et al., 2001). The cross-wavelet analysis of our results with the total solar irradiance record of Steinhilber et al. (2009) shows a correlation at a frequency of 70-110 years from 250-0 cal yr BP. This cyclicity matches the Gleissberg cycle frequency (70-100 years; Hoyt and Schatten, 1997; Beer et al., 2000). These results appear to indicate that the Gleissberg cycle may have driven some cyclicity in relatively recent times. A Gleissberg solar driver for northern hemisphere climate over recent times has also been found by numerous other researchers (Friis-Christensen and Lassen, 1991; Oh et al., 2003; Lohmann et al., 2004).

The 39-41 year cyclicity seen in spectral analysis is likely related to more the more recent 20-30 year PDO cyclicity seen in the instrumental record (Mantua et al., 1997; Chao et al., 2000; Minobe, 2000). The inconsistency of this cycle in our record is also seen in the recent 20-30 year cyclicity of instrumental and tree ring records (Mantua et al., 1997; Biondi et al., 2001). This inconsistency may be owing to the fact that the mechanisms driving the variation are complicated and not well understood (see section 2.1.1.2).

6.2.6.2. Middle High-Resolution Section (4737-3014 cal yr BP; 68.0-52.4 cm)

Spectral analysis for the middle section delineates a 101-115 year cycle in %C and C/N. Wavelet analysis of C/N shows this cycle as weak but continuous over most of the section.

There is very little evidence in the literature of any cycle in the range of 101-115 years. However, this cyclicity may represent the extreme high end of the range for the Gleissberg cycle. In order to test this, cross-wavelet analysis was performed comparing %C and C/N with the total solar irradiance ^{10}Be proxy record of Steinhilber et al. (2009). A correlation does appear to exist in the 101-115 year range, although it is relatively weak and inconsistent.

In addition to the 101-115 year frequency, a cyclicity is also apparent centered around 300 years in both the %C and C/N wavelets. This 300 year cycle also shows up in the cross-wavelet, although despite being a somewhat stronger signal, it is also an inconsistent one. Again, there is little evidence in the literature supporting the existence of a 300 year cycle in climate records, nor is there any known solar cycle with a 300 year period. However, the correlation in the cross-wavelet does support the possibility of a solar driver for this cycle. Regardless, this cycle may not be highly significant as it is at the larger end of cycle periods which can be detected with our given resolution, and as such much of the highly correlative portions of this cycle appear outside the cone of influence in the wavelets and cross-wavelet.

6.3. Horseshoe Lake Core

The extreme variability, general absence of consistent long-term trends, and complete lack of small-scale fluctuations across all isotopic proxies in the Horseshoe Lake core suggest the possibility that an isotopic paleoclimatic signal has not been well preserved. This possibility is also supported by δ^{13}C values and trends seen in the Horseshoe Lake core. These values are highly enriched compared to other lakes in similar environments (Wolfe et al., 1996; 1999; 2003), although they are very similar to those found in a nearby lake by MacDonald et al. (1993), who attributed these findings to oxidation of sediments by CO_2-respiring bacteria. These bacteria preferentially remove the lighter ^{12}C isotope from the sediment, causing the enrichment

as well as depleting the lake water DIC in ^{13}C. As this process continues, the DIC becomes ever more depleted in ^{13}C, resulting in a depletion trend for newly accumulating aquatically-derived organic material.

Despite the likely degradation of the sediments, some very general trends are present which may represent a remnant of preserved paleoenvironmental signal. However, while the next few paragraphs discuss possible paleoclimate interpretations and compare them to the Danny's Lake interpretations, it must be recognized that any interpretations from the Horseshoe Lake core are fairly speculative due to the probable low quality of sediment preservation.

In addition to isotopic analysis, pollen analysis was also completed through the core (Trainor et al., in prep.). Much of the paleoenvironmental isotopic interpretations may be aided by these pollen results, and therefore these pollen results are referenced regularly in the following discussion.

If there is some paleoenvironmental preservation in the sediments, enriched $\delta^{13}C$ values may be partially explained by the fact that Horseshoe Lake is substantially larger than Danny's Lake as well as most other lakes studied in the region. Large lakes have a higher volume of water and subsequently a greater water residence time. This allows atmospheric input to have a much more substantial input on lake water DIC than the input from catchment DIC. Because DIC sourced from the atmosphere is much more enriched in ^{13}C than that from the catchment, the DIC pool of larger lakes can therefore be expected to be more enriched than smaller lakes.

While the majority of the Horseshoe Lake $\delta^{13}C$ profile displays a depletion trend, the bottom and top experience an enrichment (fig. 28). The sharp change between the enrichment and depletion trends hint at the possibility that these shifts may be a real signal of paleoenvironmental change rather than a product of diagenetic alteration. The core can therefore be split into three sections,

with the location of these sharp changes in trend as boundaries between these sections. Changes in sediment accumulation rate also appear to be coeval with the boundaries of these sections, with an accumulation rate for the middle section (140 yr/cm) of less than half of those of the bottom and top sections (53 yr/cm and 58 yr/cm, respectively). Additionally, organic material and C/N ratio experience a minor reduction whose initiation is roughly coeval with the start of the top section.

The bottom section (8400-7200 cal yr BP) was likely dominated by algal input to lake sediments, based on the low C/N ratio. The increasing trend in $\delta^{13}C$ may be caused by DIC enrichment due to a hydrologically closed basin during a dry climate interval. A dry climate may have also reduced lake levels and allowed for an increased sedimentation rate due to a more proximal shoreline. Pollen reconstructions also support a dry tundra environment during this time (Trainor et al., in prep.).

The middle section (7200-755 cal yr BP) was likely dominated by a greater proportion of terrestrial vegetation input due to a higher C/N ratio, although the value remains low enough to suggest that algal input was still a large contributor to lake sediment organic matter. As explained above, the depletion trend in $\delta^{13}C$ may be caused by an increasingly depleted DIC due to the continual addition of ^{12}C by bacterial decay of the sediment. However, a $\delta^{13}C$ depletion trend may also represent a renewal of ^{13}C-depleted DIC from the catchment in a hydrologically open basin during a wet climate interval. Pollen analysis also suggests a wet climate during this time, with a possible advancement of the tree line to this area (Trainor et al., in prep.). A wet climate may also explain the low sedimentation rate, as water levels may be higher and therefore you would expect a less proximal shoreline and a reduced input of sediment from the catchment. Additionally, a deeper water column may have resulted in lake stratification, which could

provide the necessary anoxic conditions for sediment decay by methanogenic bacteria. In fact, the sharp changes of trend in $\delta^{13}C$ through the sections in the profile may have much to do with changes between stratified and unstratified conditions (Hodell and Schelske, 1998).

The top section (755 cal yr BP-present) appears to revert back to similar conditions as the bottom section, with an enrichment trend in $\delta^{13}C$ and a high sedimentation rate again. As in the bottom section, this section is likely experiencing a return to dry conditions and a lower lake level. Dry climate conditions are also supported by pollen analysis, with a return to tundra conditions (Trainor et al., in prep). The stagnation and slight reduction in both C/N ratio and organic matter is likely due to a reduction in terrestrial catchment vegetation due to the transition from forest to tundra. The timing of the transition into this top section suggests the possibility that climate during this time is related to the LIA.

One interesting feature in Horseshoe Lake core is a short-lived spike seen at around 3227-3025 cal yr BP. This feature stands out because it is a large, sharp excursion in an otherwise apparently featureless isotopic profile (especially evident in the C/N profile). The large increase in $\delta^{13}C$, $\delta^{15}N$ and organic matter abundance, along with the major drop in C/N ratio, suggests that these spikes record a sudden but short-lived increase in lake productivity. The timing of this event allows for the possibility that it may be related to the climatic changes seen around the same time period in Danny's Lake core and other climate records for the region (Moser and MacDonald, 1990; MacDonald et al., 1993; Pienitz et al., 1999; Ruhland and Smol, 2005).

6.4. Comparison of Danny's Lake, Horseshoe Lake, and Other Climate Records

Comparison of the paleoclimatic interpretation of the Danny's Lake and Horseshoe Lake cores may provide some insight into local vs. regional-scale changes over time. There are certain large differences between the two cores, however, which suggest that very different processes may

have affected the sediments within the two lakes. Danny's Lake core records isotopic values which are well within the expected range based on other studies from similar environments. In addition, there are clear trends in all isotopic proxies through the core which are generally consistent with climate variations seen through the Holocene in other paleoclimate records. For these reasons, Danny's Lake most likely contains well-preserved paleoenvironmental information. Horseshoe Lake, however, contains a much more erratic paleoclimate record without many clear trends, and overall values which are much different than would normally be expected from a paleoclimate record in this region. The Horseshoe Lake core most likely contains a record which has undergone significant diagenesis, and much of the paleoclimate information which may have previously been preserved within the sediments is most likely gone. Therefore, any paleoclimate interpretations made from the Horseshoe Lake core must be taken with caution. However, comparison of results from both lakes as well as previous research is still a useful exercise.

Both Danny's and Horseshoe Lake begin near 8000 cal yr BP, shortly after deglaciation, in a dry and possibly warm climate. These conditions are consistent with that seen in climate records throughout Canada (Heusser et al., 1985; Fisher and Koerner, 2003; Anderson et al., 2005; Briner et al., 2006; Finkelstein and Gajewski, 2008; Barron and Anderson, 2011). Berger and Loutre (1991) suggest that these warm, dry climate conditions are the result of higher summer insolation during the early Holocene due to optimal arrangement of the astronomical precessional cycle.

After around 7200-6900 cal yr BP, a transition to wetter climate conditions occurs in both lakes. The timing of this transition is earlier but may still correlate with other nearby records, who find a warming and wetting climate transition around 5000 yr BP (Moser and MacDonald, 1990;

MacDonald et al., 1993; Wolfe et al., 1996; Pienitz et al.,1999; Ruhland and Smol, 2005) and 6300 cal yr BP (Huang et al., 2004).

At around 4000 cal yr BP, there is a transition to cooler conditions in Danny's Lake. The timing of this transition coincides nicely with that from other records near Danny's Lake (Moser and MacDonald, 1990; MacDonald et al., 1993; Wolfe et al., 1996; Pienitz et al., 1999; Huang et al., 2004; Ruhland and Smol, 2005) as well as many records from all around Canada (Smol, 1983; Spear, 1993; Abbott et al., 2000; Anderson et al., 2005; Anderson et al., 2007; Zabenskie and Gajewski, 2007; Finkelstein and Gajewski, 2008; Rolland et al., 2008; Adams and Finkelstein, 2010; Clegg and Hu, 2010). The general consensus is that a major climate transition, to a "neoglacial" period of cooler and drier conditions, occurred over much of North America at around 4000 yr BP. However, this transition is not evident in Horseshoe Lake, except for a single large spike in the isotope proxies around 3000 cal yr BP which is suggestive of short-lived eutrophic conditions within the lake. Aside from this spike, there is a lack of substantial evidence for a transition at this point in time, likely due to the poor preservation of climate signal within the core, which is particularly evident within that section. However, without any clear evidence of a climate transition at this point, no assumptions about climate can be made.

At around 714-755 cal yr BP, another transition is evident in both Danny's and Horseshoe Lake cores, to even cooler conditions. The timing of this transition coincides with the well-recorded Little Ice Age, which caused cool and dry climate conditions throughout northern Canada (Wolfe, 2002; Finkelstein and Gajewski, 2007; Podritske and Gajewski, 2007; Peros and Gajewski, 2009; Rolland et al., 2009; Adams and Finkelstein, 2010).

7. Conclusions

A detailed modern lake survey has verified the importance of the transition from arctic tundra to boreal forest ecoclimatic regions in affecting many of the environmental parameters of the lakes within northern Canada, including the carbon and nitrogen isotopic proxies used for down-core analysis of Danny's and Horseshoe Lakes. These results strengthen the argument that changes in these isotopic proxies through time may be related to variations in terrestrial vegetation input to these lakes, which may result from changes in environmental conditions between tundra and boreal forest, or gradations of these extremes. However, values for environmental variables of sites near the all-season road between Yellowknife and Behchoko appear to be unrelated to ecoclimatic region. Rather, values for certain variables at these sites contain unique values, suggesting the possibility of an anthropogenic effect.

Analysis of both the Danny's and Horseshoe Lake cores have provided a climate record extending back over 8000 years for the central Northwest Territories. Danny's Lake core shows clear trends and cyclicity throughout most of the core, allowing for the possibility of detailed paleoenvironmental analysis. Specific intervals include an initial Early Holocene warm and dry period starting at 8145 cal yr BP, followed by an abrupt shift to wetter conditions at 6900 cal yr BP. At 4000 cal yr BP, a late Holocene neoglacial episode of cool conditions is evident, followed at 714 cal yr BP by a final transition to even cooler conditions during the Little Ice Age. It should also be noted that in the most recent time period (past 75 years), there is evidence of a large spike in productivity, which may be driven by an increase in temperatures.

The Horseshoe Lake core shows evidence of significant diagenesis, requiring that paleoclimate interpretations be made cautiously. Regardless, paleoclimate interpretations suggest an initial

dry and possibly warm period in the Early Holocene, from 8400-7200 cal yr BP, followed by a wet period up to 755 cal yr BP, and finally another dry period up to present.

Comparison of the Danny's Lake and Horseshoe Lake cores show interesting similarities in general trends throughout the Holocene. Specifically, both cores show an early warm and dry period up to around 7000 cal yr BP, followed by a wet period. However, while Danny's Lake shows evidence of a neoglacial cooling around 4000 cal yr BP, it is not apparent in Horseshoe Lake. Finally, both cores appear to show a climate shift at the beginning of the LIA, around 755-714 cal yr BP. At Danny's Lake, the shift is to cooler and possibly wetter conditions, while at Horseshoe Lake the shift appears to be to dry conditions. The similarities seen between these two cores in the Early and Middle Holocene suggest that these changes are likely regional in scale. The later discrepancies in timing and environmental conditions during the neoglacial and LIA may be due to differences in local climate conditions, or may be due to a lack of preserved paleoclimate signal at Horseshoe Lake. Paleoclimate results from these two lakes are generally in good agreement with previous research from northern Canada, which again suggests that for the most part the paleoclimate trends seen are regional in scale.

High-resolution analysis of the Danny's Lake core over the most recent 714 years allows for insight into short-term climate cycles which are likely to affect the Tibbitt to Contwoyto Winter Ice Road in the recent future. This analysis suggests that a significant cyclicity occurred during the LIA at a frequency of 70-80 years, followed by a shift to a significant cyclicity with a 50-70 year frequency over the past 150 years. Cross-wavelet analysis with tree ring PDO records suggests that these cyclicities are likely both related to the PDO. There is also some evidence of a weaker 70-110 year cyclicity over the past 300 years which may have been driven by the Gleissberg solar cycle, as indicated by cross-wavelet analysis with a ^{10}Be solar proxy record. A

much weaker and inconsistent 39-41 year cyclicity also appears to be present, which may be related to 20-30 year PDO cycles observed in recent times. While much work has been completed in attempting to understand mechanisms behind the 20-30 year PDO cyclicity, its causes are not straightforward and this may be the reason for the apparent inconsistency observed. If the 39-41 year cyclicity seen in our record is indeed related to the prominent 20-30 year cyclicity seen in recent times, predicting its future near-term pattern may be difficult without a more concrete understanding of the mechanisms driving this climate phenomena.

These high-resolution results offer an important understanding of short-term climate phenomena in the central Northwest Territories. While this is an important first step in predicting near-term climate changes, accurate predictions will require the use of climate models. Results from this study will enable greater accuracy of future climate models in predicting near-term climate scenarios within the central Northwest Territories. Such scenarios are instrumental in determining the future viability of the climate-sensitive TCWR and the economic feasibility of its continued use.

8. References

Abbott, M. B. and Stafford, T. W. (1996). Radiocarbon geochemistry of modern and ancient Arctic lake systems, Baffin Island, Canada. Quaternary Research, 45: 300–311.

Abbott, M. B., Finney, B. P., Edwards, M. E., and Kelts, K. R. (2000). Lake-Level Reconstructions and Paleohydrology of Birch Lake, Central Alaska, Based on Seismic Reflection Profiles and Core Transects. Quaternary Research, 53: 154-166.

Adams, J. K. and Finkelstein, S. A. (2010). Watershed-scale reconstruction of middle and late Holocene paleoenvironmental changes on Melville Peninsula, Nunavut, Canada. Quaternary Science Reviews, 29: 2302-2314.

Alexander, M. A. (1992). Midlatitude Atmosphere-Ocean Interaction During El Niño, Part I: The North Pacific Ocean. Journal of Climate, 5: 944-958.

Alexander, M. A., Bladé, I., Newman, M., Lanzante, J. R., Lau, N. C., and Scott, J. D. (2002). The Atmospheric Bridge: The Influence of ENSO Teleconnections on Air-Sea Interaction over the Global Oceans. Journal of Climate, 15: 2205-2231.

Alley, R. B., Mayewski, P. A., Sowers, T., Stuiver, M., Taylor, K. C., and Clark, P. U. (1997). Holocene climatic instability: A prominent, widespread event 8200 yr ago. Geology, 25: 483-486.

Anderson, L., Abbott, M. B., Finney, B. P., and Edwards, M. E. (2005). Palaeohydrology of the Southwest Yukon Territory, Canada, based on multiproxy analyses of lake sediment cores from a depth transect. The Holocene, 15: 1172-1183.

Anderson, L., Abbott, M. B., Finney, B. P., and Burns, S. J. (2007). Late Holocene moisture balance variability in the southwest Yukon Territory, Canada. Quaternary Science Reviews, 26: 130-141.

Aravena, R., Warner, B. G., MacDonald, G. M., and Hanf, K. I. (1992). Carbon Isotope Composition of Lake Sediments in Relation to Lake Productivity and Radiocarbon Dating. Quaternary Research, 37: 333-345.

Arrindell, W. A. and van der Ende., J. (1985). An empirical test of the utility of the observations-to-variables ratio in factor and components analysis. Applied Psychological Measurement, 9: 165-178.

Audry, S., Schafer, J., Blanc, G., and Jouanneau, J. M. (2004). Fifty-year sedimentary record of heavy metal pollution (Cd, Zn, Cu, Pb) in the Lot River reservoirs (France). Environmental Pollution, 132: 413-426.

Ball, D. F. (1964). Loss-On-Ignition as an estimate of organic matter and organic carbon in non-calcareous soils. Journal of Soil Science, 15: 84-92.

Barnekow, L., Possnert, G., and Sandgren, P. (1998). AMS ^{14}C chronologies of Holocene lake sediments in the Abisko area, northern Sweden – a comparison between dated bulk sediment and macrofossil samples. GFF, 120: 59-67.

Barron, J. A. and Anderson, L. (2011). Enhanced Late Holocene ENSO/PDO expression along the margins of the eastern North Pacific. Quaternary International, 235: 3-12.

Beer, J., Mende, W., and Stellmacher, R. (2000). The role of the sun in climate forcing. Quaternary Science Reviews, 19: 403-415.

Bengtsson, L. and Enell, M. (1986). Chemical analysis. In: Handbook of Holocene palaeoecology and palaeohydrology, pp. 423-451.

Berger, A. and Loutre, M. F. (1991). Insolation values for the climate of the last 10 million years. Quaternary Science Reviews, 10: 297-317.

Beuning, K. R. M., Talbot, M. R., and Kelts, K. (1997). A revised 30,000-year paleoclimatic and paleohydrologic history of Lake Albert, East Africa. Palaeogeography, Palaeoclimatology, Palaeoecology, 136: 259-279.

Biondi, F., Gershunov, A., and Cayan, D. R. (2001). North Pacific Decadal Climate Variability since 1661. Journal of Climate, 14: 5-10.

Blaauw, M. (2010). Methods and code for 'classical' age-modelling of radiocarbon sequences. Quaternary Geochronology, 5: 512-518.

Blaauw M. and Christen, J. A. (2005). Radiocarbon peat chronologies and environmental change. Applied Statistics, 54: 805-816.

Blaauw, M. and Christen, J. A. (2011). Flexible paleoclimate age-depth models using an autoregressive gamma process. Bayesian Analysis, 6: 457-474.

Blaauw, M., van Geel, B., Kristen, I., Plessen, B., Lyaruu, A., Engstrom, D. R., van der Plicht, J., and Verschuren, D. (2011). Quaternary Science Reviews, 30: 3043-3059.

Bleeker, W. (2002). Archaean tectonics: a review, with illustrations from the Slave craton. Geological Society, London, Special Publications, 199: 151–181.

Bonsal, B. R., Shabbar, A., and Higuchi, K. (2001). Impacts of low frequency variability modes on Canadian winter temperature. International Journal of Climatology, 21: 95-108.

Brenner, M., Whitmore, T. J., Curtis, J. H., Hodell, D. A., and Schelske, C. L. (1999). Stable isotope ($\delta^{13}C$ and $\delta^{15}N$) signatures of sedimented organic matter as indicators of historic lake trophic state. Journal of Paleolimnology, 22: 205-221.

Briner, J. P., Michelutti, N., Francis, D. R., Miller, G. H., Axford, Y., Wooller, M. J., and Wolfe, A. P. (2006). A multi-proxy lacustrine record of Holocene climate change on northeastern Baffin Island, Arctic Canada. Quaternary Research, 65: 431-442.

Briner, J. P., Stewart, H. A. M., Young, N. E., Phillips, W., and Losee, S. (2010). Using proglacial-threshold lakes to constrain fluctuations of the Jakobshavn Isbræ ice margin, western Greenland, during the Holocene. Quaternary Science Reviews, 29: 3861-3874.

Brodie, C. R. (2011). Evidence for bias in C/N, $\delta^{13}C$ and $\delta^{15}N$ values of aquatic and terrestrial organic materials due to acid pre-treatment methods. PAGES news, 19(2).

Brodie, C. R., Casford, J. S. L., Lloyd, J. M., Leng, M. J., Heaton, T. H. E., Kendrick, C. P., and Yongqiang, Z. (2011a). Evidence for bias in C/N, $\delta^{13}C$ and $\delta^{15}N$ values of bulk organic matter, and on environmental interpretation, from a lake sedimentary sequence by pre-analysis acid treatment methods. Quaternary Science Reviews, 30: 3076-3087.

Brodie, C. R., Leng, M. J., Casford, J. S. L., Kendrick, C. P., Lloyd, J. M., Yongqiang, Z., and Bird, M. I. (2011b). Evidence for bias in C and N concentrations and $\delta^{13}C$ composition of terrestrial and aquatic organic materials due to pre-analysis acid preparation methods. Chemical Geology, 282: 67-83.

Bronk Ramsey, C. (2009a). Dealing with outliers and offsets in radiocarbon dating. Radiocarbon, 51: 1023-1045.

Bronk Ramsey, C. (2009b). Bayesian analysis of radiocarbon dates. Radiocarbon, 51: 337–360.

Bryant, F. B. and Yarnold, P. R. (1995). Principal components analysis and exploratory and confirmatory factor analysis. In: Grimm, L. G., and Yarnold, R. R. (Eds.); Reading and understanding multivariale statistics. American Psychological Association; Washington.

Bryson, R. A., Irving, W. N., and Larsen, J. A. (1965). Radiocarbon and Soil Evidence of Former Forest in Southern Canadian Tundra. Science, 147: 46-48.

Bunn, S. E., Loneragan, N. R., and Kempster, M. A. (1995). Effects of acid washing on stable isotope ratios of C and N in penaeid shrimp and seagrass: implications for food-web studies using multiple stable isotopes. Limnology and Oceanography, 40: 622-625.

Cattell, R. B. (1978). The Scientific Use of Factor Analysis. Plenum; New York.

Ceballos, L. I., Di Lorenzo, E., and Hoyos, C. D. (2009). North Pacific Gyre Oscillation Synchronizes Climate Fluctuations in the Eastern and Western Boundary Systems. Journal of Climate, 22: 5163-5174.

Chao, Y., Ghil, M., and McWilliams, J. C. (2000). Pacific interdecadal intervariability in this century's sea surface temperatures. Geophysical Research Letters, 27: 2261-2264.

Chen, J., Wan, G., Zhang, D. D., Zhang, F., and Huang, R. (2004). Environmental records of lacustrine sediments in different time scales: Sediment grain size as an example. Science in China, 47: 954-960.

Chu, G., Sun, Q., Wang, X., Li, D., Rioual, P., Qiang, L., Han, J., and Liu, J. (2009). A 1600 year multiproxy record of paleoclimatic change from varved sediments in Lake Xiaolongwan, northeastern China. Journal of Geophysical Research, 114, D22108, doi: 10.1029/2009JD012077.

Clark, I. D. and Fritz, P. (1997). Environmental Isotopes in Hydrogeology. CRC Press; Boca Raton.

Clarke, J. U. (1998). Evaluation of Censored Data Methods To Allow Statistical Comparisons among Very Small Samples with Below Detection Limit Observations. Environmental Science & Technology Letters, 32: 177-183.

Clegg, B. F. and Hu, F. S. (2010). An oxygen-isotope record of Holocene climate change in the south-central Brooks Range, Alaska. Quaternary Science Reviews, 29: 928-939.

Clymo, R. S. (1991). Peat Growth. In: Shane, L. C. K. and Cushing, E. J. (eds); Quaternary Landscapes. University of Minnesota Press; Minnesota.

Conroy, J. L., Overpeck, J. T., Cole, J. E., Shanahan, T. M., and Steinitz-Kannan, M. (2008). Quaternary Science Reviews, 27: 1166-1180.

D'Arrigo, R. D., Villalba, R., and Wiles, G. (2001). Tree-ring estimates of Pacific decadal climate variability. Climate Dynamics, 18: 219-224.

Dean, W. E. (1974). Determination of Carbonate and Organic Matter in Calcareous Sediments and Sedimentary Rocks by Loss on Ignition: Comparison With Other Models. Journal of Sedimentary Petrology, 44: 242-248.

Douglas, M. S. V., Smol, J. P., and Blake, W. (1994). Marked Post-18th Century Environmental Change in High-Arctic Ecosystems. Science, 266: 416-419.

Dyke, A. S., and Prest, V. K. (1987). Late Wisconsinan and Holocene History of the Laurentide Ice Sheet. Géographie physique et Quaternaire, 41: 237-263.

Dyke, A. S. (2004). An outline of North American deglaciation with emphasis on central and northern Canada. Developments in Quaternary Sciences, 2: 373-424.

Edwards, M. E. and Barker, E. D. (1994). Climate and vegetation in northeastern Alaska 18,000 yr B.P.-present. Palaeogeography, Palaeoclimatology, Palaeoecology, 109: 127-135.

Everitt, S. (1975). Multivariate analysis: The need for data, and other problems. British Journal of Psychiatry, 126: 227-240.

Farnell, R., Hare, P. G., Blake, E., Bowyer, V., Schweger, C., Greer, S., and Gotthardt, R. (2004). Multidisciplinary Investigations of Alpine Ice Patches in Southwest Yukon, Canada: Paleoenvironmental and Paleobiological Investigations. Arctic, 57: 247-259.

Fernandes, M. and Krull, E. (2008). How does acid treatment to remove carbonates affect the isotopic and elemental composition of soils and sediments? Environmental Chemistry, 5: 33-39.

Fernandes, R., Korolevych, V., and Wang, S. (2007). Trends in Land Evapotranspiration over Canada for the Period 1960-2000 Based on In Situ Climate Observations and a Land Surface Model. Journal of Hydrometeorology, 8: 1016-1030.

Finkelstein, S. A. and Gajewski, K. (2007). A palaeolimnological record of diatom-community dynamics and late-Holocene climatic changes from Prescott Island, Nunavut, central Canadian Arctic. The Holocene, 17: 803-812.

Finkelstein, S. A. and Gajewski, K. (2008). Responses of Fragilarioid-dominated diatom assemblages in a small Arctic lake to Holocene climatic changes, Russell Island, Nunavut, Canada. Journal of Paleolimnology, 40: 1079-1095.

Fisher, D. A. and Koerner, R. M. (2003). Holocene ice core climate history, a multi-variable approach. In: Mackay, A. W., Battarbee, R. W., Birks, H. J. B., and Oldfield, F. (eds); Global Change in the Holocene: approaches to reconstructing fine-resolution climate change. Arnold; London.

France, R. L. (1995). Carbon-13 enrichment in benthic compared to planktonic aglae: foodweb implications. Marine Ecology Progress Series, 124: 307-312.

Francois, R. (1996). Seasonal variation in the nitrogen isotope composition of sediment trap materials collected in Lake Malawi. In: Johnson, T. C. and Odada, E. O. (eds); The limnology, climatology and paleoclimatology of the East African lakes. Gordon and Breach Science Publishers; London and New York.

Friis-Christensen, E. and Lassen, K. (1991). Length of the Solar Cycle: An Indicator of Solar Activity Closely Associated with Climate. Science, 254: 698-700.

Froelich, P. N. (1980). Analysis of organic carbon in marine sediments. Limnology and Oceanography, 25: 564-572.

Frost, P. C., Stelzer, R. S., Lamberti, G. A., and Elser, J. J. (2002). Journal of the North American Benthological Society, 21: 515-528.

Galand, P. E., Yrjälä, K., and Conrad, R. (2010). Stable carbon isotope fractionation during methanogenesis in three boreal peatland ecosystems. Biogeosciences, 7: 5497-5515.

Galloway, J. M., Macumber, A. L., Patterson, R. T., Falck, H., Hadlari, T., and Madsen, E. (2010). Paleoclimatological Assessment of the Southern Northwest Territories and Implications for the Long-Term Viability of the Tibbitt to Contwoyto Winter Road, Part I: Core Collection. Northwest Territories Geoscience Office, NWT Open Report 2010-002, 21 p.

Galy, V., Bouchez, J., and France-Lanord, C. (2007). Determination of total organic carbon content and $\delta^{13}C$ in carbonate- rich detrital sediments. Geostandards and Geoanalytical Research, 31: 199-207.

Gedalof, Z. and Smith, D. J. (2001). Interdecadal climate variability and regime-scale shifts in Pacific North America. Geophysical Research Letters, 28: 1515-1518.

Geyh, M. A., Schotterer, U., and Grosjean, M. (1998). Temporal changes of the ^{14}C reservoir effect in lakes. Radiocarbon, 40: 921-931.

Gibson, J. J. (2001). Forest-tundra water balance signals traced by isotopic enrichment in lakes. Journal of Hydrology, 251: 1-13.

Gibson, J. J. and Edwards, T. W. D. (2002). Regional water balance trends and evaporation-transpiration partitioning from a stable isotope survey of lakes in northern Canada. Global Biogeochemical Cycles, 16, 1026, 10.1029/2001GB001839.

Goldin, A. (1987). Reassessing the use of loss-on-ignition for estimating organic matter content in noncalcareous soils. Communications in Soil Science and Plant Analysis, 18: 1111-1116.

Gorsuch, R. L. (1983). Factor analysis (2nd ed.). Erlbaum; Hillsdale, NJ.

Grimm, E. C., Maher, L. J., and Nelson, D. M. (2009). The magnitude of error in conventional bulk-sediment radiocarbon dates from central North America. Quaternary Research, 72: 301-308.

Grindsted, A., Moore, J. C., and Jevrejeva, S. (2004). Application of the cross wavelet transform and wavelet coherence to geophysical time series. Nonlinear Processes in Geophysics, 11: 561-566.

Gu, B., Schelske, C. L., and Brenner, M. (1996). Relationship between sediment and plankton isotope ratios ($\delta^{13}C$ and $\delta^{15}N$) and primary productivity in Florida lakes. Canadian Journal of Fisheries and Aquatic Sciences, 53: 875-883.

Haberzettl, T., Fey, M., Lücke, A., Maidana, N., Mayr, C., Ohlendorf, C., Schäbitz, F., Schleser, G. H., Wille, M., and Zolitschka, B. (2005). Climatically induced lake level changes during the last two millennia as reflected in sediments of Laguna Potrok Aike, southern Patagonia (Santa Cruz, Argentina). Journal of Paleolimnology, 33: 283-302.

Hair, J. F. J., Anderson, R. E., Tatham, R. L., and Black, W. C. (1995). Multivariate data analysis (4th ed.). Prentice Hall; Saddle River, NJ.

Hare, S. R. and Francis, R. C. (1995). Climate change and salmon production in the Northeast Pacific Ocean. In: Beamish, R. J. (eds); Climate Change and Northern Fish Populations, Canadian Journal of Fisheries and Aquatic Sciences, 121: 357-372.

Hassan, K. M., Swinehart, J. B., and Spalding, R. F. (1997). Evidence for Holocene environmental change from C/N ratios, and $\delta^{13}C$ and $\delta^{15}N$ values in Swan Lake sediments, western Sand Hills, Nebraska. Journal of Paleolimnology, 18: 121-130.

Hassol, S.J. (2004). Arctic Climate Impact Assessment – Impacts of a warming arctic. Cambridge University Press; Cambridge.

Haston, L. and Michaelsen, J. (1994). Long-Term Central Coastal California Precipitation Variability and Relationships to El Niño-Southern Oscillation. Journal of Climate, 7: 1373-1387.

Heaton, T. H. E. (1986). Isotopic studies of nitrogen pollution in the hydrosphere and atmosphere: a review. Chemical Geology, 59: 87-102.

Heiri, O., Lotter, A. F., and Lemcke, G. (2001). Loss on ignition as a method for estimating organic and carbonate content in sediments: reproducibility and comparibility of results. Journal of Paleolimnology, 25: 101-110.

Helmstaedt, H. (2009). Crust-mantle coupling revisited: The Archean Slave craton, NWT, Canada. Lithos, 112S: 1055-1068.

Hodell, D. A. and Schelske, C. L. (1998). Production, Sedimentation and Isotopic Composition of Organic Matter in Lake Ontario. Limnology and Oceanography, 43: 200-214.

Hogarty, K. Y., Hines, C. V., Kromrey, J. D., Ferron, J. M., and Mumford, K. R. (2005). The quality of factor solutions in exploratory factor analysis: The influence of sample size, communality, and overdetermination. Educational and Psychological Measurement, 65: 202-226.

Horowitz, A. J. (1985). A Primer on Trace Metal-Sediment Chemistry. United States Geological Survey Water-Supply Paper 2277. United States Government Printing Office; Alexandria, VA.

Horowitz, A. J. and Elrick, K. A. (1987). The relation of stream sediment surface area, grain size and composition to trace element chemistry. Applied Geochemistry, 2: 437-451.

Hoyt, D. V. and Schatten, K. H. (1997). The role of the sun in climate change. Oxford University Press; New York.

Huang, C. C., MacDonald, G. M., and Cwynar, L. (2004). Palaeogeography, Palaeoclimatology, Palaeoecology, 205: 221-234.

Huesser, C. J., Huesser, L. E., and Peteet, D. M. (1985). Late-Quaternary climatic change on the American North Pacific Coast. Nature, 315: 485-487.

IPCC AR4 WG1 (2007). In: Solomon, S., Qin, D., Manning, M., Chen, Z., Marquis, M., Averyt, K. B., Tignor, M., and Miller, H.L. (eds); Climate Change 2007: The Physical Science Basis, Contribution of Working Group I to the Fourth Assessment Report of the Intergovernmental Panel on Climate Change. Cambridge University Press; Cambridge.

Junger, M. and Planas, D. (1994). Quantitative Use of Stable Carbon Isotope Analysis to Determine the Trophic Base of Invertebrate Communities in a Boreal Forest Lotic System. Canadian Journal of Fisheries and Aquatic Sciences, 51: 52-61.

Kaufman, D. S., Ager, T. A., Anderson, N. J., Anderson, P. M., Andrews, J. T., Bartlein, P. J., Brubaker, L. B., Coats, L. L., Cwynar, L. C., Duvall, M. L., Dyke, A. S., Edwards, M. E., Eisner, W. R., Gajewski, K., Geirsdóttir, A., Hu, F. S., Jennings, A. E., Kaplan, M. R., Kerwin, M. W., Lozhkin, A. V., MacDonald, G. M., Miller, G. H., Mock, C. J., Oswald, W. W., Otto-Bliesner, B. L., Porinchu, D. F., Rühland, K., Smol, J. P., Steig, E. J., and Wolfe, B. B. (2004). Holocene thermal maximum in the western Arctic (0-180°W). Quaternary Science Reviews, 23: 529-560.

Kay, P. A. (1979). Multivariate Statistical Estimates of Holocene Vegetation and Climate Change, Forest – Tundra Transition Zone, NWT, Canada. Quaternary Research, 11: 125-140.

Kaushal, S. and Binford, M. W. (1999). Relationship between C:N ratios of lake sediments, organic matter sources, and historical deforestation in Lake Pleasant, Massachusetts, USA. Journal of Paleolimnology, 22: 439-442.

Kendall, C. and McDonnell, J. J. (1998). Isotope tracers in catchment hydrology. Elsevier; Amsterdam and Oxford.

Kennedy, P., Kennedy, H., and Papadimitriou, S. (2005). The effect of acidification on the determination of organic carbon, total nitrogen and their stable isotopic composition in algae and marine sediment. Rapid Communications in Mass Spectrometry, 19: 1063-1068.

King, P., Kennedy, H., Newton, P. P., Kickells, T. D., Brand, T., Calvert, S., Cauwet, G., Etcheber, H., Head, B., Khripounoff, A., Manighetti, B., and Miquel, J. C. (1998). Analysis of total and organic carbon and total nitrogen in settling oceanic particles and a marine sediment: an interlaboratory comparison. Marine Chemistry, 60: 203-216.

Kline, P. (1979). Psychometrics and psychology. Acaderric Press; London.

Krishnamurthy, R. V., Bhattacharya, S. K., and Kusumgar, S. (1986). Palaeoclimatic changes deduced from $^{13}C/^{12}C$ and C/N ratios of Karewa lake sediments, India. Nature, 323: 150-152.

Kunce, J. T., Cook, W. D., and Miller, D. E. (1975). Random variables and correlational overkill. Educational and Psychological Measurement, 35: 529-534.

Kwon, Y. O. and Deser, C. (2007). North Pacific Decadal Variability in the Community Climate System Model Version 2. Journal of Climate, 20: 2416-2433.

Labrecque, S., Lacelle, D., Duguay, C. R., Lauriol, B., and Hawkings, J. (2009). Contemporary (1951 – 2001) Evolution of Lakes in the Old Crow Basin, Northern Yukon, Canada: Remote Sensing, Numerical Modeling, and Stable Isotope Analysis. Arctic, 62: 225-238.

Latif, M. and Barnett, T. P. (1994). Causes of Decadal Climate Variability over the North Pacific and North America. Science, 266: 634-637.

Latif, M. and Barnett, T. P. (1996). Decadal Climate Variability over the North Pacific and North America: Dynamics and Predictability. Journal of Climate, 9: 2407-2423.

Lau, N. C. and Nath, M. J. (1990). A General Circulation Model Study of the Atmospheric Response to Extratropical SST Anomalies Observed in 1950-79. Journal of Climate, 3: 965-989.

Lauriol, B., Lacelle, D., Labrecque, S., Duguay, C. R., and Telka, A. (2009). Holocene Evolution of Lakes in the Bluefin Basin, Northern Yukon, Canada. Arctic, 62: 212-224.

de Leenheer, L., van Hove, J., and van Ruymbeke, M. (1957). Détermination quantitative de la matière organique du sol. Pédologie, 7: 324-347.

Leng, M. J., Lamb, A. L., Heaton, T. H. E., Marshall, J. D., Wolfe, B. B., Jones, M. D., Holmes, J. A., and Arrowsmith, C. (2006). Isotopes in lake sediments. In: Leng, M. J. (ed); Isotopes in palaeoenvironmental research – Developments in paleoenvironmental research, Volume 10. Springer Netherlands; Dordrecht.

Letolle, R. (1980). Nitrogen-15 in the natural environment. In: Fritz, P. and Fontes, J. C. (eds); Handbook of environmental isotope geochemistry, Volume 1: The terrestrial environment. Elsevier Science Ltd.; Philadelphia.

Li, H. C. and Ku, T. L. (1997). $\delta^{13}C$ and $\delta^{18}O$ covariance as a paleohydrological indicator for closed-basin lakes. Palaeogeography, Palaeoclimatology, Palaeoecology, 133: 69-80.

Lim, D. S. S., Smol, J. P., Douglas, M. S. V. (2008). Recent environmental changes on Banks Island (N.W.T., Canadian Arctic) quantified using fossil diatom assemblages. Journal of Paleolimnology, 40: 385-398.

Lohmann, G., Rimbu, N., and Dima, M. (2004). Climate signature of solar irradiance variations: Analysis of long-term instrumental, historical and proxy data. International Journal of Climatology, 24: 1045-1056.

Lohse, L., Kloosterhuis, R. T., de Stigter, H. C., Helder, W., van Raaphorst, W., and van Weering, T. C. E. (2000). Carbonate removal by acidification causes loss of nitrogenous compounds in continental margin sediments. Marine Chemistry, 69: 193-201.

Luksch, U., von Storch, H., and Maier-Reimer, E. (1990). Modeling North Pacific SST anomalies as a response to anomalous atmospheric forcing. Journal of Marine Systems, 1: 155-168.

MacCallum, R. C., Widaman, K. F., Zhang, S., and Hong, S. (1999). Sample size in factor analysis. Psychological Methods, 4: 84-99.

MacDonald, G. M., Edwards, T. W. D., Moser, K. A., Pienitz, R., and Smol, J. P. (1993). Nature, 361: 243-246.

MacDonald, G. M. and Case, R. A. (2005). Variations in the Pacific Decadal Oscillation over the past millennium. Geophysical Research Letters, 32(8).

MacDonald, G. M., Moser, K. A., Bloom, A. M., Porinchu, D. F., Potito, A. P., Wolfe, B. B., Edwards, T. W. D., Petel, A., Orme, A. R., and Orme, A. J. (2008). Evidence of temperature depression and hydrological variations in the eastern Sierra Nevada during the Younger Dryas stade. Quaternary Research, 70: 131-140.

MacDonald, G. M., Porinchu, D. F., Rolland, N., Kremenetsky, K. V., and Kaufman, D. S. (2009). Paleolimnological evidence of the response of the central Canadian treeline zone to radiative forcing and hemispheric patterns of temperature change over the past 2000 years. Journal of Paleolimnology, 41: 129-141.

Macumber, A. L., Patterson, R. T., Neville, L. A., and Falck, H. (2011). A sledge microtome for high resolution subsampling of freeze cores. Journal of Paleolimnology, 45: 307-310.

Macumber, A. L., Neville, L. A., Galloway, J. M., Patterson, R. T., Falck, H., Swindles, G., Crann, C., Clark, I., Gammon, P., and Madsen, E. (2012). Paleoclimatological Assessment of the Northwest Territories and Implications for the Long-Term Viability of the Tibbitt to Contwoyto Winter Road, Part II: March 2010 Field Season Results. Northwest Territories Geoscience Office, NWT Open Report 2011-010, 83 p.

Mann, D. H., Peteet, D. M., Reanier, R. E., and Kunz, M. L. (2002). Responses of an arctic landscape to Lateglacial and early Holocene climatic changes: the importance of moisture. Quaternary Science Reviews, 21: 997-1021.

Mantua, N. J., Hare, S. R., Zhang, Y., Wallace, J. M., and Francis, R. C. (1997). The Pacific Decadal Oscillation. Bulletin of the American Meteorological Society, 78: 1069-1079.

Mantua, N. J. and Hare, S. R. (2002). The Pacific Decadal Oscillation. Journal of Oceanography, 58: 35-44.

Marascuilo, A. and Levin, J. R. (1983). Multivariate statistics in the social sciences. Brooks/Cole; Monterey, CA.

McArthur, J. M., Tyson, R. V., Thomson, J., and Mattey, D. (1992). Early diagenesis of marine organic matter: Alteration of the carbon isotopic composition. Marine Geology, 105: 51-61.

McKenzie, J. A. (1985). Carbon istopes and productivity in the lacustrine and marine environment. Chemical Processes in Lakes, 1985.

Menking, K. M. (1997). Climatic signals in clay mineralogy and grain-size variations in Owens Lake core OL-92, southeast California. Geological Society of America Special Papers, 317: 25-36.

Meyers, P. A. and Ishiwatari, R. (1993). Lacustrine organic geochemistry – an overview of indicators of organic matter sources and diagenesis in lake sediments. Organic Geochemistry, 20: 867-900.

Meyers, P. A. (1994). Preservation of elemental and isotopic source identification of sedimentary organic matter. Chemical Geology, 114: 289-302.

Michelutti, N., Holtham, A. J., Douglas, M. S. V., and Smol, J. P. (2003). Periphytic diatom assemblages from ultra-oligotrophic and UV transparent lakes and ponds on Victoria Island and comparisons with other diatom surveys in the Canadian Arctic. Journal of Phycology, 39: 465-480.

Miller, A. J. and Schneider, N. (2000). Interdecadal climate regime dynamics in the North Pacific Ocean: theories, observations and ecosystem impacts. Progress in Oceanography, 47: 355-379.

Miller, A. J., Chai, F., Chiba, S., Moisan, J. R., and Neilson, D. J. (2004). Decadal-scale climate and ecosystem interactions in the North Pacific Ocean. Journal of Oceanography, 60: 163-188.

Minobe, S. (1997). A 50-70 year climatic oscillation over the North Pacific and North America. Geophysical Research Letters, 24: 683-686.

Minobe, S. (2000). Spatio-temporal structure of the pentadecadal variability over the North Pacific. Progress in Oceanography, 47: 381-408.

Moberg, A., Sonechkin, D. M., Holmgren, K., Datsenko, N. M., and Karlén, W. (2005). Highly variable Northern Hemisphere temperatures reconstructed from low- and high-resolution proxy data. Nature, 433: 613-617.

Morrill, C., Overpeck, J. T., Cole, J. E., Liu, K., Shen, C., and Tang, L. (2006). Holocene variations in the Asian monsoon inferred from the geochemistry of lake sediments in central Tibet. Quaternary Research, 65: 232-243.

Moser, K. A. and MacDonald, G. M. (1990). Holocene Vegetation Change at Treeline North of Yellowknife, Northwest Territories, Canada. Quaternary Research, 34: 227-239.

Muzuka, A. N. N., Ryner, M., and Holmgren, K. (2004). 12,000-Year, preliminary results of the stable nitrogen and carbon isotope record from the Empakai Crater lake sediments, Northern Tanzania. Journal of African Earth Sciences, 40: 293-303.

Natural Resouces Canada (1993). Canada-Permafrost [map]. Fifth Edition, National Atlas of Canada.

Nichols, H. (1970). Late Quaternary Pollen Diagrams from the Canadian Arctic Barren Grounds at Pelly Lake, Northern Keewatin, N.W.T. Arctic and Alpine Research, 2: 43-61.

Nunnally, J. C. (1978). Psychometric theory (2nd Ed.). McGraw-Hill; New York.

Oh, H. S., Ammann, C. M., Naveau, P., Nychka, D., and Otto-Bliesner, B. L. (2003). Multi-resolution time series analysis applied to solar irradiance and climate reconstructions. Journal of Atmospheric and Solar-Terrestrial Physics, 65: 191-201.

O'Reilly, C. M., Alin, S. R., Plisnier, P. D., Cohen, A. S., and McKee, B. A. (2003). Climate change decreases aquatic ecosystem productivity of Lake Tanganyika, Africa. Nature, 424: 766-768.

Padgham, W. A. and Fyson, W. K. (1992). The slave province: a distinct Archean craton. Canadian Journal of Earth Science, 29: 2072–2086.

Park, J. H., An, S. I., Yeh, S. W., and Schneider, N. (2012). Quantitative assessment of the climate components driving the pacific decadal oscillation in climate models. Theoretical and Applied Climatology, 112: 431-445.

Paul, C. A., Rühland, K. M., and Smol, J. P. (2010). Diatom-inferred climatic and environmental changes over the last ~9000 years from a low Arctic (Nunavut, Canada) tundra lake. Palaeogeography, Palaeoclimatology, Palaeoecology, 291: 205-216.

Peros, M. C. and Gajewski, K. (2009). Pollen-based reconstructions of late Holocene climate from the central and western Canadian Arctic. Journal of Paleolimnology, 41: 161-175.

Perren, B. B., Bradley, R. S., and Francus, P. (2003). Rapid Lacustrine Response to Recent High Arctic Warming: A Diatom Record from Sawtooth Lake, Ellesmere Island, Nunavut. Arctic, Antarctic, and Alpine Research, 35: 271-278.

Pienitz, R. and Smol, J. P. (1993). Diatom assemblages and their relationship to environmental variables in lakes from the boreal forest-tundra ecotone near Yellowknife, Northwest Territories, Canada. Hydrobiologia, 269/270: 391-404.

Pienitz, R., Smol, J. P., and MacDonald, G. M. (1999). Paleolimnological Reconstruction of Holocene Climatic Trends from Two Boreal Treeline Lakes, Northwest Territories, Canada. Arctic, Antarctic, and Alpine Research, 31: 82-93.

Pienitz, R., Smol, J. P., Last, W., Leavitt, P., and Cumming, B. (2000). Multi-proxy Holocene palaeoclimatic record from a saline lake in the Canadian Subarctic. The Holocene, 10: 673-686.

Pierce, D. W., Barnett, T. P., Schneider, N., Saravanan, R., Dommenget, D., and Latif, M. (2001). The role of ocean dynamics in producing decadal climate variability in the North Pacific. Climate Dynamics, 18: 51-70.

Pilskaln, C. H. (2004). Seasonal and interannual particle export in an African rift valley lake: A 5-yr record from Lake Malawi, southern East Africa. Limnology and Oceanography, 49: 964-977.

Pisaric, M. F. J., St-Onge, S. M., Kokelj, S. V. (2009). Tree-ring Reconstruction of Early-growing Season Precipitation from Yellowknife, Northwest Territories, Canada. Arctic, Antarctic, and Alpine Research, 41: 486-496.

Podritske, B. and Gajewski, K. (2007). Diatom community response to multiple scales of Holocene climate variability on a small lake on Victoria Island, NWT, Canada. Quaternary Science Reviews, 26: 3179-3196.

Prentice and Thomson (2004). Economics of Airships for Northern Re-supply. Transport Institute, Asper School of Business, University of Manitoba.

Reimer, P. J., Baillie, M. G.L., Bard, E., Bayliss, A., Beck, J. W., Blackwell, P. G., Bronk Ramsey, C., Buck, C. E., Burr, G. S., Edwards, R. L., Friedrich, M., Grootes, P. M., Guilderson, T. P., Hajdas, I., Heaton, T. J., Hogg, A. G., Hughen, K. A., Kaiser, K. F., Kromer, B., McCormac, F. G., Manning, S. W., Reimer, R. W., Richards, D. A., Southon, J. R., Talamo, S., Turney, C. S. M., van der Plicht, J., and Weyhenmeyer, C. E. (2009). IntCal09 and Marine09 radiocarbon age calibration curves, 0-50,000 years cal BP. Radiocarbon, 51:1111-1150.

Ritchie, J. C. (1984). A Holocene pollen record of boreal forest history from the Travaillant Lake area, Lower Mackenzie River Basin. Canadian Journal of Botany, 62: 1385-1392.

Rolland, N., Larocque, I., Francus, P., Pienitz. R., and Laperrière, L. (2008). Holocene climate inferred from biological (Diptera: Chironomidae) analyses in a Southampton Island (Nunavut, Canada) lake. The Holocene, 18: 229-241.

Rolland, N., Larocque, I., Francus, P., Pienitz, R., and Laperrière, L. (2009). Evidence for a warmer period during the 12^{th} and 13^{th} centuries AD from chironomid assemblages in Southampton Island, Nunavut, Canada. Quaternary Research, 72: 27-37.

Rühland, K. and Smol, J. P. (1998). Limnological Characteristics of 70 Lakes Spanning Arctic Treeline from Coronation Gulf to Great Slave Lake in the Central Northwest Territories, Canada. International Review of Hydrobiology, 83: 183-203.

Rühland, K. and Smol, J. P. (2005). Diatom shifts as evidence for recent Subarctic warming in a remote tundra lake, NWT, Canada. Palaeogeography, Palaeoclimatology, Palaeoecology, 226: 1-16.

Ryba, S. A. and Burgess, R. M. (2002). Effects of sample preparation on the measurement of organic carbon, hydrogen, nitrogen, sulfur, and oxygen concentrations in marine sediments. Chemosphere, 48: 139-147.

Sampei, Y. and Matsumoto, E. (2001). C/N ratios in a sediment core Nakaumi Lagoon, southwest Japan – usefulness as an organic source indicator. Geochemical Journal, 35: 189-205.

Sand-Jensen, K. and Borum, J. (1991). Interactions among phytoplankton, periphyton, and macrophytes in temperate freshwaters and estuaries. Aquatic Botany, 41: 137-175.

Schelske, C. L. and Hodell, D. A. (1991). Recent Changes in Productivity and Climate of Lake Ontario Detected by Isotopic Analysis of Sediments. Limnology and Oceanography, 36: 961-975.

Schmidt, M. W. I. and Gleixner, G. (2005). Carbon and nitrogen isotope composition of bulk soils, particle-size fractions and organic material after treatment with hydrofluoric acid. European Journal of Soil Science, 56: 407-416.

Schneider, N., Miller, A. J., and Pierce, D. W. (2002). Anatomy of North Pacific Decadal Variability. Journal of Climate, 15: 586-605.

Schubert, C. J. and Nielsen, B. (2000). Effects of decarbonation treatments on $\delta^{13}C$ values in marine sediments. Marine Chemistry, 72: 55-59.

Shannon, C. E. (1949). Communication in the Presence of Noise. Proceedings of the IRE, January, pp. 10-21.

Shen, C., Wang, W. C., Gong, W., and Hao, Z. (2006). A Pacific Decadal Oscillation record since 1470 AD reconstructed from proxy data of summer rainfall over eastern China. Geophysical Research Letters, 33(3).

Singh, M., Ansari, A. A., Müller, G., and Singh, I. B. (1997). Heavy metals in freshly deposited sediments of the Gomati River (a tributary of the Ganga River): effects of human activities. Environmental Geology, 29: 246-252.

Smol, J. P. (1983). Paleophycology of a high arctic lake near Cape Herschel, Ellesmere Island. The Canadian Journal of Botany, 61: 2195-2204.

Sorenson, C. J., Knox, J. C., Larsen, J. A., and Bryson, R. A. (1971). Paleosols and the forest border in Keewatin, N.W.T. Quaternary Research, 1: 468-473.

Sorenson, C. J. (1977). Reconstructed Holocene Bioclimates. Annals of the Association of American Geographers, 67: 214-222.

Spear, R. W. (1993). The palynological record of Late-Quaternary arctic tree-line in northwest Canada. Review of Palaeobotany and Palynology, 79: 99-111.

Spence, C. and Rouse, W. R. (2002). The Energy Budget of Canadian Shield Subarctic Terrain and Its Impact on Hillslope Hydrological Processes. Journal of Hydrometeorology, 3: 208-218.

Spiker, E. C. and Hatcher, P. G. (1984). Carbon isotope fractionation of sapropelic organic matter during early diagenesis. Organic Geochemistry, 5: 283-290.

Stainton, M. P. (1973). A Syringe Gas-Stripping Procedure for Gas-Chromatographic Determination of Dissolved Inorganic and Organic Carbon in Fresh Water and Carbonates in Sediments. Journal of the Fisheries Research Board of Canada, 30: 1441-1445.

Steinhilber, F., Beer, J., and Frohlich, C. (2009). Total solar irradiance during the Holocene. Geophysical Research Letters, 36(19).

Stevenson, F. J. and Cheng, C. N. (1971). Organic geochemistry of the Argentine Basin sediments: carbon-nitrogen relationships and Quaternary correlations. Geochimica et Cosmochimica Acta, 36: 653-671.

Strong, W. L., Zoltai, S. C., and Ironside, G. R. (1989). Ecoclimatic regions of Canada, Ecological Land Classification Series, No. 23. Canadian Wildlife Service; Ottawa.

Stuiver, M. and Reimer, P. J. (1993). Extended ^{14}C data base and revised Calib 3.0 ^{14}C age calibration program. Radiocarbon, 35: 215-230.

Sun, D., Bloemendal, J., Rea, D. K., Vandenberghe, J., Jiang, F., An, Z., and Su, R. (2002). Grain-size distribution function of polymodal sediments in hydraulic and aeolian environments, and numerical partitioning of the sedimentary components. Sedimentary Geology, 152: 263-277.

Sun, H., Nelson, M., Chen, F., and Husch, J. M. (2007). Effect of structural water in clay minerals on the estimation of soil organic matter content by the LOI analytical method. Presented at the GSA Denver Annual Meeting – poster, Session 81, Booth #14.

Taguchi, B., Xie, S. P., Schneider, N., Nonaka, M., Sasaki, H., and Sasai, Y. (2007). Decadal Variability of the Kuroshio Extension: Observations and an Eddy-Resolving Model Hindcast. Journal of Climate, 20: 2357-2377.

Talbot, M. R. and Livingstone, D. A. (1989). Hydrogen index and carbon isotopes of lacustrine organic matter as lake level indicators. Palaeogeography, Palaeoclimatology, Palaeoecology, 70: 121-137.

Talbot, M. R. and Johannessen, T. (1992). A high resolution palaeoclimatic record for the last 27,500 years in tropical West Africa from the carbon and nitrogen isotopic composition of lacustrine organic matter. Earth and Planetary Science Letters, 110: 23-37.

Talbot, M. R. (2001). Nitrogen isotopes in palaeolimnology. In: Last, W. M. and Smol, J. P. (eds); Tracking environmental hange using lake sediments, Volume 2: Physical and geochemical methods. Kluwer Academic Press; Dordrecht.

Trenberth, K. E. and Hurrell, J. W. (1994). Decadal atmosphere-ocean variations in the Pacific. Climate Dynamics, 9: 303-319.

Velicer, W. F. and Fava, J. L. (1998). Effects of variable and subject sampling on factor pattern recovery. Psychological Methods, 3: 231-251.

Velinsky, D. J., Fogel, M. L., Todd, J. F., and Tebo, B. M. (1991). Isotope fractionation of dissolved ammonium at the oxygen-hydrogen sulfide interface in anoxic waters. Geophysical Research Letters, 18: 649-652.

Wang, H., Liu, H., Cui, H., and Abrahamsen, N. (2001). Terminal Pleistocene/Holocene palaeoenvironmental changes revealed by mineral-magnetism measurements of lake sediments for Dali Nor area, southeastern Inner Mongolia Plateau, China. Palaeogeography, Palaeoclimatology, Palaeoecology, 170: 115-132.

Wang, X. S., Qin, Y., and Chen, Y. K. (2006). Heavy metals in urban roadside soils, part 1: effect of particle size fractions on heavy metals partitioning. Environmental Geology, 50: 1061-1066.

Watanabe, T., Naraoka, H., Nishimura, M., and Kawai, T. (2004). Biological and environmental changes in Lake Baikal during the late Quaternary inferred from carbon, nitrogen and sulfur isotopes. Earth and Planetary Science Letters, 222: 285-299.

Wiles, G. C., D'Arrigo, R. D., and Jacoby, G. C. (1998). Gulf of Alaska atmosphere-ocean variability over recent centuries inferred from coastal tree-ring records. Climatic Change, 38: 289-306.

Willemse, N. W. and Törnqvist, T. E. (1999). Holocene century-scale temperature variability from West Greenland lake records. Geology, 27: 580-584.

Wolfe, A. P. (2002). Climate modulates the acidity of Arctic lakes on millennial time scales. Geology, 30: 215-218.

Wolfe, B. B., Edwards, T. W. D., Aravena, R., and MacDonald, G. M. (1996). Rapid Holocene hydrologic change along boreal tree-line revealed by $\delta^{13}C$ and $\delta^{18}O$ in organic lake sediments, Northwest Territories, Canada. Journal of Paleolimnology, 15: 171-181.

Wolfe, B. B., Edwards, T. W. D., and Aravena, R. (1999). Changes in carbon and nitrogen cycling during tree-line retreat recorded in the isotopic content of lacustrine organic matter, western Taimyr Peninsula, Russia. The Holocene, 9: 215-222.

Wolfe, B. B., Edwards, T. W. D., Jiang, H., MacDonald, G. M., Gervais, B. R., and Snyder, J. A. (2003). Effect of varying oceanicity on early- to mid-Holocene palaeohydrology, Kola Peninsula, Russia: isotopic evidence from treeline lakes. The Holocene, 13: 153-160.

Wu, L. and Liu, Z. (2003). Decadal Variability in the North Pacific: The Eastern North Pacific Mode. Journal of Climate, 16: 3111-3131.

Wu, Y., Hou, X., Cheng, X., Yao, S., Xia, W., and Wang, S. (2007). Combining geochemical and statistical methods to distinguish anthropogenic source of metals in lacustrine sediment: a case study in Dongjiu Lake, Taihu Lake catchment, China. Environmental Geology, 52: 1467-1474.

Yamamuro, M. and Kayanne, H. (1995). Rapid direct determination of organic carbon and nitrogen in carbonate-bearing sediments with a Tanaco MT-5 CHN analyzer. Limnology and Oceanography, 40: 1001-1005.

Zabenskie, S. and Gajewski, K. (2007). Post-Glacial climatic change on Boothia Peninsula, Nunavut, Canada. Quaternary Research, 68: 261-270.

Zhang, Y., Wallace, J. M., and Iwasaka, N. (1996). Is Climate Variability over the North Pacific a Linear Response to ENSO? Journal of Climate, 9: 1468-1478.

Appendix

Modern Lake Survey Data

Sample	Latitude	δ13C	δ15N	%C	%N	C/N	Depth	pH	DO	Cond.	Cu	Pb	Zn	Ni	Mn	Fe	As	U	Cd	Ca	P	Mg	Ti	Al	Na	K	S	Hg	Li
R09 PROPS 01	62.540	-26.850	2.820	2.318	0.255	9.090	0.750	6.550	7.800	Missing	18.900	10.370	65.300	29.500	281.000	22200.000	5.000	5.000	0.130	3400.000	660.000	7600.000	730.000	16200.00	230.000	2300.000	700.000	0.014	29.300
R09 STIB 02	62.541	Missing	Missing	Missing	Missing	Missing	1.600	8.460	10.660	259.300	26.720	6.340	96.300	41.800	435.000	12600.000	7.500	1.800	0.440	15700.000	117	5300.000	210.000	7600.000	780.000	1500.000	12900.000	0.118	17.200
R09-LK04S4	62.490	-28.500	3.400	0.533	0.074	7.203	5.100	7.970	10.430	108.400	4.850	2.350	18.900	8.500	120.000	8900.000	1.900	0.800	0.040	1100.000	350.000	2600.000	240.000	4800.000	100.000	900.000	300.000	0.009	14.100
R09-LK05S1	62.508	-30.630	0.980	30.120	2.450	12.294	1.100	7.660	8.320	247.200	27.600	5.910	81.200	30.800	333.000	15000.000	8.500	3.800	0.250	15200.000	101	6300.000	290.000	9500.000	650.000	1900.000	15300.000	0.089	14.500
R09-0702	62.550	-31.820	1.400	36.200	2.806	12.901	4.000	7.810	9.800	202.700	31.420	5.020	84.800	31.200	209.000	7900.000	26.000	2.300	0.170	15600.000	164	4800.000	180.000	6900.000	550.000	1500.000	12700.000	0.142	8.700
R09-0803	62.504	-29.570	0.980	38.950	2.595	15.010	2.100	7.820	7.310	351.000	20.710	2.760	42.000	22.300	399.000	8000.000	5.500	3.700	0.190	18400.000	840.000	4200.000	120.000	5000.000	410.000	7000.000	17500.000	0.069	4.800
R09 09.00	62.523	-26.120	1.730	14.150	1.193	11.861	1.100	8.070	10.660	106.800	24.830	8.830	60.800	32.900	641.000	17000.000	8.000	2.200	0.150	6400.000	720.000	6000.000	460.000	14600.00	150.000	2300.000	3300.000	0.053	24.500
R09-10-01	62.524	-28.480	1.750	5.483	0.432	12.692	3.200	7.580	1.250	94.100	32.150	11.620	66.200	38.500	265.000	21500.000	5.100	4.700	0.130	5400.000	660.000	7300.000	580.000	20300.00	280.000	2600.000	1500.000	0.051	32.400
R09-11-01	62.548	-28.040	0.570	43.300	2.351	18.418	7.100	7.650	0.100	196.800	53.190	5.830	65.100	34.800	242.000	17400.000	21.300	4.300	0.310	15400.000	117	6100.000	280.000	11000.00	300.000	1600.000	15800.000	0.100	15.500
R09-12-02	62.539	-29.580	1.640	29.620	2.286	12.957	3.100	7.820	7.640	327.300	22.520	6.490	75.400	29.800	307.000	19200.000	17.600	3.400	0.210	12600.000	930.000	6800.000	300.000	10800.00	790.000	2300.000	7800.000	0.062	18.200
R09 13-03	62.552	-23.170	4.720	23.950	2.009	11.921	5.100	8.230	8.540	349.900	18.240	4.410	60.600	19.800	458.000	12100.000	18.800	7.900	0.190	10800.000	790.000	4900.000	270.000	8000.000	690.000	1800.000	9200.000	0.029	21.100
R09 14-02	62.497	-28.780	1.430	13.100	1.078	12.152	1.100	7.970	7.600	255.300	36.710	12.550	89.200	41.500	492.000	28700.000	101.600	3.500	0.400	8300.000	105	9900.000	630.000	21400.00	720.000	4700.000	6000.000	0.070	31.100
R09 15-01	62.518	-21.010	6.000	1.003	0.141	7.113	1.500	8.300	4.430	50.600	30.010	9.890	67.100	22.400	357.000	18300.000	25.600	4.100	0.060	3200.000	780.000	6000.000	590.000	11900.00	270.000	2300.000	400.000	0.003	24.000
R09 16-01	62.460	-29.330	1.360	12.210	1.048	11.651	2.000	7.880	5.210	129.000	27.270	9.500	100.10	33.800	353.000	20000.000	81.000	5.000	0.310	10300.000	690.000	7800.000	500.000	16800.00	270.000	2700.000	4800.000	0.080	28.900
R09 17-01	62.486	-28.570	1.340	32.020	1.931	16.582	1.100	7.720	4.310	66.300	20.750	6.890	84.800	24.800	730.000	16600.000	85.400	5.000	0.370	15400.000	940.000	4600.000	270.000	9100.000	390.000	1400.000	7100.000	0.154	12.300
R09 18-01	62.480	-28.440	1.920	19.080	1.051	18.154	6.100	7.540	0.220	135.300	26.290	9.260	190.10	27.000	364.000	18400.000	39.800	7.200	0.300	25500.000	700.000	16200.000	410.000	14100.00	300.000	2600.000	2900.000	0.149	23.900
R09 19-01	62.467	-25.970	4.000	1.416	0.147	9.633	2.000	7.750	5.230	124.800	3.870	2.280	11.600	5.400	87.000	4600.000	23.900	0.600	0.040	1200.000	290.000	1200.000	90.000	2300.000	70.000	200.000	900.000	0.003	4.900
R11-13-01	64.333	-18.760	4.480	8.660	0.684	12.661	6.300	6.630	9.230	8.800	Missing	Missing	Missing	Missing	Missing	Missing	Missing	Missing	Missing	Missing	Missing	Missing	Missing	Missing	Missing	Missing	Missing	Missing	Missing
R11-13-02	64.412	-21.060	3.620	2.232	0.206	10.835	2.400	6.650	5.340	9.400	17.170	2.270	33.600	14.500	166.000	12600.000	7.200	1.800	0.110	800.000	250.000	2100.000	230.000	5500.000	70.000	1400.000	800.000	0.031	13.700
R11-13-03	64.419	-25.	3.780	9.786	0.891	10.983	7.000	6.480	8.500	10.200	69.670	7.180	107.10	39.500	219.000	29200.00	16.000	6.300	0.380	1700.000	122 0.00	3400.000	280.000	1390 0.00	90.000	180 0.00	3000.000	0.079	19.400

		470											0			0					0			0		0			
R11-13-04	64.290	-23.450	2.020	10.590	0.884	11.980	3.900	6.590	9.350	9.300	59.350	4.930	55.900	27.900	84.000	9800.000	4.100	5.700	0.370	2400.000	660.000	2000.000	160.000	8800.000	80.000	900.000	3300.000	0.073	13.700
R11-13-05	64.268	-25.280	3.530	10.660	0.939	11.353	3.100	6.570	8.570	12.800	48.490	4.160	52.700	33.100	100.000	10200.000	6.800	3.100	0.260	2200.000	770.000	2800.000	240.000	8600.000	90.000	12000.000	2500.000	0.074	19.700
R11-13-06	64.259	-25.230	3.120	6.034	0.608	9.924	1.900	6.450	6.100	11.200	39.600	4.510	58.600	30.100	142.000	12700.000	4.700	1.900	0.230	2200.000	700.000	3900.000	370.000	10900.000	130.000	2000.000	1800.000	0.063	26.700
R11-13-07	64.037	-25.500	3.450	10.270	0.856	11.998	3.000	6.400	8.830	7.700	54.970	5.280	81.500	38.300	115.000	16100.000	15.100	7.900	0.350	2400.000	940.000	2800.000	230.000	12300.000	70.000	12000.000	3100.000	0.066	16.600
R11-14-01	65.383	-23.230	3.220	10.810	1.230	8.789	4.400	6.570	9.570	9.900	45.650	6.440	52.900	32.800	214.000	17700.000	14.800	1.500	0.260	2900.000	129000	4900.000	240.000	10000.000	130.000	16000.000	3000.000	0.061	19.400
R11-14-02	65.258	-21.970	5.340	0.931	0.075	12.413	4.400	6.550	2.040	9.600	14.770	2.050	35.500	16.800	326.000	12400.000	7.100	1.100	0.040	500.000	220.000	2600.000	250.000	6200.000	50.000	9000.000	400.000	0.012	12.400
R11-14-03	65.140	-22.690	4.000	5.031	0.600	8.385	3.200	6.690	9.730	10.300	70.290	5.750	65.200	46.500	297.000	24100.000	47.800	1.900	0.420	2000.000	720.000	5400.000	440.000	14300.000	100.000	24000.000	2100.000	0.046	25.100
R11-14-05	64.950	-22.830	3.550	11.650	0.818	14.242	7.200	6.520	9.380	9.300	94.450	6.350	101.100	50.800	223.000	30800.000	28.500	7.800	0.560	2100.000	830.000	5500.000	400.000	18300.000	90.000	27000.000	2900.000	0.035	27.000
R11-14-06	64.924	-26.820	3.070	6.875	0.579	11.874	5.500	6.570	7.040	11.600	71.420	7.410	126.800	60.200	324.000	29400.000	25.200	7.800	0.420	2000.000	920.000	8300.000	930.000	23600.000	130.000	43000.000	1600.000	0.066	48.700
R11-14-07	64.839	-26.650	2.850	7.561	0.617	12.254	4.500	6.760	9.780	12.500	60.520	5.630	78.500	34.500	423.000	57300.000	65.000	8.000	0.290	1400.000	134000	5800.000	580.000	17000.000	100.000	31000.000	1400.000	0.061	32.400
R11-14-08	64.721	-22.090	2.810	2.663	0.216	12.329	2.800	6.690	9.460	8.800	25.060	3.170	105.200	42.900	164.000	15200.000	9.300	4.000	0.090	1200.000	420.000	4500.000	560.000	12000.000	70.000	25000.000	900.000	0.017	29.300
R11-14-09	64.653	-22.460	2.910	8.866	0.760	11.666	6.500	6.750	8.800	10.400	69.500	7.010	122.200	53.000	349.000	31300.000	17.800	5.800	0.420	1700.000	163000	7700.000	710.000	20800.000	140.000	41000.000	2200.000	0.039	42.800
R11-14-10	64.499	-24.970	4.520	12.610	1.173	10.750	7.100	6.550	10.030	11.700	83.330	7.800	95.800	45.900	340.000	40300.000	27.900	5.100	0.230	1800.000	134000	6500.000	590.000	18400.000	130.000	33000.000	2500.000	0.083	34.400
R11-14-11	64.430	-23.520	4.980	0.742	0.073	10.164	5.400	6.720	11.290	14.800	15.820	2.880	33.300	21.900	523.000	20700.000	49.400	2.000	0.060	800.000	650.000	3300.000	450.000	6700.000	90.000	20000.000	200.000	0.003	19.400
R11-18-01	64.294	-24.040	2.920	6.661	0.554	12.023	3.500	6.530	3.500	9.800	86.920	5.290	122.800	68.800	85.000	14500.000	10.100	2.300	0.390	2400.000	650.000	3000.000	160.000	10800.000	70.000	10000.000	3400.000	0.050	15.100
R11-18-02	64.251	-26.810	2.750	11.220	0.856	13.107	9.000	6.620	9.480	7.400	74.590	5.010	103.500	31.600	237.000	34600.000	28.000	5.700	0.530	2200.000	133000	2700.000	260.000	16500.000	80.000	10000.000	2500.000	0.077	16.400
R11-19-13	64.127	-25.160	3.070	13.130	0.937	14.013	2.000	6.530	10.690	7.800	44.830	2.990	71.200	26.900	83.000	12100.000	11.500	4.000	0.280	1800.000	540.000	2300.000	230.000	8600.000	70.000	10000.000	2100.000	0.035	15.500
R11-19-14	64.125	-23.160	3.270	6.070	0.465	13.054	6.700	6.570	9.690	8.000	40.590	4.140	57.300	24.400	154.000	15700.000	10.500	4.000	0.240	1300.000	830.000	3400.000	320.000	10800.000	70.000	14000.000	1300.000	0.026	19.400
R11-15-01	63.902	-24.710	3.110	12.380	0.991	12.492	3.200	6.700	9.270	12.100	84.170	4.990	133.000	49.800	164.000	21500.000	9.800	4.200	0.470	2900.000	750.000	3400.000	330.000	14800.000	70.000	18000.000	3900.000	0.064	19.800
R11-15-02	63.887	-26.330	2.860	7.760	0.555	13.982	5.000	6.830	8.670	10.900	60.600	5.480	90.600	42.600	171200	33700.000	55.400	5.200	0.360	1800.000	850.000	3000.000	290.000	16800.000	70.000	13000.000	1900.000	0.040	18.100
R11-15-03	63.811	-22.300	3.100	18.720	1.398	13.391	3.600	6.800	8.730	14.700	72.870	6.360	125.000	36.700	213.000	18400.000	5.900	15.800	0.830	3700.000	940.000	3100.000	200.000	13300.000	90.000	11000.000	4700.000	0.072	16.300

R11-15-04	63.742	-22.490	3.860	17.480	1.638	10.672	3.000	7.000	8.630	17.400	69.610	7.790	114.600	43.900	246.000	25900.000	5.500	24.100	0.280	4200.000	830.000	5500.000	480.000	14800.000	150.000	250.000	3900.000	0.071	32.400
R11-15-06	63.677	-28.110	3.530	14.570	1.176	12.389	5.900	6.680	7.130	14.500	63.210	7.250	89.400	30.200	269.000	24900.000	3.800	39.900	0.380	3200.000	1410.000	4000.000	270.000	16700.000	110.000	120.000	2600.000	0.131	17.900
R11-18-12	63.761	-26.770	3.680	9.681	0.928	10.432	3.000	6.810	9.370	13.300	55.500	11.910	149.900	45.600	274.000	24600.000	5.400	40.700	0.520	3000.000	830.000	8000.000	840.000	23100.000	240.000	420.000	2400.000	0.085	46.800
R11-19-01	63.816	-26.490	3.560	6.514	0.565	11.529	2.500	6.670	10.270	11.200	52.820	6.050	120.700	54.100	327.000	26700.000	7.100	13.700	0.260	2700.000	760.000	10400.000	1100.000	22700.000	240.000	530.000	1200.000	0.051	55.300
R11-19-02	63.800	-26.850	2.620	22.220	1.607	13.827	2.000	6.660	10.680	12.000	42.600	5.350	64.400	20.800	115.000	7900.000	7.700	10.600	0.380	3700.000	770.000	2000.000	160.000	8600.000	100.000	800.000	2800.000	0.095	11.600
R11-19-06	64.106	-26.510	2.250	18.110	1.408	12.862	3.000	6.650	10.360	9.800	141.320	3.090	189.600	35.700	87.000	7300.000	7.600	3.500	0.950	3100.000	800.000	2400.000	190.000	12100.000	50.000	900.000	2800.000	0.084	12.800
R11-19-07	64.056	-23.720	3.260	16.280	1.267	12.849		6.570	7.740	22.300	73.120	3.530	126.700	84.100	99.000	14100.000	16.400	2.000	0.530	2300.000	670.000	2400.000	170.000	8700.000	60.000	800.000	5200.000	0.059	12.000
R11-19-08	64.004	-23.820	3.870	14.110	0.982	14.369	6.500	6.760	9.990	12.200	83.260	5.160	137.600	65.800	208.000	2640	21.500	2.800	0.400	2900.000	1020.000	2900.000	190.000	12900.000	70.000	1100.000	3300.000	0.055	15.400
R11-19-09	63.983	-27.640	2.760	11.080	0.908	12.203	5.000	6.480	9.930	9.600	Missing	Missing	Missing	Missing	Missing	Missing	Missing	Missing	Missing	Missing	Missing	Missing	Missing	Missing	Missing	Missing	Missing	Missing	Missing	Missing
R11-19-10	63.988	-27.530	3.290	8.084	0.559	14.462	3.000	6.560	10.390	12.200	27.550	3.300	36.300	19.200	94.000	10900.000	8.100	2.000	0.120	2200.000	830.000	2700.000	250.000	8200.000	80.000	1200.000	1200.000	0.059	15.200
R11-19-11	63.982	-27.120	3.760	9.581	0.687	13.946	9.500	6.550	10.120	14.700	84.040	5.840	130.000	101.100	222.000	3160	15.500	3.000	0.290	2200.000	1410.000	3600.000	360.000	14600.000	80.000	1500.000	2500.000	0.156	20.500
R11-19-12	64.033	-26.670	3.660	14.450	1.143	12.642		6.610	10.130	12.000	89.140	5.750	82.800	44.600	147.000	16600.000	18.600	3.300	0.380	3100.000	1150.000	3300.000	230.000	12100.000	80.000	1300.000	2900.000	0.102	18.000
R11-17-01	62.849	Missing	Missing	Missing	Missing	Missing	1.900	7.170	5.580	59.800	Missing	Missing	Missing	Missing	Missing	Missing	Missing	Missing	Missing	Missing	Missing	Missing	Missing	Missing	Missing	Missing	Missing	Missing	Missing	Missing
R11-17-02	62.771	-29.510	3.760	5.299	0.556	9.531	6.000	7.260	0.710	72.800	26.030	7.160	108.600	39.000	544.000	29700.000	6.600	18.400	0.180	3800.000	1060.000	6800.000	740.000	18800.000	240.000	3000.000	1300.000	0.060	39.000
R11-17-03	62.953	Missing	Missing	Missing	Missing	Missing	5.400	7.300	1.510	146.300	104.330	4.100	119.800	126.600	174.000	19400.000	11.600	4.300	0.530	9700.000	780.000	3900.000	280.000	7200.000	170.000	1000.000	2080.000	0.033	17.300
R11-17-04	63.015	Missing	Missing	Missing	Missing	Missing	4.300	7.260	0.230	40.300	Missing	Missing	Missing	Missing	Missing	Missing	Missing	Missing	Missing	Missing	Missing	Missing	Missing	Missing	Missing	Missing	Missing	Missing	Missing	Missing
R11-17-06	63.318	Missing	Missing	Missing	Missing	Missing	3.400	7.440	8.960	83.800	91.810	11.280	229.600	158.500	289.200	8800.000	28.900	7.700	0.890	9200.000	1210.000	1800.000	90.000	12200.000	80.000	400.000	8300.000	0.109	7.600
R11-17-07	63.392	-29.990	5.660	19.570	2.305	8.490	7.200	7.160	3.020	23.700	42.800	9.940	65.300	14.700	263.000	9500.000	2.200	98.600	0.500	3800.000	1820.000	1600.000	120.000	14100.000	160.000	800.000	3700.000	0.138	7.600
R11-18-03	63.401	-24.940	5.430	19.910	1.911	10.419	5.500	6.930	7.190	23.500	38.960	6.480	66.700	16.500	149.000	10700.000	1.100	109.700	0.460	4000.000	1380.000	1400.000	70.000	12600.000	160.000	500.000	4100.000	0.064	7.500
R11-18-04	63.417	-24.950	3.570	17.480	1.672	10.455	6.100	6.910	7.610	18.400	108.870	5.390	137.100	43.200	191.000	21000.000	1.500	69.100	0.840	4200.000	1030.000	1200.000	110.000	22500.000	70.000	400.000	3900.000	0.082	5.200
R11-18-05	63.458	-25.210	2.820	20.740	1.740	11.920	3.800	6.990	9.450	32.400	51.440	4.610	64.600	23.000	84.000	46000.000	0.300	67.800	0.390	4500.000	850.000	1400.000	60.000	9400.000	160.000	400.000	4700.000	0.102	5.400
R11-18-06	63.477	-27.780	3.040	8.046	0.710	11.332	4.000	7.070	6.500	46.100	29.070	3.700	167.000	22.300	498.000	41000.000	3.200	26.300	0.360	4100.000	1870.000	2300.000	260.000	19100.000	90.000	600.000	1300.000	0.085	9.800

R11-18-07	63.517	-28.710	3.650	19.550	1.535	12.736	10.000	6.330	0.200	31.800	66.710	6.350	71.600	20.200	299.000	140000.000	1.900	22.300	0.470	4200.000	21700.000	2400.000	240.000	170000.000	270.000	10000.000	2800.000	0.207	13.900
R11-18-08	63.587	-25.310	2.450	12.850	1.120	11.473	2.000	6.810	9.680	18.000	33.100	2.220	66.800	17.000	52.000	54000.000	0.600	5.500	0.240	2600.000	330.000	1500.000	180.000	6300.000	80.000	500.000	2100.000	0.030	9.300
R11-18-09	63.594	-28.080	1.720	38.930	2.021	19.263	1.500	6.860	9.770	23.000	67.800	2.630	88.700	23.200	88.000	61000.000	1.200	18.800	0.530	8800.000	620.000	1400.000	90.000	6900.000	130.000	300.000	4800.000	0.101	2.100
R11-18-10	63.600	-27.750	1.940	51.790	2.323	22.294	1.200	Missing	9.790	18.000	32.300	1.730	40.600	10.600	107.000	73000.000	1.400	9.700	0.440	135000.000	560.000	2200.000	70.000	4100.000	60.000	200.000	3900.000	0.082	0.800
R11-18-11	63.659	-25.950	4.840	12.470	1.368	9.115	4.800	Missing	9.360	13.700	28.880	5.500	66.300	21.000	129.000	134000.000	1.800	20.300	0.260	2500.000	810.000	2600.000	240.000	123000.000	100.000	110000.000	2000.000	0.070	16.700
R11-19-03	63.759	-22.210	2.010	23.210	1.824	12.725	2.300	6.780	10.450	11.300	51.250	2.540	67.300	28.100	88.000	57000.000	1.800	4.200	0.370	3600.000	590.000	1600.000	130.000	7900.000	70.000	400.000	4000.000	0.028	8.600
R11-19-04	63.788	-24.320	2.880	29.350	2.289	12.822	2.000	6.670	10.670	17.100	55.540	4.070	100.600	36.900	183.000	111000.000	4.900	6.100	0.550	5600.000	830.000	2400.000	200.000	107000.000	100.000	800.000	4500.000	0.087	11.500
R11-19-05	63.799	-25.090	3.370	24.470	1.836	13.328	2.000	7.000	8.910	11.600	64.410	4.320	77.800	28.600	124.000	101000.000	2.500	6.800	0.480	3700.000	860.000	1500.000	120.000	114000.000	80.000	600.000	4600.000	0.086	6.400

Purple samples=R09, blue samples=Arctic Tundra, red samples=Transition Zone, green samples=Boreal Forest. Water depth in meters, dissolved oxygen in (µm/l), conductivity in (µm/S), elemental data in ppm.

Tukey Boxplots of Variables

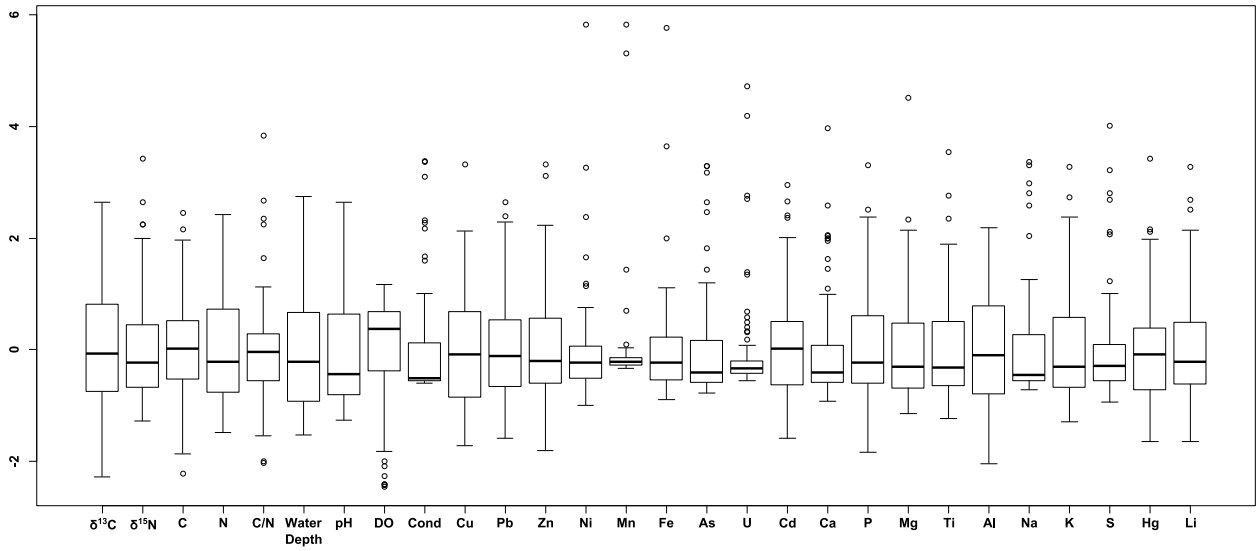

Variable values have been centered and scaled against an arbitrary y-axis to fit on the same graph.

Box-Cox Test for λ

Variable	λ value
δ13C	0.5
δ15N	0.75
%C	0.5
%N	1.25
C/N Ratio	0.66
Water Depth (m)	0.33
Surface pH	-2
DO (µm/l)	1.5
Conductivity (µm/S)	-0.5
Cu	0.5
Pb	0.33
Zn	0.33
Ni	-0.2
Mn	-0.33
Fe	-0.2
As	0
U	-0.25
Cd	0.66
Ca	-0.2
P	0.33
Mg	0
Ti	0.2
Al	0.66
Na	-0.75
K	0.25
S	0.2
Hg	0.66
Li	0.5

Kendall's Tau Rank Correlation Coefficient

	δ13C	δ15N	%C	%N	C/N	Depth (m)	pH	DO	Cond.	Cu	Pb	Zn	Ni	Mn	Fe	As	U	Cd	Ca	P	Mg	Ti	Al	Na	K	S	Hg	Li
δ13C		0.330	-0.166	-0.166	-0.132	0.051	-0.232	0.107	-0.391	0.154	-0.177	-0.007	0.109	-0.115	0.004	-0.002	-0.093	0.030	-0.336	-0.196	-0.120	-0.022	-0.091	-0.344	-0.011	-0.111	-0.362	0.074
δ15N			-0.296	-0.185	-0.252	0.292	-0.181	-0.032	-0.157	0.102	0.040	-0.014	0.040	0.022	0.095	-0.023	0.075	-0.042	-0.328	0.065	-0.086	0.046	0.071	-0.130	0.026	-0.277	-0.161	0.107
%C				0.677	0.873	-0.066	0.204	0.033	0.262	0.144	-0.022	0.109	-0.035	-0.052	-0.233	-0.069	0.176	0.336	0.534	0.166	-0.132	-0.348	-0.166	0.145	-0.261	0.646	0.438	-0.357
%N					0.625	-0.071	0.222	0.006	0.272	0.090	0.054	0.002	-0.088	-0.056	-0.247	-0.186	0.226	0.284	0.501	0.242	-0.117	-0.324	-0.113	0.211	-0.224	0.595	0.436	-0.310
C/N						-0.010	0.074	0.063	0.139	0.211	-0.077	0.088	-0.051	-0.131	-0.225	-0.098	0.208	0.345	0.416	0.177	-0.190	-0.369	-0.155	0.051	-0.291	0.554	0.429	-0.380
Depth (m)							-0.205	-0.087	-0.152	0.265	0.112	0.154	0.136	0.084	0.266	0.115	0.139	0.110	0.178	0.324	0.016	0.074	0.230	0.053	0.052	0.073	0.046	0.104
pH								-0.163	0.640	-0.298	0.115	-0.031	-0.130	0.233	-0.108	0.035	0.017	-0.089	0.456	0.014	0.107	-0.030	-0.084	0.380	-0.006	0.258	0.068	-0.100
DO									-0.232	0.081	-0.204	0.040	0.040	-0.185	-0.085	-0.040	-0.120	0.034	-0.159	0.078	-0.120	-0.080	-0.135	-0.214	-0.073	-0.077	-0.022	-0.029
Cond.										-0.278	0.172	-0.035	-0.106	0.222	-0.108	-0.021	0.004	-0.081	0.532	0.091	0.130	-0.023	-0.067	0.494	-0.007	0.302	0.170	-0.087
Cu											0.092	0.451	0.495	-0.140	0.200	0.055	0.183	0.577	-0.096	0.233	-0.088	-0.061	0.284	-0.253	-0.056	0.159	0.193	0.011
Pb												0.254	0.262	0.401	0.364	0.197	0.225	0.073	0.220	0.367	0.486	0.379	0.528	0.432	0.447	0.094	0.216	0.399
Zn													0.562	0.145	0.347	0.136	0.240	0.411	0.106	0.238	0.156	0.162	0.423	-0.015	0.156	0.143	0.222	0.173
Ni														0.154	0.421	0.279	0.008	0.301	-0.026	0.180	0.292	0.283	0.396	-0.020	0.306	0.128	0.027	0.347
Mn															0.403	0.358	0.109	-0.073	0.204	0.269	0.431	0.397	0.317	0.401	0.374	0.036	0.051	0.291
Fe																0.346	0.142	0.046	-0.133	0.290	0.458	0.560	0.590	0.094	0.532	-0.159	-0.044	0.544
As																	-0.200	-0.040	-0.067	0.129	0.361	0.322	0.138	0.100	0.374	0.025	-0.067	0.300
U																		0.308	0.191	0.251	-0.047	-0.002	0.347	0.133	-0.034	0.116	0.273	-0.006
Cd																			0.148	0.238	-0.197	-0.235	0.201	-0.121	-0.217	0.350	0.346	-0.189
Ca																				0.169	0.110	-0.127	-0.032	0.474	-0.071	0.608	0.390	-0.162
P																					0.117	0.009	0.346	0.229	0.067	0.199	0.409	0.017
Mg																						0.687	0.344	0.451	0.779	-0.015	-0.062	0.682
Ti																							0.449	0.276	0.791	-0.271	-0.171	0.802
Al																								0.137	0.425	-0.144	0.116	0.458
Na																									0.331	0.257	0.185	0.225
K																										-0.153	-0.117	0.816
S																											0.362	-0.245
Hg																												-0.168
Li																												

Values are Kendall's Tau: orange=moderate correlation, red=strong correlation, bright red=very strong correlation. Dissolved oxygen in (µm/l), conductivity in (µm/S), elemental data in ppm.

Ward's Hierarchical Cluster Analysis of Variables

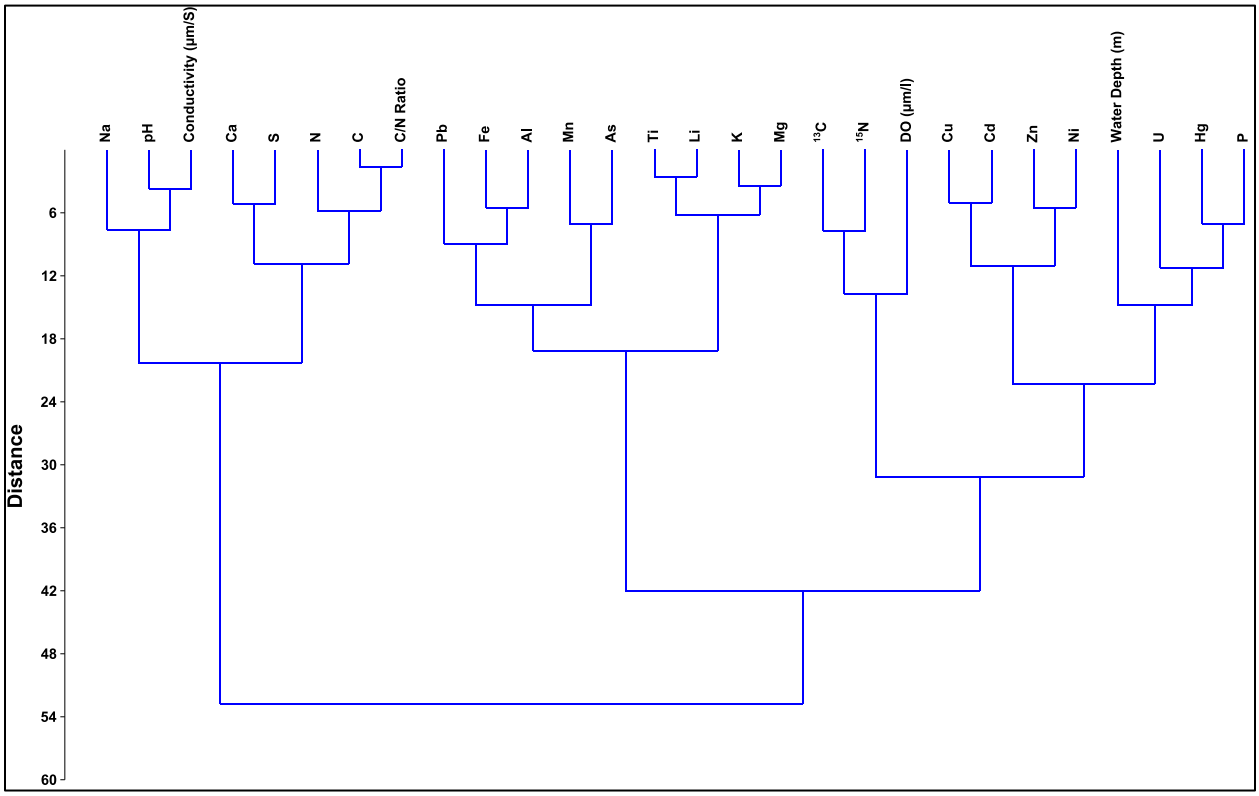

Ward's Hierarchical Cluster Analysis of Samples

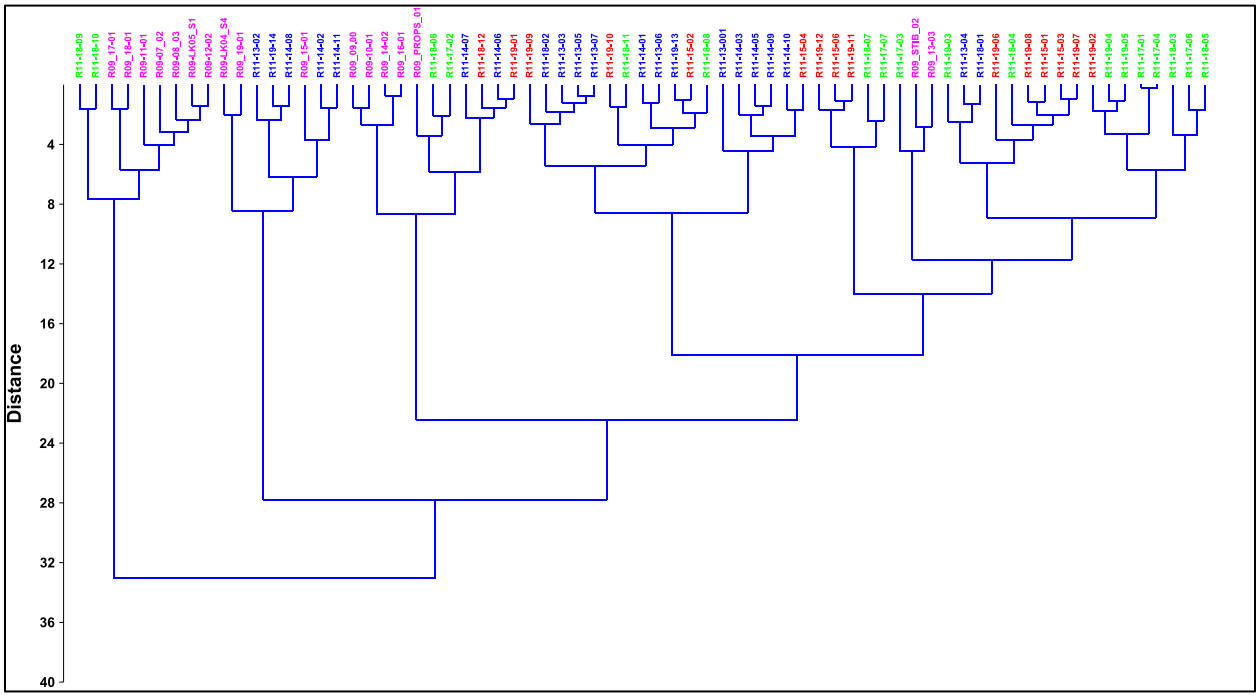

Purple samples=R09, blue samples=Arctic Tundra, red samples=Transition Zone, green samples=Boreal Forest.

Scatterplot of Ward's Hierarchical Cluster Analysis of Samples vs. Latitude

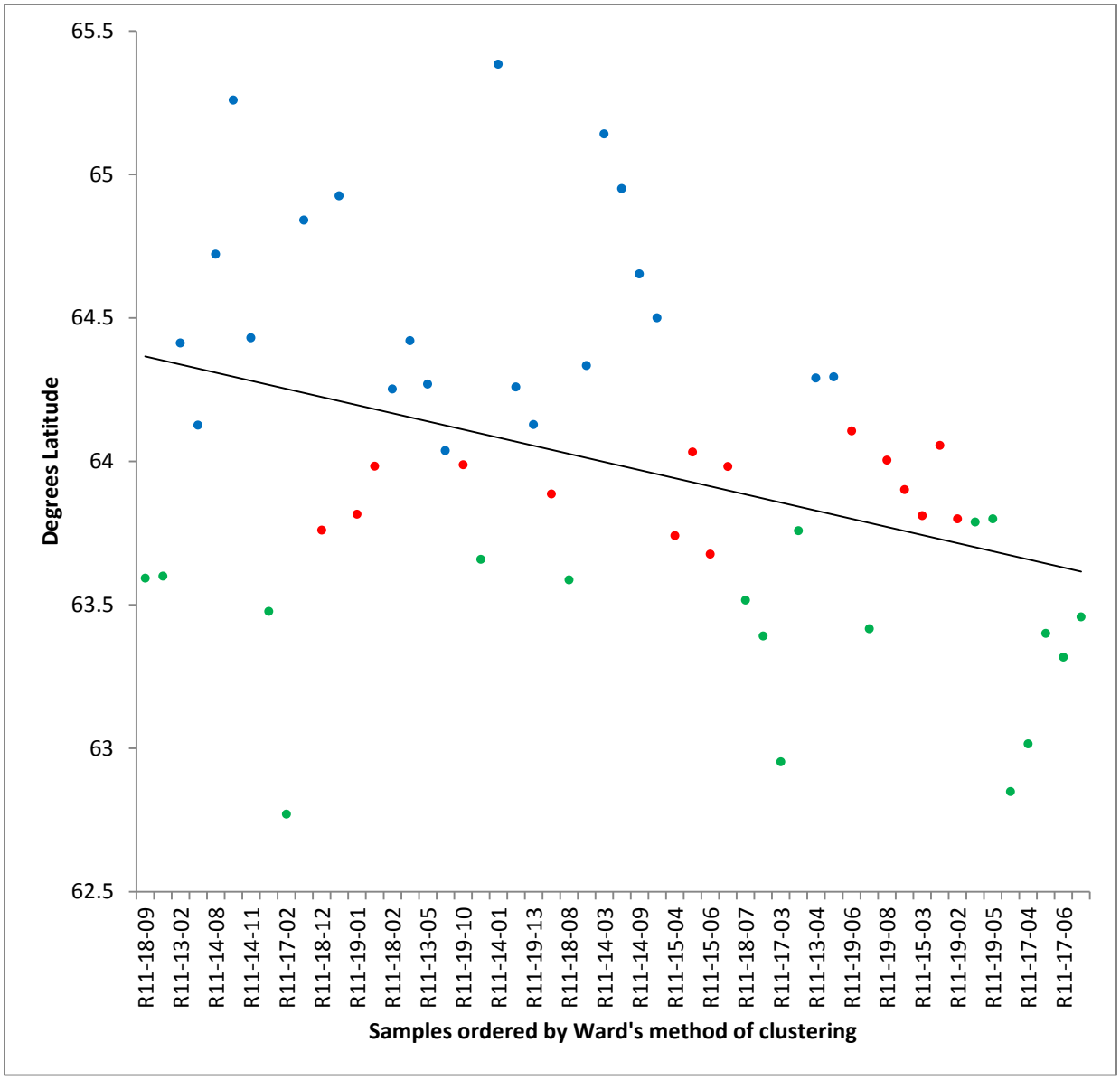

Blue samples=Arctic Tundra, red samples=Transition Zone, green samples=Boreal Forest. Black line is the trendline.

Principle Components Analysis Eigenvalues and Variable Loadings

Principle Components			Loadings								
PC	Eigenvalue	% Variance	$\delta^{13}C$	$\delta^{15}N$	C	Cond. (µm/S)	Cu	Ca	Ti	S	Hg
1	7.50172	48.039	-0.2907	-0.3471	0.4552	0.2346	0.06311	0.4255	-0.1642	0.4378	0.3593
2	2.8212	18.066	0.3496	0.235	0.2317	-0.4689	0.6014	-0.1203	-0.2998	0.1402	0.2515
3	1.7015	10.896	-0.245	-0.1395	-0.09075	-0.1668	0.3707	-0.01014	0.778	-0.1311	0.3528
4	1.29757	8.3093	0.4773	-0.462	0.1037	-0.04015	0.1703	0.1157	0.2998	0.305	-0.5667
5	1.08682	6.9597	0.2458	0.6583	-0.1404	0.4182	0.09352	0.3488	0.2689	0.3282	0.03322
6	0.504424	3.2302	0.4341	0.06546	0.4063	-0.2877	-0.5804	0.1923	0.2453	-0.1865	0.3011
7	0.308524	1.9758	0.4557	-0.3858	-0.5654	0.2137	-0.02989	-0.02965	-0.1538	0.03383	0.5016
8	0.261963	1.6775	0.1425	-0.06913	0.1459	0.2875	0.3416	0.4465	-0.1302	-0.7286	-0.0846
9	0.132157	0.8463	0.1693	-0.007849	0.4408	0.5565	0.06822	-0.6574	0.1223	-0.06338	0.1071

Orange=moderate loading, red=strong loading, bright red=very strong loading.

Principle Components Analysis – PC 1 vs. PC 2

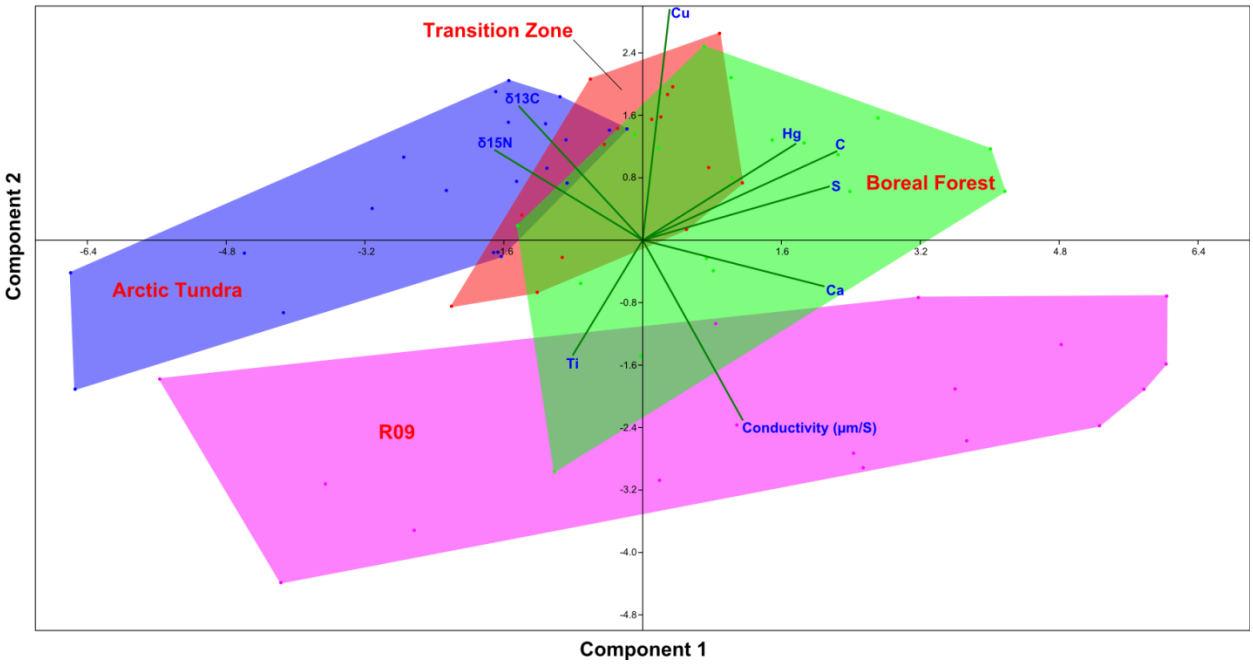

Kruskal-Wallis One-Way Analysis of Variance

	Arctic Tundra								
	$\delta^{13}C$	**$\delta^{15}N$**	**%C**	**Cond. (µm/S)**	**Cu**	**Ca**	**Ti**	**S**	**Hg**
Transition	0.00851	0.78500	0.00067	0.00079	0.08602	0.00023	0.41270	0.05805	0.01407
Boreal Forest	0.00203	0.52590	0.00002	0.00000	0.83260	0.00000	0.00166	0.00083	0.00423
R09	0.00007	0.00383	0.02379	0.00000	0.00053	0.00004	0.98830	0.02195	0.25200

	Transition Zone								
	$\delta^{13}C$	**$\delta^{15}N$**	**%C**	**Cond. (µm/S)**	**Cu**	**Ca**	**Ti**	**S**	**Hg**
Arctic Tundra	0.00851	0.78500	0.00067	0.00079	0.08602	0.00023	0.41270	0.05805	0.01407
Boreal Forest	0.84220	0.63800	0.13320	0.00021	0.07941	0.00081	0.01253	0.08870	0.66420
R09	0.01648	0.01410	0.45010	0.00000	0.00001	0.00083	0.58380	0.12140	0.50860

	Boreal Forest								
	$\delta^{13}C$	**$\delta^{15}N$**	**%C**	**Cond. (µm/S)**	**Cu**	**Ca**	**Ti**	**S**	**Hg**
Arctic Tundra	0.00203	0.52590	0.00002	0.00000	0.83260	0.00000	0.00166	0.00083	0.00423
Transition	0.84220	0.63800	0.13320	0.00021	0.07941	0.00081	0.01253	0.08870	0.66420
R09	0.02357	0.01200	0.72860	0.00001	0.00005	0.02373	0.00708	0.42820	0.39070

	R09								
	$\delta^{13}C$	**$\delta^{15}N$**	**%C**	**Cond. (µm/S)**	**Cu**	**Ca**	**Ti**	**S**	**Hg**
Arctic Tundra	0.00007	0.00383	0.02379	0.00000	0.00053	0.00004	0.98830	0.02195	0.25200
Transition	0.01648	0.01410	0.45010	0.00000	0.00001	0.00083	0.58380	0.12140	0.50860
Boreal Forest	0.02357	0.01200	0.72860	0.00001	0.00005	0.02373	0.00708	0.42820	0.39070

Displayed values are p(same): probability of both data sets originating from the same population. Red highlighted areas denote a significant probability that the datasets are from different populations.